

R-06-78

**Rock types and ductile structures
on a rock domain basis, and
fracture orientation and mineralogy
on a deformation zone basis**

**Preliminary site description
Forsmark area – version 1.2**

Michael Stephens, Geological Survey of Sweden

Ola Forssberg, Golder Associates AB

September 2006

Svensk Kärnbränslehantering AB

Swedish Nuclear Fuel
and Waste Management Co

Box 5864

SE-102 40 Stockholm Sweden

Tel 08-459 84 00

+46 8 459 84 00

Fax 08-661 57 19

+46 8 661 57 19



Rock types and ductile structures on a rock domain basis, and fracture orientation and mineralogy on a deformation zone basis

Preliminary site description Forsmark area – version 1.2

Michael Stephens, Geological Survey of Sweden

Ola Forssberg, Golder Associates AB

September 2006

Keywords: Rock type, Ductile structure, Rock domain, Fracture orientation, Fracture mineralogy, Deformation zone, Model version 1.2, Histogram, Stereographic projection.

This report concerns a study which was conducted for SKB. The conclusions and viewpoints presented in the report are those of the authors and do not necessarily coincide with those of the client.

A pdf version of this document can be downloaded from www.skb.se

Abstract

This report presents the results of the analysis of base geological data in order to establish the dominant rock type, the subordinate rock types and the orientation of ductile mineral fabrics within each rock domain included in the regional geological model, version 1.2. An assessment of the degree of homogeneity of each domain is also provided. The analytical work has utilised the presentation of data in the form of histograms and stereographic projections. Fisher means and K values or best-fit great circles and corresponding pole values have been calculated for the ductile structural data. These values have been used in the geometric modelling of rock domains in the regional model, version 1.2. Furthermore, all analytical results have been used in the assignment of properties to rock domains in this model.

A second analytical component reported here addresses the orientation and mineralogy of fractures in the deterministic deformation zones that are included in the regional geological model, version 1.2. The analytical work has once again utilised the presentation of data in the form of histograms and stereographic projections. Fisher means and K values are presented for the orientation of fracture sets in the deterministic deformation zones that have been identified with the help of new borehole data. The frequencies of occurrence of different minerals along the fractures in these deformation zones as well as the orientation of fractures in the zones, along which different minerals occur, are also presented. The results of the analyses have been used in the establishment of a conceptual structural model for the Forsmark site and in the assignment of properties to deterministic deformation zones in model version 1.2.

Sammanfattning

Denna rapport presenterar resultat av analyser av geologiska data med syfte att karakterisera den dominerande bergarten och de underordnade bergarterna, samt orienteringen av plastiska strukturer inom varje bergdomän som ingår i version 1.2 av den regionala bergdomänmodellen. Vidare har en bedömning av homogeniteten av varje bergdomän gjorts. Förekomsten av olika bergarter presenteras i histogram och strukturmätningar i stereogram. För de plastiska strukturerna har Fishers medelvärde och K-värdet eller storcirkeln ("best-fit great circle") och motsvarande polvärden beräknats. Dessa värden har använts i den geometriska modelleringen i version 1.2 av den regionala bergdomänmodellen. Vidare har alla analysdata använts för bestämningen av de egenskaper som karakteriserar varje bergdomän i version 1.2 modellen.

Förutom analysering av ovan nämnda data omfattar rapporten även orienteringen och mineralogin i sprickor i de deterministiska deformationszonerna som är modellerade i version 1.2 av den geologiska modellen. I enlighet med de ovan nämnda data, presenteras sprickdata som histogram och stereogram. För de olika sprickgrupperna i de deterministiska deformationszonerna vilka har identifierats med hjälp av nya borrhålsdata har Fishers medelvärde och K-värdet beräknats. Förekomsten av olika sprickmineral samt orienteringen av sprickor längs vilka olika mineral förekommer har också presenterats för varje deformationszon. Resultaten av analyserna har använts i samband med konstruktionen av en konceptuell strukturmodell för Forsmark och för bestämningen av egenskaper i de deterministiska deformationszonerna i modell version 1.2.

Contents

1	Introduction	7
2	Rock domains	9
2.1	Methodological considerations	9
2.2	Data	11
2.3	Results	13
3	Deterministic deformation zones	19
3.1	Methodological considerations	19
3.2	Data	23
3.3	Results	23
4	References	27
Appendix 1	Rock types – codes and nomenclature	29
Appendix 2	Dominant and subordinate rock types in rock domains	31
Appendix 3	Orientation of ductile structures in rock domains	67
Appendix 4	Orientation of fractures in deterministic deformation zones	109
Appendix 5	Mineral coating or filling along fractures in deterministic deformation zones	133

1 Introduction

A key component in the geological modelling work concerns the assignment of properties to both rock domains and deterministic deformation zones recognised in the modelling work /Munier et al. 2003/. Several of these properties are needed directly in the geological modelling (e.g. orientation of ductile structures for the geometric modelling of rock domains, fracture mineralogy along deterministic deformation zones for the conceptual understanding of the site) and several are important both for the geological modelling and for other site investigation work (e.g. orientation of fractures along deterministic deformation zones). The properties that need to be assigned to each of these geological features, including a subgroup that concerns the properties assigned to the dominant rock type in each domain, are summarised in Tables 1-1, 1-2 and 1-3.

Table 1-1. Properties assigned to each rock domain.

Property	Comment
Rock domain ID	RFM***
Dominant rock type	
Subordinate rock types	
Degree of homogeneity	
Metamorphism/alteration	
Mineral fabric	Type and orientation with Fisher mean and K value or best-fit great circle and pole, as deemed appropriate

Table 1-2. Properties assigned to the dominant rock type in each domain.

Property	Comment
Mineralogical composition (%)	Only the dominant minerals are listed. Range/mean/standard deviation/number of samples
Grain size	Classification according to the nomenclature used by the Geological Survey of Sweden
Age (million years)	Range or value and 95% confidence interval
Structure	
Texture	
Density (kg/m ³)	Range/mean/standard deviation/number of samples
Porosity (%)	Range/mean/standard deviation/number of samples
Magnetic susceptibility (SI units)	Range/mean/standard deviation/number of samples
Electric resistivity in fresh water (ohm m)	Range/mean/standard deviation/number of samples
Uranium content based on gamma ray spectrometry data (ppm)	Range/mean/standard deviation/number of samples
Natural exposure rate (microR/h)	Range/mean/standard deviation/number of samples

Table 1-3. Properties assigned to deterministic deformation zones.

Property	Comment
Deformation zone ID code	ZFM*****
Position	With numerical estimate of uncertainty
Orientation (strike/dip)	With numerical estimate of uncertainty
Thickness	With numerical estimate of uncertainty
Length	With numerical estimate of uncertainty
Ductile deformation	Indicated if present along the zone
Brittle deformation	Indicated if present along the zone
Alteration	Indicated if present along the zone. Type of alteration specified
Fracture orientation	Fisher mean/K value/number of samples of each major fracture set
Fracture frequency	Mean/range
Fracture mineralogy	Mineral coating or filling specified

This report presents the results of the analysis of base geological data that have been used to establish:

- The dominant rock type, the subordinate rock types and the orientation of ductile mineral fabrics within each rock domain that has been included in the regional geological model, version 1.2. An assessment of the degree of homogeneity of each domain is also provided.
- The orientation and mineralogy of fractures in the deterministic deformation zones that have also been identified in the regional geological model, version 1.2.

The analytical work has utilised the presentation of data in the form of histograms and stereographic projections (Appendices 1–5) and the results are presented in a series of summary tables. The results of the analytical work have been used in the geometric modelling of rock domains, in the establishment of a conceptual structural model for the Forsmark site, and in the assignment of properties to rock domains and deterministic deformation zones. These aspects are addressed in the version 1.2 main modelling report /SKB 2005/.

2 Rock domains

2.1 Methodological considerations

The thirty-five rock domains that have been included in the version 1.2 geological model are shown in Figure 2-1. The rationale employed for the division of the regional model volume into rock domains is described in Section 5.3.3 in /SKB 2005/.

The composition and grain size of the dominant rock type together form one of the geological characteristics that have been used to distinguish domains. However, several domains consist of the same dominant rock type but have been distinguished on the basis of a second geological feature, the degree of homogeneity combined with the character and degree of ductile deformation. The degree of homogeneity addresses the frequency of occurrence of subordinate rock types in a domain. Different degrees of homogeneity and ductile deformation are critical for the separation of, for example, rock domains RFM012 and RFM029 as well as rock domains RFM018 and RFM035. Bearing in mind the procedures adopted to define rock domains, it is clear that a documentation of dominant rock type and subordinate rock types within each domain as well as a judgement of the degree of homogeneity are necessary in the modelling work.

With the exception of rock domains RFM007, RFM012, RFM017, RFM018, RFM023, RFM026 and RFM029, only surface data are available for the identification and characterisation of rock domains (Figure 2-1). Furthermore, the surface data are judged to be far more representative of the character of these domains. For these two reasons, data bearing on the character of rock type in the outcrop data have been selected for analysis in this report and divided up according to each rock domain.

Inspection of the various rock units that are described in the single hole interpretations /Carlsten et al. 2004abcdef/ has permitted a correlation between the rock units identified in the boreholes and the domains that have been recognised at the surface. In this manner, an identification of rock domains at depth along the boreholes can be carried out (Table 2-1). Since only the relative order of spatial significance of each rock type at each observation point has been documented in the bedrock mapping at the surface /Stephens et al. 2003a, Bergman et al. 2004/, there are no quantitative estimates of the proportions of different rock types in the surface data. Rock domains RFM012 and RFM029 are exceptions to this general rule. In these two domains, it is judged that the borehole data are sufficient to provide such quantitative information (see /SKB 2005/).

Bearing in mind that the bedrock at the Forsmark site has been affected by pervasive, ductile strain under amphibolite facies metamorphic conditions, the orientation of ductile structures are important for the geometric modelling of the various domains. This procedure can be adopted on the basis of the assumption that the character and orientation of ductile structures in such tectonic domains are not dependent on scale. Nevertheless, it is necessary to consider the variation in the orientation of these fabrics with depth and, for this reason, data from both the surface and from boreholes have been selected and divided up according to each rock domain. Unfortunately, no routine has been developed to measure linear structural features in the boreholes. For this reason, linear fabrics are only available from the surface.

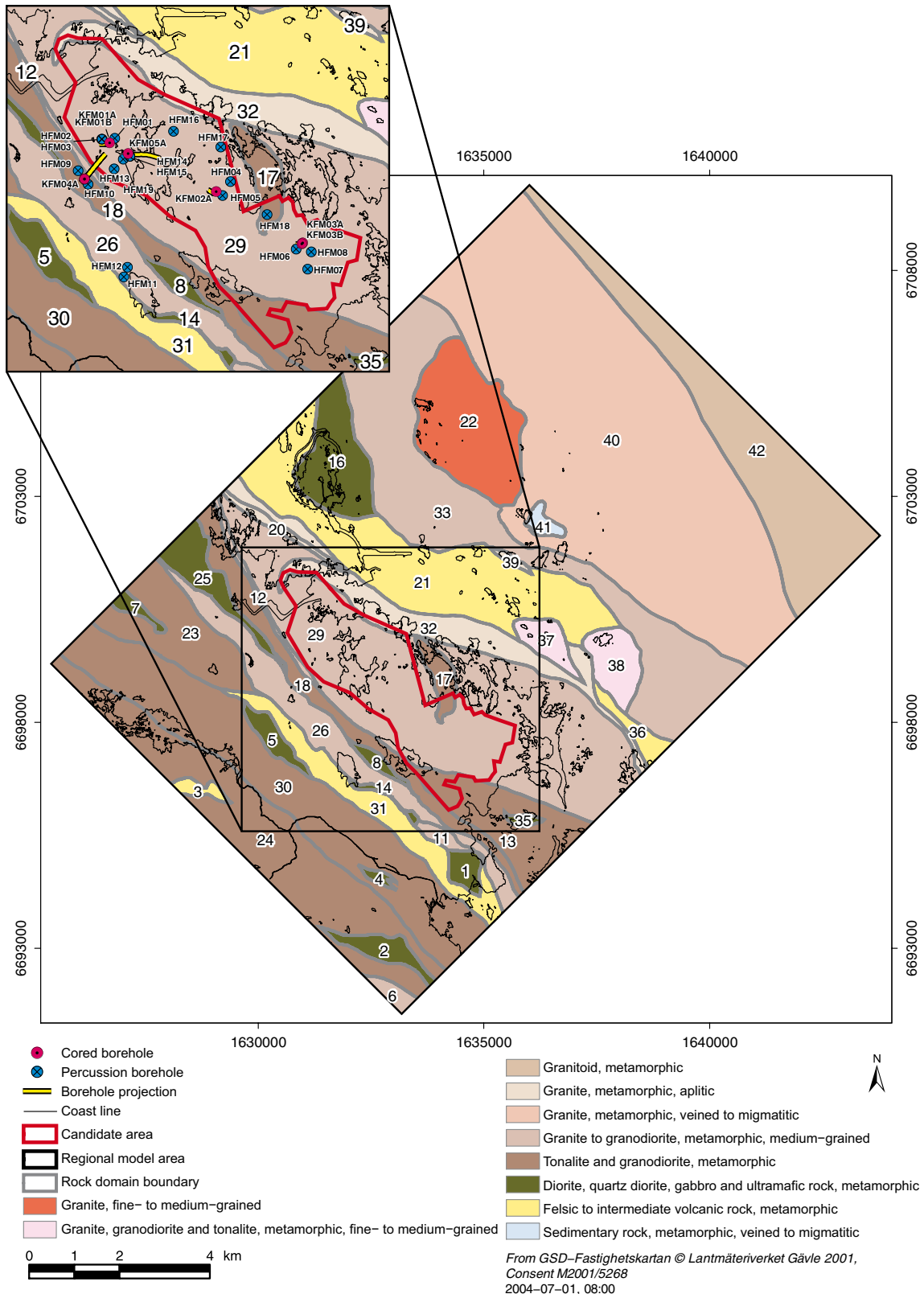


Figure 2-1. Rock domains identified at the surface in the version 1.2 modelling work, numbered from 1 to 42 /after SKB 2005/. The colours show the rock units that can be defined on the basis of the composition and grain size of the dominant rock type (see text).

Table 2-1. Summary of the correlation of rock units that have been recognised in the single hole interpretations /Carlsten et al. 2004abcdef/ and rock domains in boreholes KFM03A, KFM04A, HFM09, HFM10, HFM11, HFM12, HFM18 and KFO01. All other rock units in the single hole interpretations have been included in rock domain RFM029. Correlation based on /SKB 2005/.

Borehole	Rock unit	Rock domain
KFM03A	RU1, RU3, RU4, RU5	RFM029
KFM03A	RU2	RFM017
KFM04A	RU1, RU2	RFM018
KFM04A	RU3, RU4, RU5	RFM012
KFM04A	RU6, RU7, RU8	RFM029
HFM09	RU1	RFM018
HFM10	RU1	RFM018
HFM11	RU1, RU2	RFM026
HFM12	RU1	RFM026
HFM18	RU1	RFM017
HFM18	RU2	RFM029
KFO01	0–270.7 m	RFM007
KFO01	270.7–478.3 m	RFM023

Measurements of the orientation of both tectonic foliation and tectonic banding are included in the analysis of planar ductile structures at the surface. In the boreholes, measurements of the orientation of tectonic foliation, ductile shear zones and ductile-brittle shear zones are available. Data bearing on the orientation of linear structures at the surface have been divided into one group that is inferred to show fold axes and a second group that is inferred to represent the mineral stretching lineation. All these structures have been plotted in the lower hemisphere of various stereographic projections.

Bearing in mind the variation in the character and degree of ductile deformation inside the regional model area /SKB 2005/, Fisher mean and K values have been estimated in the domains where tectonic foliation and banding are more prominent and the ductile strain is inferred to be higher (e.g. rock domains RFM012, RFM018 and RFM031), while best-fit great circles and corresponding pole values have been calculated in the areas inferred to show major folding of the tectonic foliation (e.g. RFM017, RFM029 and RFM032). The Fisher K value, which is a measure of the dispersion of the data, has been estimated using the relationship between the number of poles and the magnitude of the vector sum of all pole vectors in a particular set of structures /Fisher 1953/. Considerable data are necessary to calculate a reliable K value. Except for a few cases, where few measurements are available and no K value is provided, all data sets with Fisher mean and K values have been treated in the same manner.

2.2 Data

The following data have been extracted from the SICADA database in order to analyse the character of the dominant rock type, the character of the subordinate rock types, the degree of homogeneity, and the nature and orientation of the ductile mineral fabrics in each rock domain:

- The character of the rock type at 2,119 outcrop observations (Figure 2-2). These point objects were studied in connection with the bedrock mapping programme at the scale 1:10,000 during both 2002 and 2003. The field data were subsequently synthesised in /Stephens et al. 2003a, Bergman et al. 2004/.

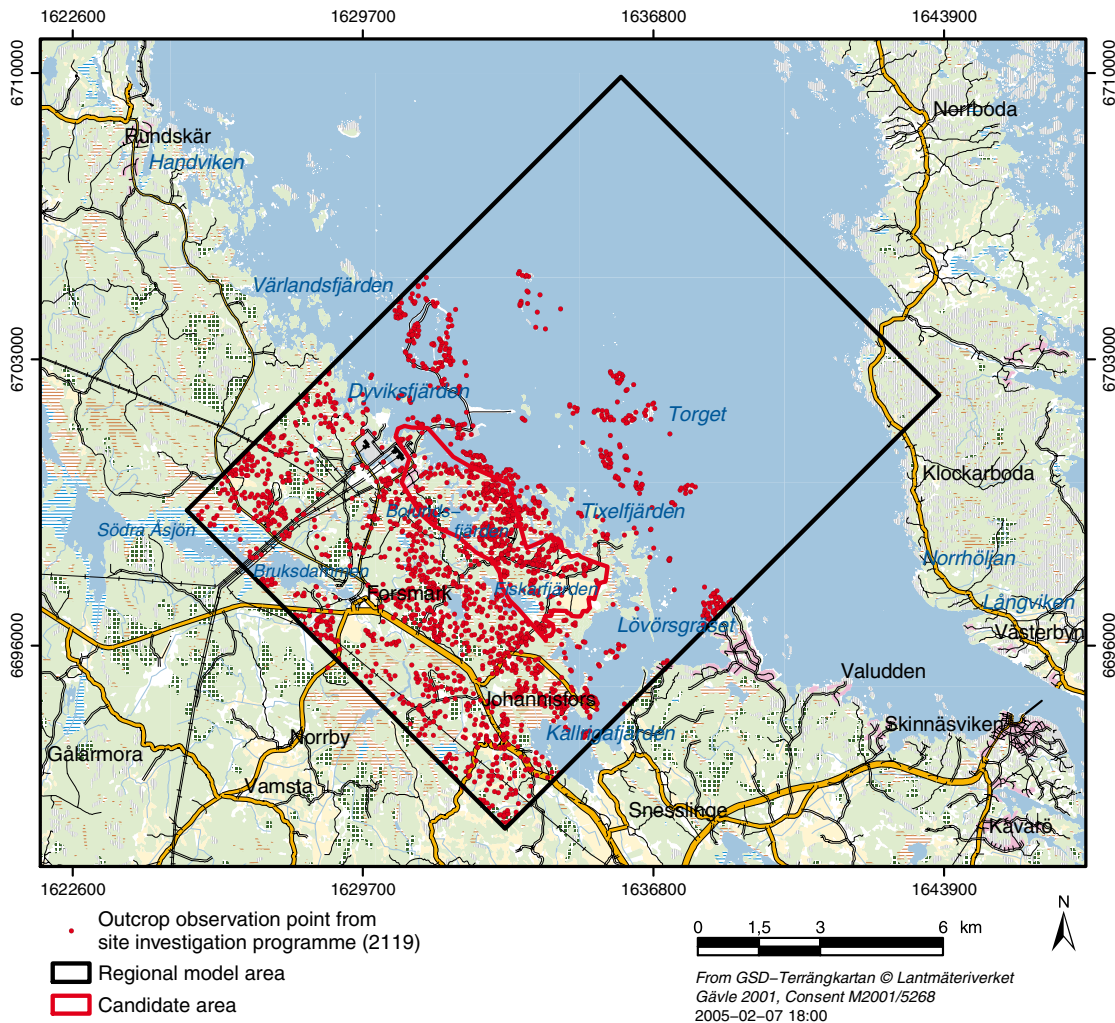


Figure 2-2. Outcrop observation points (2,119) at which data bearing on the character of rock type have been analysed. Measurements of the orientation of ductile structures are available at c. 75% of these observation points.

- The single hole interpretations of the cored boreholes KFM01A, KFM01B, KFM02A, KFM03A, KFM03B, KFM04A and KFM05A, and the percussion boreholes HFM01 to HFM19 (Figure 2-1), with focus on the identification of rock units /Carlsten et al. 2004abcdef/.
- The measurements of the orientation of both planar and linear, ductile structures at the surface (Figure 2-2). These data were also assembled in connection with the bedrock mapping programme /Stephens et al. 2003a, Bergman et al. 2004/.
- The measurements of the orientation of planar ductile structures in the cored boreholes KFM01A, KFM01B, KFM02A, KFM03A, KFM03B and KFM04A (Figure 2-1). At the time when the rock domain modelling work was completed, the data from KFM05A were not available. These data were also assembled in connection with the bedrock mapping of the boreholes using the Boremap methodology adopted by SKB /Petersson and Wängnerud 2003, Berglund et al. 2004, Petersson et al. 2004abc/.

At each surface observation point, the dominant rock type as well as the subordinate rock types are documented. On the basis of their spatial significance in the outcrop, the various rock types are arranged in a relative order of importance (order in outcrop, 1 to x). However, as pointed out above, no quantitative data are available that document the volumetric proportions of each rock type. The various codes and nomenclature for all the rock types identified at the Forsmark site are provided in Appendix 1.

2.3 Results

In Appendix 2, three histograms for rock type, which make use of the surface outcrop data, are shown for each rock domain. The upper histogram shows the number of observation points where a particular rock type is dominant. The second histogram, in the middle of each figure, shows the number of observation points that are composed solely of one rock type. Finally, the lower histogram shows the number of recordings of each rock type in the domain, irrespective of which order the rock type occurs at a particular observation point. Since rocks of the same composition but with different properties (e.g. grain size, texture, structure, etc) at an observation point are recorded separately in the outcrop database, the number of occurrences shown in the lower histogram commonly exceeds the number of outcrops observed in a domain. The first two histograms provide an assessment of the dominant rock type in the domain. The third histogram provides a basis for the definition of subordinate rock types in the domain.

An inspection of the histograms in Appendix 2 forms the basis for the results presented in tabular format in Table 2-2. The estimation of dominant rock type, subordinate rock types and degree of homogeneity have been exported to the rock domain property tables in /SKB 2005/. The extent and geometry of the rock domains at the surface are shown in Figure 2-1.

Table 2-2. Dominant rock type and subordinate rock types within the different domains, and the inferred degree of homogeneity of these domains based on the analysis of surface data, regional model version 1.2 (see Appendix 2).

Rock domain ID (model version 1.2)	Dominant rock type (SKB code)	Subordinate rock types (SKB code)	Degree of homogeneity
RFM001	Ultramafic rock, metamorphic (101004).	Diorite, quartz diorite and gabbro, metamorphic (101033).	High
RFM002	Diorite, quartz diorite and gabbro, metamorphic (101033).	Ultramafic rock, metamorphic (101004). Amphibolite (102017). Pegmatite, pegmatitic granite (101061). Granitoid, metamorphic (111051).	High
RFM003	Felsic to intermediate volcanic rock, metamorphic (103076).	Pegmatite, pegmatitic granite (101061). Diorite, quartz diorite and gabbro, metamorphic (101033). Amphibolite (102017). Granitoid, metamorphic (111051).	Low
RFM004	Ultramafic rock, metamorphic (101004).	Diorite, quartz diorite and gabbro, metamorphic (101033). Pegmatite, pegmatitic granite (101061). Amphibolite (102017). Tonalite to granodiorite, metamorphic (101054).	High
RFM005	Diorite, quartz diorite and gabbro, metamorphic (101033).	Pegmatite, pegmatitic granite (101061). Ultramafic rock, metamorphic (101004). Amphibolite (102017). Tonalite to granodiorite, metamorphic (101054).	High
RFM006	Granite (to granodiorite), metamorphic (101057).	Tonalite to granodiorite, metamorphic (101054). Pegmatite, pegmatitic granite (101061). Amphibolite (102017). Felsic to intermediate volcanic rock, metamorphic (103076).	High
RFM007	Diorite, quartz diorite and gabbro, metamorphic (101033).	Granite to granodiorite, metamorphic (101057). Pegmatite, pegmatitic granite (101061). Granite, fine- to medium-grained (111058).	High
RFM008	Diorite, quartz diorite and gabbro, metamorphic (101033).	Pegmatite, pegmatitic granite (101061).	High
RFM011	Granite (to granodiorite), metamorphic (101057).	Amphibolite (102017). Pegmatite, pegmatitic granite (101061).	High

Rock domain ID (model version 1.2)	Dominant rock type (SKB code)	Subordinate rock types (SKB code)	Degree of homogeneity
RFM012	Granite (to granodiorite), metamorphic (101057).	Granitoid, metamorphic, fine- to medium-grained (101051). Pegmatite, pegmatitic granite (101061). Amphibolite (102017). Felsic to intermediate volcanic rock, metamorphic (103076).	High
RFM013	Tonalite to granodiorite, metamorphic (101054).	Granodiorite, metamorphic (101056). Pegmatite, pegmatitic granite (101061). Diorite, quartz diorite and gabbro, metamorphic (101033). Amphibolite (102017).	Low
RFM014	Diorite, quartz diorite and gabbro, metamorphic (101033).	Ultramafic rock, metamorphic (101004). Pegmatite, pegmatitic granite (101061). Granitoid, metamorphic (111051). Felsic to intermediate volcanic rock, metamorphic (103076).	High
RFM016	Diorite, quartz diorite and gabbro, metamorphic (101033).	Pegmatite, pegmatitic granite (101061). Amphibolite (102017).	High
RFM017	Tonalite to granodiorite, metamorphic (101054).	Pegmatite, pegmatitic granite (101061). Granitoid (tonalitic), metamorphic, fine- to medium-grained (101051).	High
RFM018	Tonalite to granodiorite, metamorphic (101054).	Granite to granodiorite, metamorphic (101057). Granodiorite, metamorphic (101056). Felsic to intermediate volcanic rock, metamorphic (103076). Pegmatite, pegmatitic granite (101061). Amphibolite (102017). Granitoid, metamorphic, fine-to medium-grained (101051). Diorite, quartz diorite and gabbro, metamorphic (101033). Granite, fine- to medium-grained (111058). Magnetite mineralisation associated with calc-silicate rock (109014).	Low
RFM020	Granite, metamorphic, aplitic (101058).	Pegmatite, pegmatitic granite (101061). Granite to granodiorite, metamorphic (101057). Amphibolite (102017).	Low
RFM021	Felsic to intermediate volcanic rock, metamorphic (103076).	Pegmatite, pegmatitic granite (101061). Diorite, quartz diorite and gabbro, metamorphic (101033). Amphibolite (102017). Granitoid, metamorphic (111051). Granite, fine- to medium-grained (111058). Granitoid, metamorphic, fine- to medium-grained (101051)	Low
RFM022	Granite, fine- to medium-grained (111058).	Pegmatite, pegmatitic granite (101061). Felsic to intermediate volcanic rock, metamorphic (103076).	High
RFM023	Tonalite to granodiorite, metamorphic (101054).	Pegmatite, pegmatitic granite (101061). Granite to granodiorite, metamorphic (101057). Diorite, quartz diorite and gabbro, metamorphic (101033). Amphibolite (102017). Granitoid, metamorphic, fine- to medium-grained (101051). Granite, Fine- to medium-grained (111058).	High

Rock domain ID (model version 1.2)	Dominant rock type (SKB code)	Subordinate rock types (SKB code)	Degree of homogeneity
RFM024	Tonalite to granodiorite, metamorphic (101054).	Granodiorite, metamorphic (101056). Granite to granodiorite, metamorphic (101057). Diorite, quartz diorite and gabbro, metamorphic (101033). Pegmatite, pegmatitic granite (101061). Amphibolite (102017). Granite, metamorphic, aplitic (101058).	High
RFM025	Diorite, quartz diorite and gabbro, metamorphic (101033).	Pegmatite, pegmatitic granite (101061). Amphibolite (102017). Tonalite to granodiorite, metamorphic (101054).	High
RFM026	Granite (to granodiorite), metamorphic (101057).	Granite, metamorphic, aplitic (101058). Granodiorite, metamorphic (101056). Pegmatite, pegmatitic granite (101061). Diorite, quartz diorite and gabbro, metamorphic (101033). Felsic to intermediate volcanic rock, metamorphic (103076). Amphibolite (102017).	High
RFM029	Granite (to granodiorite), metamorphic (101057).	Granitoid, metamorphic, fine- to medium-grained (101051). Amphibolite (102017). Pegmatite, pegmatitic granite (101061). Granite, fine- to medium-grained (111058). Granite, metamorphic, aplitic (101058).	High
RFM030	Tonalite to granodiorite, metamorphic (101054).	Granodiorite, metamorphic (101056). Diorite, quartz diorite and gabbro, metamorphic (101033). Pegmatite, pegmatitic granite (101061). Amphibolite (102017). Granite to granodiorite, metamorphic (101057). Felsic to intermediate volcanic rock, metamorphic (103076). Granitoid, metamorphic, fine- to medium-grained (101051). Granite, fine- to medium-grained (111058). Sulphide mineralisation (109010).	Low
RFM031	Felsic to intermediate volcanic rock, metamorphic (103076).	Amphibolite (102017). Tonalite to granodiorite, metamorphic (101054). Pegmatite, pegmatitic granite (101061). Diorite, quartz diorite and gabbro, metamorphic (101033). Granodiorite, metamorphic (101056). Magnetite mineralisation associated with calc-silicate rock (109014)	Low
RFM032	Granite, metamorphic, aplitic (101058).	Granite to granodiorite, metamorphic (101057). Pegmatite, pegmatitic granite (101061). Amphibolite (102017). Granitoid, metamorphic, fine- to medium-grained (101051). Granite, fine- to medium-grained (111058). Felsic to intermediate volcanic rock, metamorphic (103076).	Low
RFM033	Granite (to granodiorite), metamorphic (101057).	Pegmatite, pegmatitic granite (101061). Amphibolite (102017). Granitoid, metamorphic, fine- to medium-grained (101051). Granite, fine- to medium-grained (111058). Granite, metamorphic, aplitic (101058).	High
RFM035	Diorite, quartz diorite and gabbro, metamorphic (101033).	Pegmatite, pegmatitic granite (101061). Amphibolite (102017).	High

Rock domain ID (model version 1.2)	Dominant rock type (SKB code)	Subordinate rock types (SKB code)	Degree of homogeneity
RFM036	Felsic to intermediate volcanic rock, metamorphic (103076).	Pegmatite, pegmatitic granite (101061). Amphibolite (102017). Granite, fine- to medium-grained (111058). Granite, metamorphic, aplitic (101058).	Low
RFM037	Granodiorite, tonalite and granite, metamorphic, fine- to medium-grained (101051).	Pegmatite, pegmatitic granite (101061). Felsic to intermediate volcanic rock, metamorphic (103076). Granite, fine- to medium-grained (111058). Amphibolite (102017).	High
RFM038	Granodiorite, tonalite and granite, metamorphic, fine- to medium-grained (101051).	Pegmatite, pegmatitic granite (101061). Granite, fine- to medium-grained (111058). Amphibolite (102017).	High
RFM039	Granite, metamorphic, aplitic (101058).	Pegmatite, pegmatitic granite (101061). Amphibolite (102017). Granite to granodiorite, metamorphic, medium-grained (101057). Granitoid, metamorphic, fine- to medium-grained (101051).	Low
RFM040	Granite (to granodiorite), metamorphic, veined to migmatitic (111057).	Pegmatite, pegmatitic granite (101061). Granitoid, metamorphic, fine- to medium-grained (101051). Granite, metamorphic, aplitic (101058). Granite, fine- to medium-grained (111058). Felsic to intermediate volcanic rock, metamorphic (103076).	Low
RFM041	Sedimentary rock, metamorphic, veined to migmatitic (106001).	Pegmatite, pegmatitic granite (101061). Granitoid, metamorphic, fine- to medium-grained (101051). Granite, fine- to medium-grained (111058). Amphibolite (102017).	Low
RFM042	Granitoid, metamorphic (111051).	Pegmatite, pegmatitic granite (101061). Granite, fine- to medium-grained (111058).	High

In Appendix 3, the orientations of tectonic foliation/banding, fold axis and mineral stretching lineation in each rock domain are shown on the lower hemisphere of separate stereographic projections. The planar structures (tectonic foliation/banding) have been plotted as poles to planes. Where both surface and borehole data are available, plots of both data sets as well as a combination of data sets are provided.

The analysis of ductile structures in the bedrock provides a basis for the projection of the various rock domains at depth and for a visualisation of the variation in plunge of the mineral stretching lineation within the rock domains /SKB 2005/. The orientations of the ductile structures that have been used in the geological modelling work are shown in Table 2-3. Furthermore, the orientation of the various ductile structures have been exported to the rock domain property tables in /SKB 2005/.

Table 2-3. Mean values of the orientation of ductile structures that have been used in the projection of rock domains at depth in the geological regional modelling work, version 1.2. The analysis of both surface and borehole data have been used (see Appendix 3). The estimated trend and plunge for the Fisher mean orientation of tectonic foliation/banding have been converted to a strike and dip notation (right-hand-rule).

Rock domain ID (model version 1.2)	Dominant rock type (SKB code)	Strike and dip of tectonic foliation/banding (mean orientation)	Trend and plunge of mineral stretching lineation (mean orientation)
RFM001	Ultramafic rock, metamorphic (101004)	No data	No data
RFM002	Diorite, quartz diorite and gabbro, metamorphic (101033)	No data	124/36
RFM003	Felsic to intermediate volcanic rock, metamorphic (103076)	108/75	136/40
RFM004	Ultramafic rock, metamorphic (101004)	No data	No data
RFM005	Diorite, quartz diorite and gabbro, metamorphic (101033)	136/89	137/41
RFM006	Granite (to granodiorite), metamorphic (101057)	127/77	143/44
RFM007	Diorite, quartz diorite and gabbro, metamorphic (101033)	No data	147/34
RFM008	Diorite, quartz diorite and gabbro, metamorphic (101033)	133/82	137/41
RFM011	Granite (to granodiorite), metamorphic (101057)	Variable	141/46
RFM012	Granite (to granodiorite), metamorphic (101057)	139/79 (surface data and data from KFM04A)	155/37 (surface data)
RFM013	Tonalite to granodiorite, metamorphic (101054)	112/57 (undulating)	144/36
RFM014	Diorite, quartz diorite and gabbro, metamorphic (101033)	No data	145/41
RFM016	Diorite, quartz diorite and gabbro, metamorphic (101033)	344/74 (undulating) Pole to best-fit great circle is 124/64	163/27
RFM017	Tonalite to granodiorite, metamorphic (101054)	Pole to best-fit great circle is 126/23 (surface data and data from KFM03A)	134/32 (surface data)
RFM018	Tonalite to granodiorite, metamorphic (101054)	141/81 (surface data and data from KFM04A)	143/35 (surface data)
RFM020	Granite, metamorphic, aplitic (101058)	120/84	123/40
RFM021 (northern part)	Felsic to intermediate volcanic rock, metamorphic (103076)	Pole to best-fit great circle is 124/64	Few data, variable
RFM021 (southern part)	Felsic to intermediate volcanic rock, metamorphic (103076)	127/83	127/30 (variable plunge)
RFM022	Granite, fine- to medium-grained (111058)	319/72 (few data and uncertain geological significance)	137/22
RFM023	Tonalite to granodiorite, metamorphic (101054)	Variable	144/33
RFM024	Tonalite to granodiorite, metamorphic (101054)	118/73	131/38
RFM025	Diorite, quartz diorite and gabbro, metamorphic (101033)	146/88	145/42
RFM026	Granite (to granodiorite), metamorphic (101057)	138/87	139/41

Rock domain ID (model version 1.2)	Dominant rock type (SKB code)	Strike and dip of tectonic foliation/ banding (mean orientation)	Trend and plunge of mineral stretching lineation (mean orientation)
RFM029	Granite (to granodiorite), metamorphic (101057)	Pole to best-fit great circle is 143/45 (surface data) Pole to best-fit great circle is 163/41 (data from KFM01A, KFM01B, KFM02A, KFM03A, KFM03B, KFM04A) Pole to best-fit great circle is 154/45 (all surface and borehole data)	142/38 (surface data)
RFM030	Tonalite to granodiorite, metamorphic (101054)	126/81	136/40
RFM031	Felsic to intermediate volcanic rock, metamorphic (103076)	131/85	139/41
RFM032 (whole domain)	Granite, metamorphic, aplitic (101058)	Pole to best-fit great circle is 126/65	118/37
RFM032 (eastern part)	Granite, metamorphic, aplitic (101058)	135/84	No data
RFM033	Granite (to granodiorite), metamorphic (101057)	Few data and variable	129/24
RFM035	Diorite, quartz diorite and gabbro, metamorphic (101033)	No data	137/32 (few data)
RFM036	Felsic to intermediate volcanic rock, metamorphic (103076)	No data	No data
RFM037	Granodiorite, tonalite and granite, metamorphic, fine- to medium-grained (101051)	Few data and variable	129/25
RFM038	Granodiorite, tonalite and granite, metamorphic, fine- to medium-grained (101051)	Few data and variable	126/24
RFM039	Granite, metamorphic, aplitic (101058)	303/81 (few data)	133/29
RFM040	Granite (to granodiorite), metamorphic, veined to migmatitic (111057)	Few data	123/32
RFM041	Sedimentary rock, metamorphic, veined to migmatitic (106001)	Few data	122/29
RFM042	Granitoid, metamorphic (111051)	No data	No data

3 Deterministic deformation zones

3.1 Methodological considerations

The surface intersection of the deterministic deformation zones in the version 1.2 base geological model are shown in Figures 3-1 (vertical and steeply dipping zones) and 3-2 (gently dipping zones). Ten deformation zones (ZFMNE1189, ZFMNE00B4, ZFMNE1195, ZFMNEB23A, ZFMNEB23B, ZFMNE0B5A, ZFMNE0B5B, ZFMNE00C1, ZFMNE00C2 and ZFMNW00E1), most of which are gently dipping, fail to intersect the surface, and for this reason, are not present in the two figures. The rationale used to determine the occurrence and properties of deterministic deformation zones is described in Section 5.4.3 in /SKB 2005/.

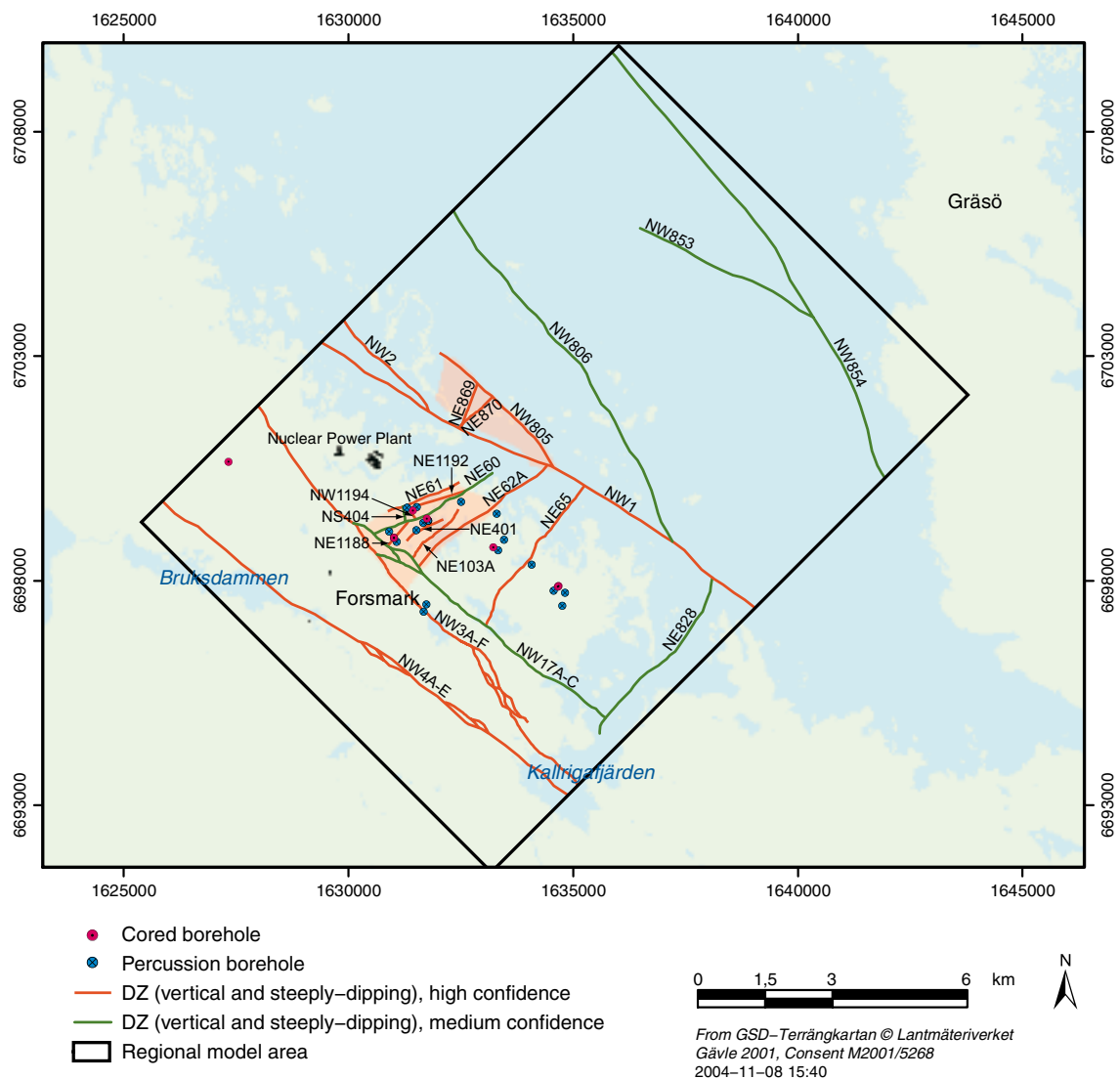


Figure 3-1. Map showing the surface traces of all the vertical and steeply dipping deformation zones in the base geological model, version 1.2. The map also shows the two areas (beige colour) in which vertical and steeply dipping deformation zones, which are predominantly longer than 1,000 m, have been handled deterministically. Outside these two areas, only vertical and steeply dipping zones mostly longer than 4,000 m have been handled deterministically.

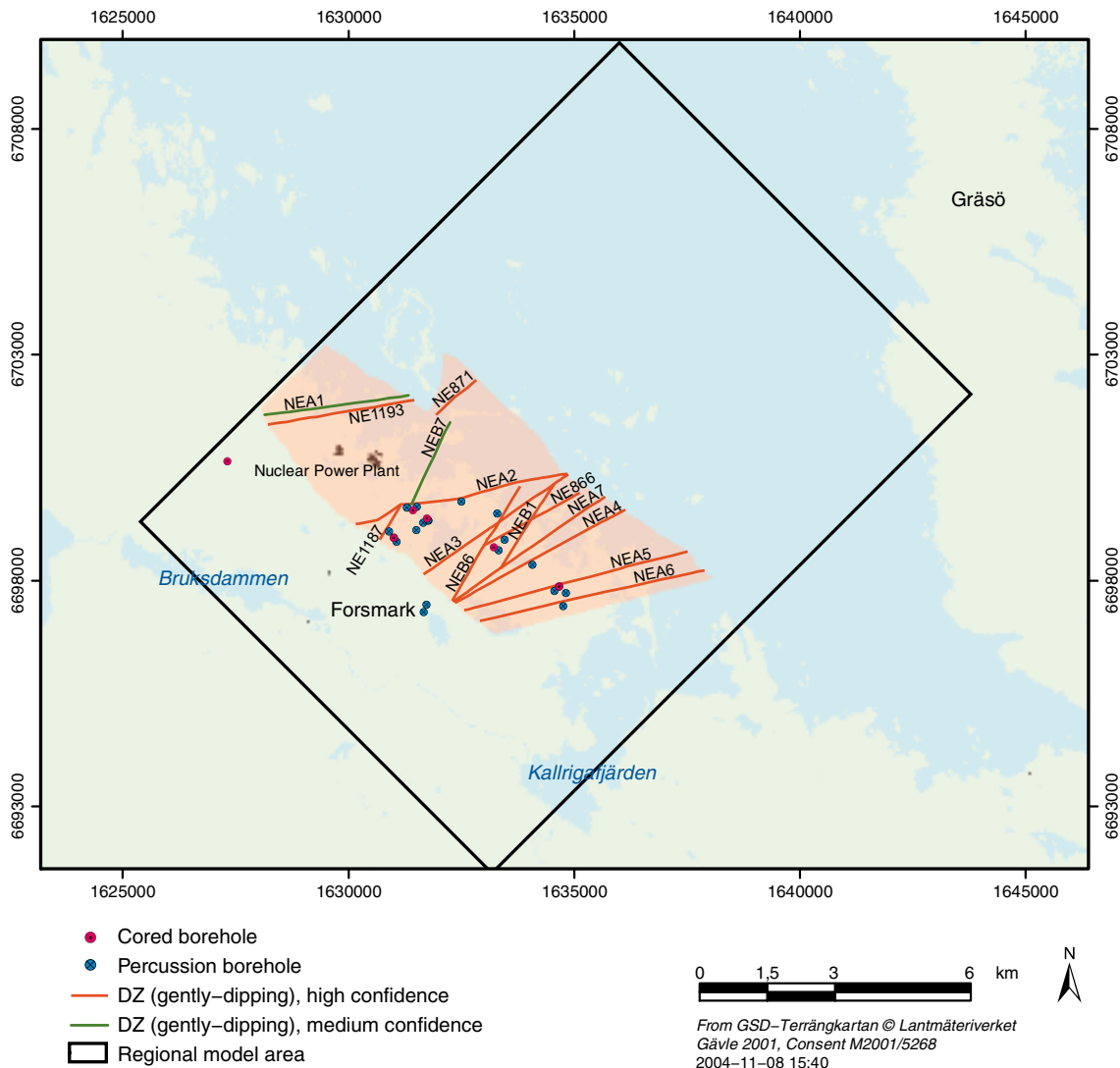


Figure 3-2. Map showing the surface traces of all the gently dipping deformation zones in the base geological model, version 1.2. The map also shows the area (beige colour) in which gently dipping deformation zones, which are predominantly longer than 1,000 m, have been handled deterministically.

The orientation and the mineral coating or filling of fractures within the deterministic deformation zones are two of the properties that have been selected for inclusion in the property table for each zone (Table 1-3). Older fracture data were used to characterise the deformation zones that transect tunnels 1–2 and 3, close to the nuclear power plants, and the tunnels in the vicinity of SFR (zones ZFMNW0001, ZFMNW0002, ZFMNW0805, ZFMNE0869, ZFMNE0870 and ZFMNE0871). These data are summarised in /Carlsson and Christiansson 1987, Axelsson and Hansen 1997/. No new data from the site investigation work are available for these deformation zones.

The deterministic deformation zones at the Forsmark site are poorly exposed at the surface. Only the Eckarfjärden deformation zone (ZFMNW003A–F) is exposed at a few, small inland outcrops. On account of the limited size and poor outcrop quality, no systematic assembly of fracture orientation and fracture mineralogical data has been completed at these outcrops. Furthermore, no temporary excavations of deterministic deformation zones have been carried out in connection with the initial site investigation work. In summary, little information on the orientation and mineralogy of fractures along deformation zones at the site have been obtained from surface data.

For the reasons outlined above, all new data that concern the orientation and mineralogy of fractures along deterministic deformation zones come from boreholes. The fixed point intersections of the deterministic deformation zones along the cored and percussion boreholes are shown in Table 3-1. All possible deformation zones in the single hole interpretations, except DZ4, DZ7 and DZ9 in KFM02A, DZ5 in KFM03A, a part of DZ3 (see Table 3-1) in KFM05A, DZ1 in HFM10 and DZ1 in HFM18, have been modelled deterministically, i.e. nearly 90% of the possible deformation zones that have been identified in the single hole interpretations.

Fracture orientation data along deformation zones are available from both percussion and cored boreholes. Since there are difficulties to assess the mineral coatings and fillings along fractures intersected by percussion boreholes, the quality of such data in SICADA is judged to be poor. For this reason, attention has been focussed on fracture mineralogical data from cored boreholes. Mineralogical data from percussion boreholes have only been used when cored borehole data are lacking.

Table 3-1. Correlation of deterministic deformation zones (model version 1.2) and fixed point intersections in the boreholes drilled during the initial site investigation at Forsmark. DZ1, DZ2 etc refer to possible deformation zones documented in the various single hole interpretations. All zones except ZFMNE1189 are high confidence zones. Site investigation data bearing on the orientation and mineralogy of fractures along deformation zones have been extracted from the boreholes or combination of boreholes listed in column 2 (see also Section 3.2).

Deterministic deformation zone ID (model version 1.2)	Fixed point intersections along boreholes in the initial site investigation
Vertical and steeply, SW-dipping brittle and ductile deformation zones with WNW and NW strike	
ZFMNW003A-F (Eckarfjärden deformation zone)	DZ1 in HFM11 and DZ1 in HFM12
ZFMNW1194	DZ2 in KFM01B
Steeply dipping brittle deformation zones with NE strike	
ZFMNE0061	DZ3 in KFM01A
ZFMNE062A, B	DZ4 and DZ5 in KFM05A
ZFMNE0065	DZ3 in HFM18
ZFMNE103A, B	Parts of DZ3 (609–616 m and 712–720 m borehole length) in KFM05A
ZFMNE0401	DZ1 in HFM13 and DZ2 in KFM05A
ZFMNE1188	DZ4 and DZ5 in KFM04A
ZFMNE1189	DZ5 in KFM02A
ZFMNE1192	DZ2 in KFM01A
Steeply dipping brittle deformation zones with NS strike	
ZFMNS0404	DZ3 in KFM01B
Gently SE- and S-dipping brittle deformation zones	
ZFMNE00A2	Deeper crustal levels: DZ6 in KFM02A, DZ1, DZ2 and DZ3 in KFM04A
ZFMNE00A3	DZ3 in KFM02A and DZ4 in KFM03A
ZFMNE00A4	DZ1 in KFM03A and DZ2 in HFM18
ZFMNE00A5	DZ1 and DZ2 in KFM03B, DZ1 in HFM06 and DZ1 in HFM08
ZFMNE00A6	DZ1 in HFM07
ZFMNE00A7	DZ2 in KFM03A and DZ3 in HFM18
ZFMNE00B1	DZ3 in KFM03A
ZFMNE00B4	DZ10 in KFM02A
ZFMNE00B6	DZ2 in KFM02A and DZ2 in HFM04
ZFMNE0866	DZ1 in KFM02A, DZ1 in HFM04 and DZ1 in HFM05
ZFMNE1187	DZ1 in HFM09 and DZ2 in HFM10
ZFMNE1195	DZ8 in KFM02A

Fracture orientation data for each deterministic deformation zone have been extracted from SICADA in accordance with the fixed point intersections listed in Table 3-1 (see also Section 3.2). For each deformation zone, the poles to the fractures along the zone have been plotted on the lower hemisphere of an equal area stereographic projection. Open and partly open fractures have been separated from sealed fractures in these plots. Since fracture orientation data are virtually absent from crush zones and sealed fracture networks, these structural features are not addressed in the analysis. For this reason, fracture frequencies are somewhat lower than that registered in SICADA for the zones that contain such structures.

Prior to contouring, a Terzhagi bias correction has been applied with a minimum bias angle of 15 degrees. The Fisher mean and K value for one or more, dominant sets of fractures in the contoured diagram have been calculated. The Fisher K value, which is a measure of the dispersion of the data, has been estimated using the relationship between the number of poles and the magnitude of the vector sum of all pole vectors in a selected set of fractures /Fisher 1953/. The first step in the selection of fracture sets has involved an optical comparison of the contoured plot with the fracture orientation sets defined from fracture data outside deformation zones, in the statistical model of fractures at Forsmark, version 1.2 /La Pointe et al. 2005/. The definitions of the different fracture sets in this model are provided in Table 3-2. If deemed necessary, the boundaries between orientation sets in the fracture data from deformation zones have been modified in order to achieve a better fit to the contoured data. The alternative interpretations are presented.

On the basis of the study of mineral growth relationships along especially the fractures that bear groundwater, six generations of fracture mineralisation have been identified at the Forsmark site /Sandström et al. 2004/. These are summarised below in order of decreasing age:

- Generation 1 (oldest): Epidote, quartz and chlorite.
- Generation 2/Generation 3: Prehnite/Laumontite. In addition, growth of calcite, chlorite-corrensite, adularia and quartz. Generations 2 and 3 are grouped together since stable isotope data for calcite in the two generations are similar /Sandström et al. 2004/.
- Generation 4/Generation 5: Quartz, adularia, albite, analcime, chlorite-corrensite and calcite/Calcite and pyrite. Once again, generations 4 and 5 are grouped together on the basis of the stable isotope composition of the calcite in the two generations /Sandström et al. 2004/.
- Generation 6 (youngest): Calcite, clay minerals, possibly also asphaltite.

In the analysis carried out in this study, mineralogical data along the fractures in each deterministic deformation zone have been extracted from SICADA in accordance with the fixed point intersections listed in Table 3-1 (see also Section 3.2). On the basis of the results of the detailed study in /Sandström et al. 2004/, attention is focused on a selection of eight common minerals. In alphabetical order, these minerals are calcite, chlorite, clay minerals, epidote, hematite (commonly associated with adularia), laumontite, prehnite and quartz. The fractures along which other minerals are present, where no mineral coating or filling has been identified, and where oxidised wall-rock alteration is present in the adjacent host rock are also included in the analysis.

Table 3-2. Definition of fracture orientation sets based on outcrop data obtained outside deterministic deformation zones at the Forsmark site /after La Pointe et al. 2005/.

Fracture orientation set	Strike range	Dip range
NE	020–080 and 200–260	50–90
NS	155–200 and 335–020	50–90
NW	115–155 and 295–335	50–90
EW	080–115 and 260–295	50–90
Gently dipping	No restriction	0–50

3.2 Data

The following data have been extracted from the SICADA database in order to analyse the orientation and mineralogy of fractures along the deterministic deformation zones modelled in version 1.2:

- The single hole interpretations of the cored boreholes KFM01A, KFM01B, KFM02A, KFM03A, KFM03B, KFM04A and KFM05A, and the percussion boreholes HFM01 to HFM19 (Figure 2-1), with focus on the identification of possible deformation zones /Carlsten et al. 2004abcdef/.
- The measurements of the orientation of fractures and the character of mineral coatings and fillings (MIN1 to MIN4) along fractures in the parts of the cored boreholes KFM01A, KFM01B, KFM02A, KFM03A, KFM03B, KFM04A and KFM05A, and the percussion boreholes HFM01 to HFM19, which are inferred, in the single hole interpretations, to represent intersections through possible deformation zones. These data were assembled in connection with the bedrock mapping of the boreholes using the Boremap methodology adopted by SKB /Nordman 2003abc, 2004ab, Nordman and Samuelsson 2004, Petersson and Wängnerud 2003, Berglund et al. 2004, Petersson et al. 2004abcd/.

3.3 Results

The fracture orientation data for each deterministic deformation zone at the Forsmark site, which has been identified with the help of new borehole data, are presented in the form of lower hemisphere, equal area stereographic projections (Appendix 4). The Fisher mean and K value for one or more fracture sets along each zone have been calculated according to the procedure described in Section 3.1. The sensitivity of adopting alternative boundaries between fracture sets can be judged by comparing the Fisher mean and K values for the different sets. Only very minor differences are noted in these values in the zones where this procedure has been implemented.

Histograms that show the number of fractures along which a particular mineral or wall-rock alteration has been identified are presented for the deterministic deformation zones (Appendix 5). In each histogram, mineral coatings or fillings and wall-rock alteration along open and partly open fractures have been separated from the same features along sealed fractures. Furthermore, for each deformation zone, the poles to fractures along which a particular mineral coating or filling and wall-rock alteration is present have been plotted in a series of lower hemisphere, equal area stereographic projections (Appendix 5). In this manner, the mineralogy and orientation of fractures along each deterministic deformation zone are linked together.

An inspection of the stereographic projections and histograms in Appendices 4 and 5 forms the basis for the results presented for each deterministic deformation zone in Table 3-3. The focus here is on the Fisher mean and K value for the orientation of one or more fracture sets in each zone, the number of fractures upon which these values are based, and the principal minerals that form coatings or fillings along fractures in the zone. It is emphasised again that orientation data are not available for the fractures in crush zones and sealed fracture networks.

Table 3-3. Orientation of dominant fracture sets and mineralogy of fractures along the deterministic deformation zones, which have been identified with the help of new borehole data, in regional model version 1.2. Surface data are also available for the Eckarfjärden deformation zone (ZFMNW003A–F). The estimated trend and plunge for the Fisher mean orientation of inferred fracture sets have been converted to a strike and dip notation (right-hand-rule).

Deterministic deformation zone ID (model version 1.2)	Fracture orientation		Total fractures (N)	Fracture coating or filling
	Fisher mean (strike/dip)	K value		
Vertical and steeply, SW-dipping brittle and ductile deformation zones with WNW and NW strike				
ZFMNW003A–F (Eckarfjärden deformation zone)	NW set 130/88	NW set 17	482	Surface and percussion borehole data available. Epidote, quartz, calcite, chlorite. Note also fractures with oxidized walls
ZFMNW1194	Gently-dipping set 168/11 NW set 145/81	Gently-dipping set 21 NW set 21	226	Cored borehole data. Chlorite, calcite, epidote, quartz, clay minerals. Note also fractures with oxidized walls and fractures without mineral coating/filling
Steeply dipping brittle deformation zones with NE strike				
ZFMNE0061	NE set 040/76	NE set 69	246	Cored borehole data. Laumontite, chlorite, hematite, calcite, quartz. Note also fractures with oxidized walls
ZFMNE062A, B	NE set 241/90	NE set 33	244	Cored borehole data. Calcite, laumontite, chlorite, hematite, quartz, prehnite. Note also fractures with oxidized walls
ZFMNE0065	NE set 030/77	NE set 13	132	Only percussion borehole data available. Chlorite, calcite, quartz. Note also fractures with oxidized walls
ZFMNE103A, B	NE set 227/87 NS set 182/87	NE set 15 NS set 15	102	Cored borehole data. Laumontite, chlorite, calcite, hematite, quartz. Note also fractures with oxidized walls
ZFMNE0401	NE set 239/81 NW to NS set 154/81	NE set 33 NW to NS set 21	226	Cored borehole data. Chlorite, calcite, prehnite, hematite, laumontite, epidote, clay minerals, quartz. Note also fractures with oxidized walls
ZFMNE1188	NW set 139/84 NE set 237/86	NW set 27 NE set 12	423	Cored and percussion borehole data. Chlorite, calcite, laumontite, hematite, quartz, clay minerals, epidote, prehnite. Note also fractures with oxidized walls
ZFMNE1189	NE set 038/65	NE set 33	36	Cored borehole data. Calcite, chlorite, hematite, quartz. Note also fractures with oxidized walls
ZFMNE1192	NE set 067/81 Gently-dipping set 115/06	NE set 87 Gently-dipping set 25	113	Cored borehole data. Chlorite, laumontite, hematite, calcite, quartz. Note also fractures with oxidized walls
Steeply dipping brittle deformation zones with NS strike				
ZFMNS0404	NS set 347/86 Gently-dipping set 074/07	NS set 33 Gently-dipping set 13	258	Cored borehole data. Chlorite, calcite, laumontite, prehnite, quartz, hematite, epidote, clay minerals. Note also fractures with oxidized walls

Gently SE- and S-dipping brittle deformation zones

ZFMNE00A2	Gently-dipping set 027/11 NE set 053/75 NW set 313/88	Gently-dipping set 18 NE set 10 NW set 13	1,058	Cored and percussion borehole data. Chlorite, calcite, hematite, clay minerals, epidote, laumontite, prehnite, quartz. Note also fractures with oxidized walls and fractures without mineral coating/filling
ZFMNE00A3	Gently-dipping set 034/04	Gently-dipping set 13	224	Cored borehole data. Calcite, chlorite, hematite, quartz, clay minerals, prehnite. Note also fractures without mineral coating/filling
ZFMNE00A4	Gently-dipping set 042/04	Gently-dipping set 13	216	Cored and percussion borehole data. Chlorite, calcite, laumontite. Note also fractures without mineral coating/filling
ZFMNE00A5	Gently-dipping set 038/14	Gently-dipping set 12	155	Cored and percussion borehole data. Chlorite, calcite, clay minerals, prehnite, hematite, quartz
ZFMNE00A6	Gently-dipping set 045/70	Gently-dipping set 11	98	Only percussion borehole data available. Chlorite, calcite
ZFMNE00A7	Gently-dipping set 028/34 NE set 043/79 EW set 096/89	Gently-dipping set 15 NE set 12 EW set 11	180	Cored and percussion borehole data. Calcite, chlorite, clay minerals, hematite, prehnite. Note also fractures with oxidized walls
ZFMNE00B1	Gently-dipping set 128/12	Gently-dipping set 9	46	Cored borehole data. Chlorite, calcite, prehnite, hematite, quartz, clay minerals, laumontite. Note also some fractures with oxidized walls
ZFMNE00B4	Gently-dipping set 068/52	Gently-dipping set 9	27	Cored borehole data. Calcite, clay minerals, chlorite, hematite, prehnite. Note also fractures without mineral coating/filling
ZFMNE00B6	Gently-dipping set 038/15	Gently-dipping set 15	105	Cored and percussion borehole data. Chlorite, calcite, prehnite. Note also fractures with oxidized walls
ZFMNE0866	Gently-dipping set 001/11	Gently-dipping set 13	58	Only percussion borehole data available. Chlorite, calcite
ZFMNE1187	Gently-dipping set 037/12 NE set 231/78	Gently-dipping set 28 NE set 34	68	Only percussion borehole data available. Chlorite, calcite, epidote
ZFMNE1195	Moderately dipping set 080/40	Moderately dipping set 28	57	Cored borehole data. Chlorite, calcite. Note also fractures without mineral coating/filling

An integrated assessment of the different generations of mineral assemblages /Sandström et al. 2004/, the orientation of mineral coatings and fillings along fractures (this report), and the available geochronological data /Page et al. 2004/ is discussed further in connection with the development of a conceptual structural model for the Forsmark site (see Section 5.4.2 in /SKB 2005/). Apart from older data that describe the cross-cutting relations between fractures with different mineral fillings along zone ZFMNW0001, the Singö deformation zone /Larsson 1973, Carlsson 1979/, there are virtually no data that describe the time relationships between different fracture minerals along deterministic deformation zones at the site. Such zone-specific data are planned to be available during the complementary site investigation phase. The results of the analytical work presented in this report, together with the information in older summary reports for the zones north-east of the power plant and around SFR, have been used in the assignment of properties of deterministic deformation zones /SKB 2005/.

4 References

- Axelsson C-L, Hansen L M, 1997.** Update of structural models at SFR nuclear waste repository, Forsmark, Sweden. SKB R-98-05, Svensk Kärnbränslehantering AB.
- Berglund J, Petersson J, Wängnerud A, Danielsson P, 2004.** Boremap mapping of core drilled borehole KFM01B. Forsmark site investigation. SKB P-04-114, Svensk Kärnbränslehantering AB.
- Bergman T, Andersson J, Hermansson T, Zetterström E, Albrecht L, Stephens M B, Petersson J, Nordman C, 2004.** Bedrock mapping. Stage 2 (2003) – bedrock data from outcrops and the basal parts of trenches and shallow boreholes through the Quaternary cover. Forsmark site investigation. SKB P-04-91, Svensk Kärnbränslehantering AB.
- Carlsson A, 1979.** Characteristic features of a superficial rock mass in southern central Sweden – Horizontal and subhorizontal fractures and filling material. Striae 11.
- Carlsson A, Christiansson R, 1987.** Geology and tectonics at Forsmark, Sweden. SKB SFR-87-04, Svensk Kärnbränslehantering AB.
- Carlsten S, Petersson J, Stephens M, Mattsson H, Gustafsson J, 2004a.** Geological single-hole interpretation of KFM01A, KFM01B and HFM01–03 (DS1). Forsmark site investigation. SKB P-04-116, Svensk Kärnbränslehantering AB.
- Carlsten S, Petersson J, Stephens M, Mattsson H, Gustafsson J, 2004b.** Geological single-hole interpretation of KFM02A and HFM04–05 (DS2). Forsmark site investigation. SKB P-04-117, Svensk Kärnbränslehantering AB.
- Carlsten S, Petersson J, Stephens M, Thunehed H, Gustafsson J, 2004c.** Geological single-hole interpretation of KFM03B, KFM03A and HFM06–08 (DS3). Forsmark site investigation. SKB P-04-118, Svensk Kärnbränslehantering AB.
- Carlsten S, Petersson J, Stephens M, Mattsson H, Gustafsson J, 2004d.** Geological single-hole interpretation of KFM04A and HFM09–10 (DS4). Forsmark site investigation. SKB P-04-119, Svensk Kärnbränslehantering AB.
- Carlsten S, Petersson J, Stephens M, Thunehed H, Gustafsson J, 2004e.** Geological single-hole interpretation of HFM11–13 and HFM16–18. Forsmark site investigation. SKB P-04-120, Svensk Kärnbränslehantering AB.
- Carlsten S, Petersson J, Stephens M, Thunehed H, Gustafsson J, 2004f.** Geological single-hole interpretation of KFM05A, HFM14–15 and HFM19 (DS5). Forsmark site investigation. SKB P-04-296, Svensk Kärnbränslehantering AB.
- Fisher R, 1953.** Dispersion on a sphere. Proceedings of the Royal Society of London A217.
- La Pointe P R, Olofsson I, Hermanson J, 2005.** Statistical model of fractures and deformation zones for Forsmark. Preliminary site description Forsmark area – version 1.2. SKB R-05-26, Svensk Kärnbränslehantering AB.
- Larsson W, 1973.** Forsmark kraftstation, aggregat 1 och 2, avloppstunneln: Berggeologiska förhållanden efter tunnellen. Technical Report, Swedish State Power Board, Stockholm.
- Munier R, Stenberg L, Stanfors R, Milnes A G, Hermanson J, Triumf C-A, 2003.** Geological Site Descriptive Model. A strategy for the model development during site investigations. SKB R-03-07, Svensk Kärnbränslehantering AB.

- Nordman C, 2003a.** Boremap mapping of percussion boreholes HFM01–03. Forsmark site investigation. SKB P-03-20, Svensk Kärnbränslehantering AB.
- Nordman C, 2003b.** Boremap mapping of percussion boreholes HFM04 and HFM05. Forsmark site investigation. SKB P-03-21, Svensk Kärnbränslehantering AB.
- Nordman C, 2003c.** Boremap mapping of percussion boreholes HFM06–08. Forsmark site investigation. SKB P-03-22, Svensk Kärnbränslehantering AB.
- Nordman C, 2004a.** Boremap mapping of percussion boreholes HFM09–12. Forsmark site investigation. SKB P-04-101, Svensk Kärnbränslehantering AB.
- Nordman C, 2004b.** Boremap mapping of percussion boreholes HFM13-15 and HFM19. Forsmark site investigation. SKB P-04-112, Svensk Kärnbränslehantering AB.
- Nordman C, Samuelsson E, 2004.** Boremap mapping of percussion boreholes HFM16–18. Forsmark site investigation. SKB P-04-113, Svensk Kärnbränslehantering AB.
- Page L, Hermansson T, Söderlund P, Andersson J, Stephens M B, 2004.** Bedrock mapping. U-Pb, $^{40}\text{Ar}/^{39}\text{Ar}$ and (U-Th)/He geochronology. Forsmark site investigation. SKB P-04-126, Svensk Kärnbränslehantering AB.
- Petersson J, Wängnerud A, 2003.** Boremap mapping of telescopic drilled borehole KFM01A. Forsmark site investigation. SKB P-03-23, Svensk Kärnbränslehantering AB.
- Petersson J, Wängnerud A, Stråhle A, 2004a.** Boremap mapping of telescopic drilled borehole KFM02A. Forsmark site investigation. SKB P-03-98, Svensk Kärnbränslehantering AB.
- Petersson J, Wängnerud A, Danielsson P, Stråhle A, 2004b.** Boremap mapping of telescopic drilled borehole KFM03A and core drilled borehole KFM03B. Forsmark site investigation. SKB P-03-116, Svensk Kärnbränslehantering AB.
- Petersson J, Wängnerud A, Berglund J, Danielsson P, Stråhle A, 2004c.** Boremap mapping of telescopic drilled borehole KFM04A. Forsmark site investigation. SKB P-04-115, Svensk Kärnbränslehantering AB.
- Petersson J, Berglund J, Wängnerud A, Danielsson P, Stråhle A, 2004d.** Boremap mapping of telescopic drilled borehole KFM05A. Forsmark site investigation. SKB P-04-295, Svensk Kärnbränslehantering AB.
- Sandström B, Savolainen M, Tullborg E-L, 2004.** Fracture mineralogy. Results from fracture minerals and wall rock alteration in boreholes KFM01A, KFM02A, KFM03A and KFM03B. Forsmark site investigation. SKB P-04-149, Svensk Kärnbränslehantering AB.
- SKB, 2005.** Preliminary site description. Forsmark area – version 1.2. SKB R-05-18, Svensk Kärnbränslehantering AB.
- Stephens M B, Bergman T, Andersson J, Hermansson T, Wahlgren C-H, Albrecht L, Mikko H, 2003a.** Bedrock mapping. Stage 1 (2002) – Outcrop data including fracture data. Forsmark. SKB P-03-09, Svensk Kärnbränslehantering AB.
- Stephens M B, Lundqvist S, Ekström M, Bergman T, Andersson J, 2003b.** Bedrock mapping. Rock types, their petrographic and geochemical characteristics, and a structural analysis of the bedrock based on stage 1 (2002) surface data. Forsmark site investigation. SKB P-03-75, Svensk Kärnbränslehantering AB.

Rock types – codes and nomenclature

The table below translates the various rock codes, which are used in all databases and in this report, to rock names. The different groups (A to D) are essentially a stratigraphic classification of the rocks /Stephens et al. 2003b/. The oldest rocks, which are supracrustal in character, are included in Group A. The rocks in Groups B and C belong to two separate generations of younger, calc-alkaline intrusive rocks. The youngest intrusive rocks are included in Group D. Pegmatite and pegmatitic granite (101061) are included in Group D, but show both younger (dominant) and older relationships to the Group C rocks.

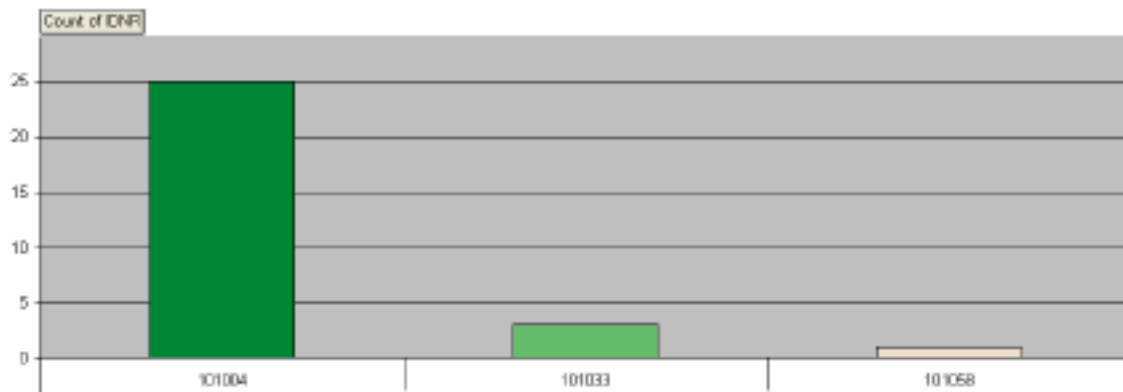
Rock code	Rock composition	Complementary characteristics		
Rock codes and rock names adopted by SKB				
111058	Granite		Fine- to medium-grained	Group D
101061	Pegmatite, pegmatitic granite			Group D
101051	Granite, granodiorite and tonalite	Metamorphic	Fine- to medium-grained	Group C
111051	Granitoid	Metamorphic		Group B
101058	Granite	Metamorphic	Aplitic	Group B
111057	Granite to granodiorite	Metamorphic, veined to migmatitic		Group B
101057	Granite to granodiorite	Metamorphic	Medium-grained	Group B
101056	Granodiorite	Metamorphic		Group B
101054	Tonalite to granodiorite	Metamorphic		Group B
101033	Diorite, quartz diorite, gabbro	Metamorphic		Group B
102017	Amphibolite			Group B
101004	Ultramafic rock	Metamorphic		Group B
108019	Calc-silicate rock (skarn)			Group A
109014	Magnetite mineralisation associated with calc-silicate rock (skarn)			Group A
109010	Sulphide mineralisation			Group A
103076	Felsic to intermediate volcanic rock	Metamorphic		Group A
106001	Sedimentary rock	Metamorphic, veined to migmatitic		Group A
106000	Sedimentary rock	Metamorphic		Group A
Additional rock codes and rock names of strongly subordinate character				
1051	Granitoid	Metamorphic	Uncertain classification 101051, 111051	Group B or Group C
1053	Tonalite	Metamorphic	Uncertain classification 101051 or 101054	Group B or Group C
1054	Tonalite to granodiorite	Metamorphic	Uncertain classification 101051 or 101054	Group B or Group C

Rock code	Rock composition	Complementary characteristics		
1056	Granodiorite	Metamorphic	Uncertain classification 101051 or 101056	Group B or Group C
1057	Granite to granodiorite	Metamorphic	Uncertain classification 101051 or 101057	Group B or Group C
1058_120	Granite	Metamorphic	Uncertain classification 101057 or 101058	Group B
1058	Granite		Uncertain classification 101051, 101057, 101058 or 111058	Group B, Group C or Group D
1059	Leucocratic granite		Uncertain classification 101058 or 111058	Group B or Group D
1062	Aplite		Uncertain classification 101058 or 111058	Group B or Group D
111058_101051	Granite		Uncertain classification 101051 or 111058	Group C or Group D
5103	Felsic rock	Metamorphic	Uncertain classification 103076 or 101058	Group A or Group B
6053	Quartz-hematite rock			
8003	Cataclastic rock			
8004	Mylonite			
8011	Gneiss			
8020	Hydrothermal vein or segregation			
8021	Quartz-rich hydrothermal vein or segregation			
8023	Hydrothermally altered rock			

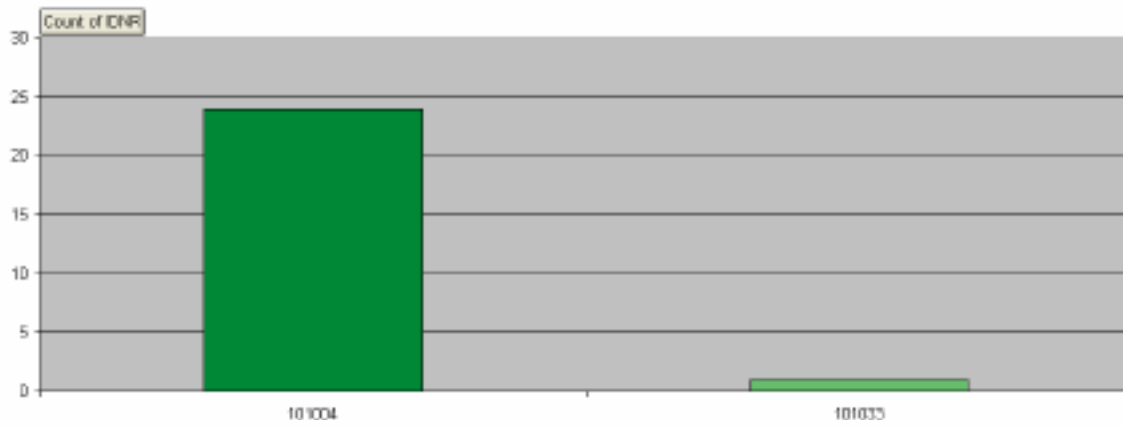
Dominant and subordinate rock types in rock domains

Three histograms for rock type, which make use of the surface outcrop data, are shown for each rock domain. The upper histogram shows the number of observation points (outcrops) where a particular rock type is dominant and, as a consequence, the number of observation points in the rock domain. The second histogram, in the middle of each figure, shows the number of observation points that are composed solely of one rock type. The lower histogram shows the number of recordings of each rock type in the domain, irrespective of which order the rock type occurs at a particular observation point. Since rocks of the same composition but with different properties (e.g. grain size, texture, structure, etc) at each observation point are recorded separately in the outcrop database, the number of occurrences shown in the lower histogram commonly exceeds the number of outcrops observed in a domain. No data are available for rock domain RFM042.

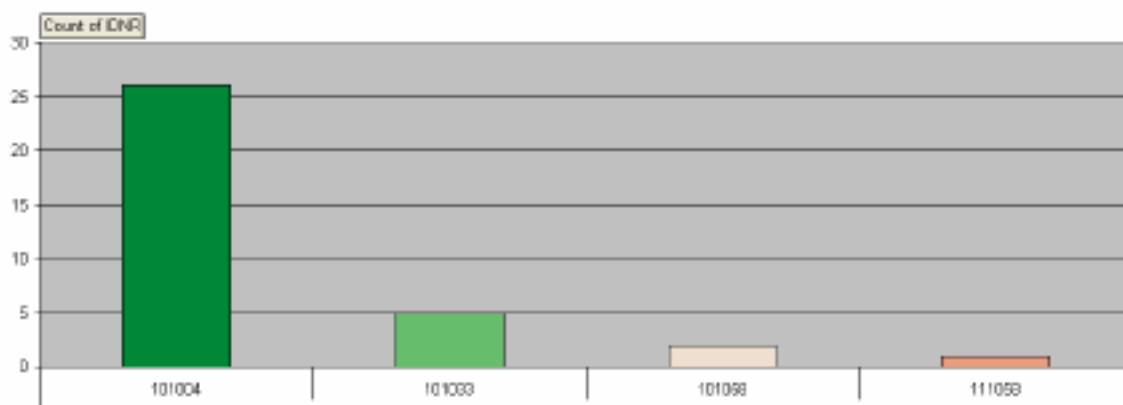
Rock domain 1
 Number of outcrops where each rock type is dominating.
 Y-axis indicates total number of outcrops in the rock domain. [N = 29]



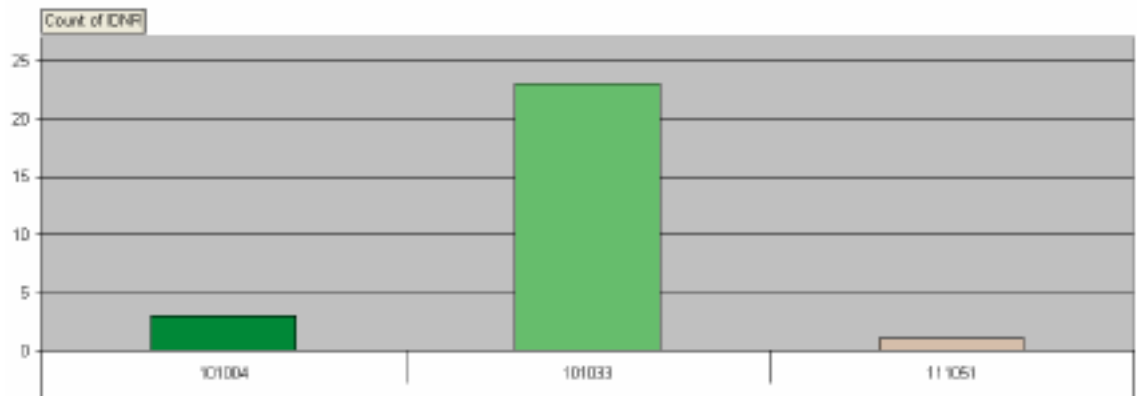
Rock domain 1
 Number of outcrops composed solely of one rock type.
 Y-axis indicates total number of outcrops in the rock domain.



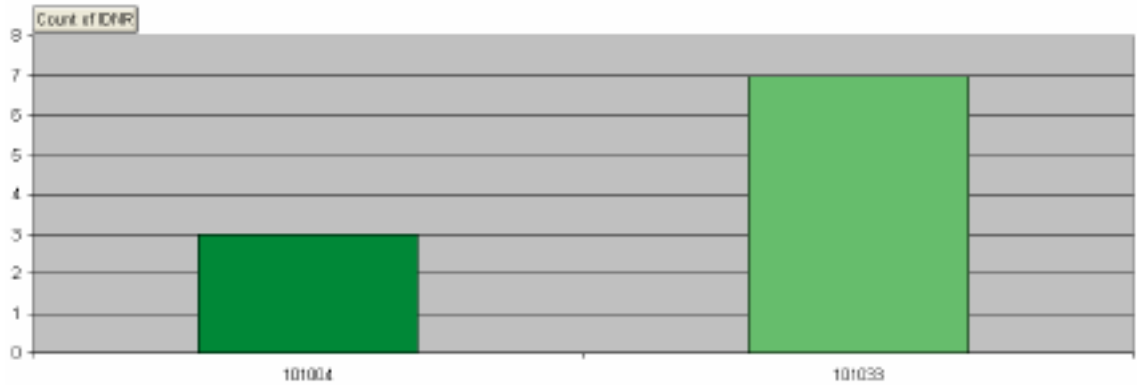
Rock domain 1
 Number of occurrences of each rock type. [N = 34]



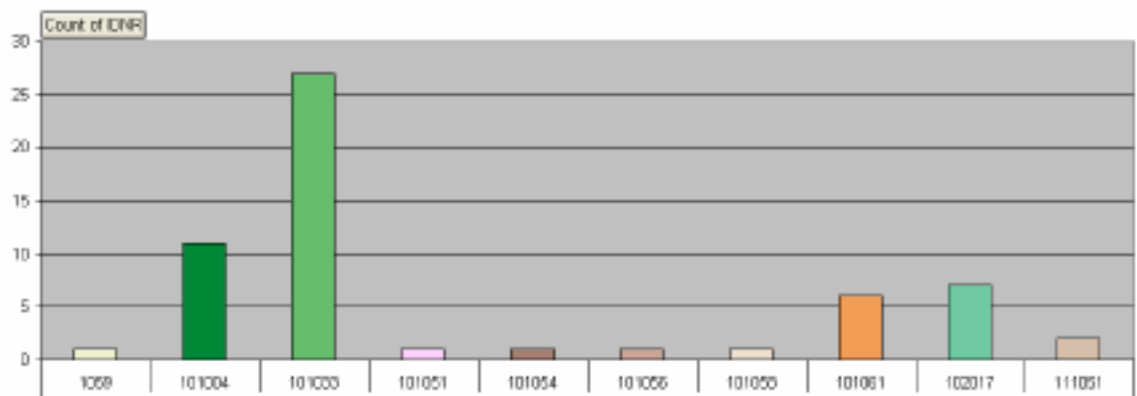
Rock domain 2
 Number of outcrops where each rock type is dominating.
 Y-axis indicates total number of outcrops in the rock domain. [N = 27]



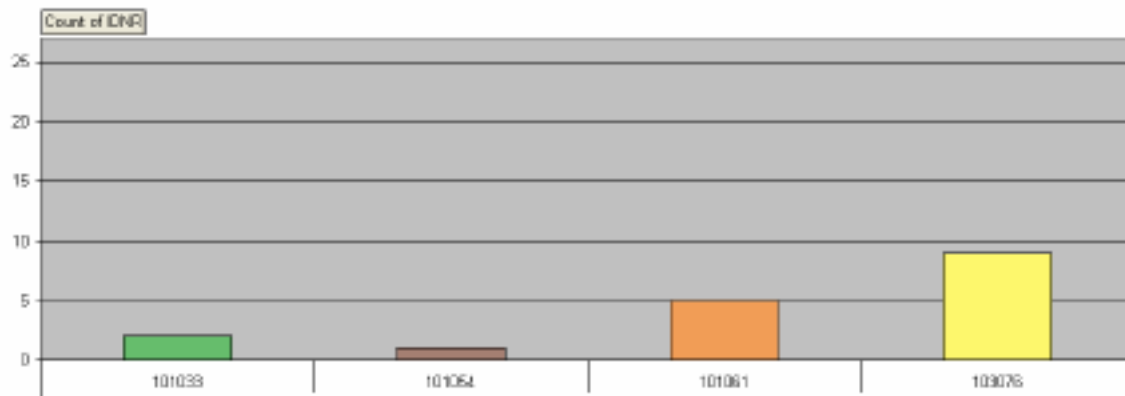
Rock domain 2
 Number of outcrops composed solely of one rock type.
 Y-axis indicates total number of outcrops in the rock domain.



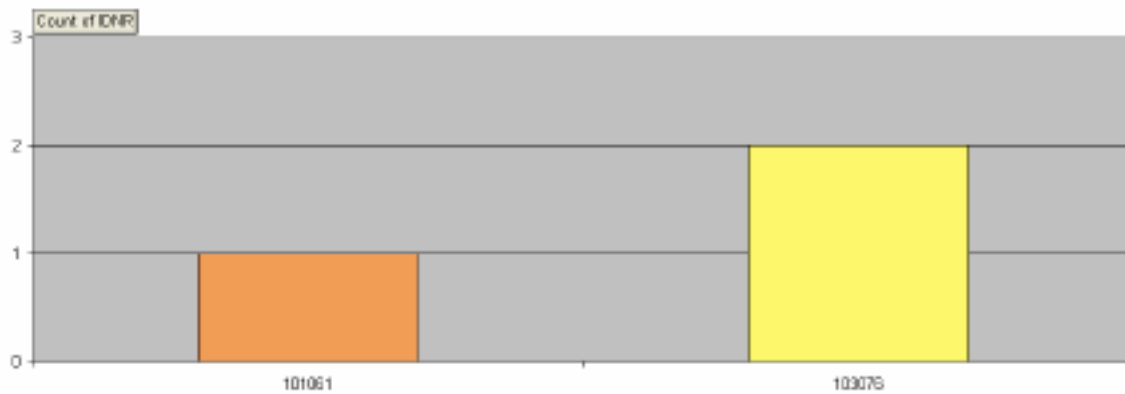
Rock domain 2
 Number of occurrences of each rock type [N = 56]



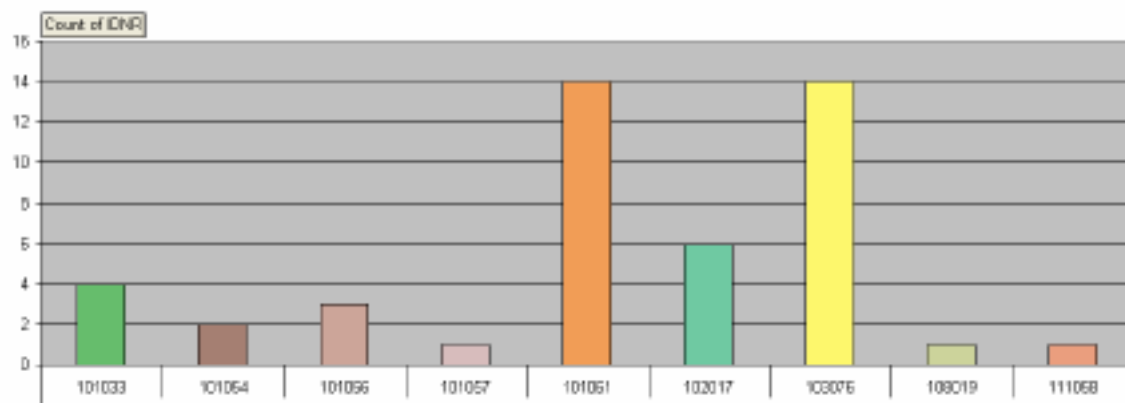
Rock domain 3
 Number of outcrops where each rock type is dominating.
 Y-axis indicates total number of outcrops in the rock domain. [N = 17]



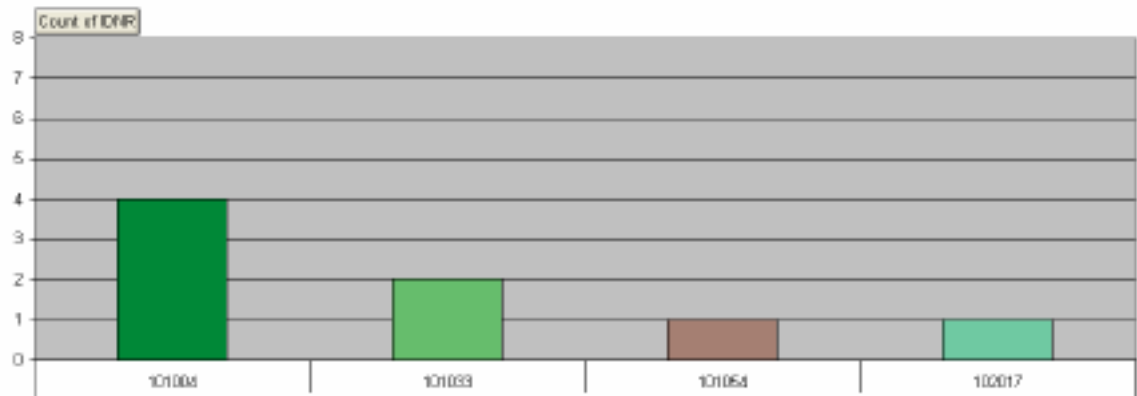
Rock domain 3
 Number of outcrops composed solely of one rock type.
 Y-axis indicates total number of outcrops in the rock domain.



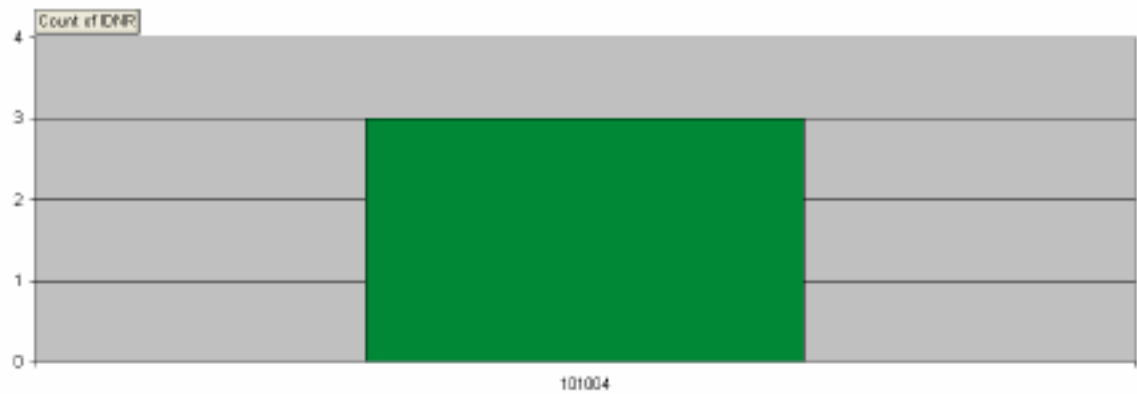
Rock domain 3
 Number of occurrences of each rock type [N = 46]



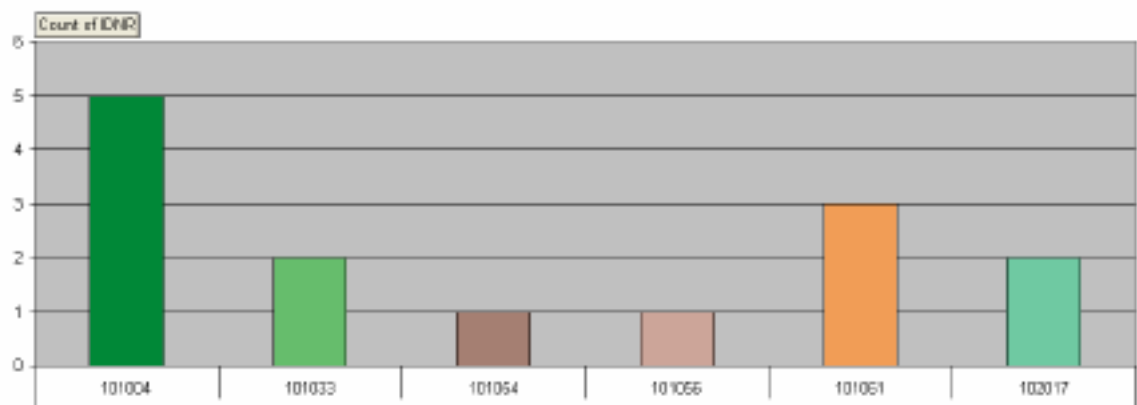
Rock domain 4
 Number of outcrops where each rock type is dominating.
 Y-axis indicates total number of outcrops in the rock domain. [N = 8]



Rock domain 4
 Number of outcrops composed solely of one rock type.
 Y-axis indicates total number of outcrops in the rock domain.

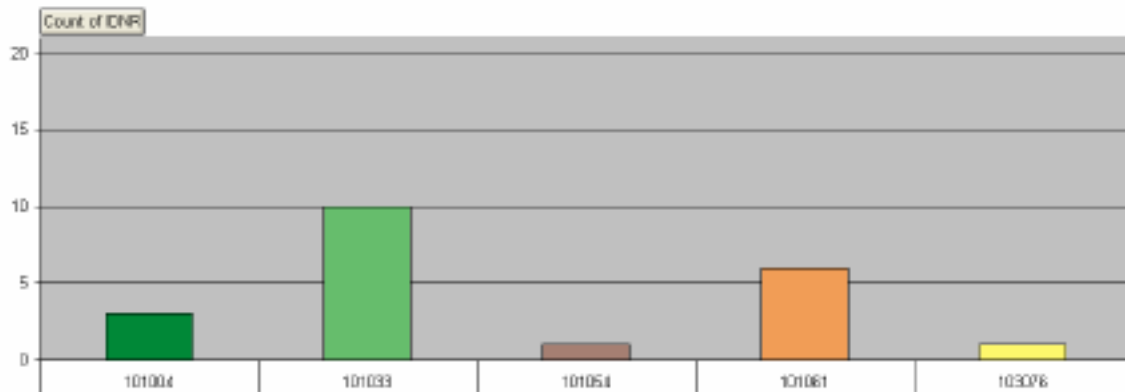


Rock domain 4
 Number of occurrences of each rock type [N = 14]



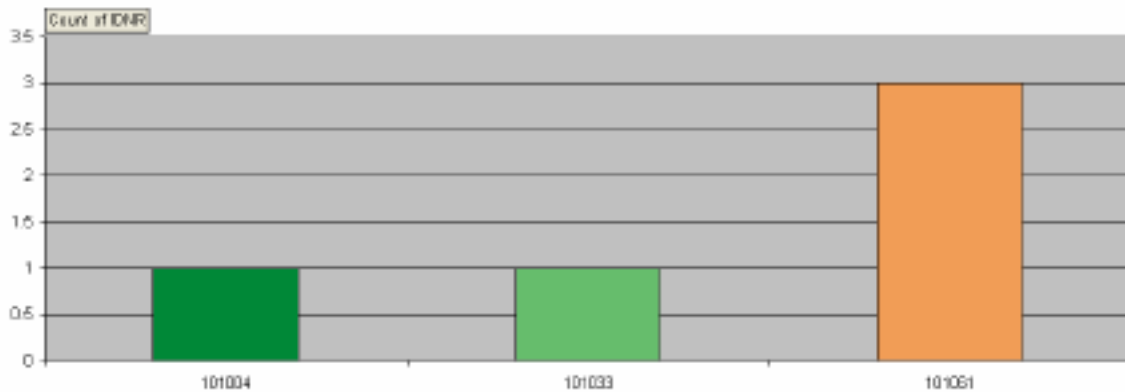
Rock domain 5

Number of outcrops where each rock type is dominating.
 Y-axis indicates total number of outcrops in the rock domain. [N = 21]



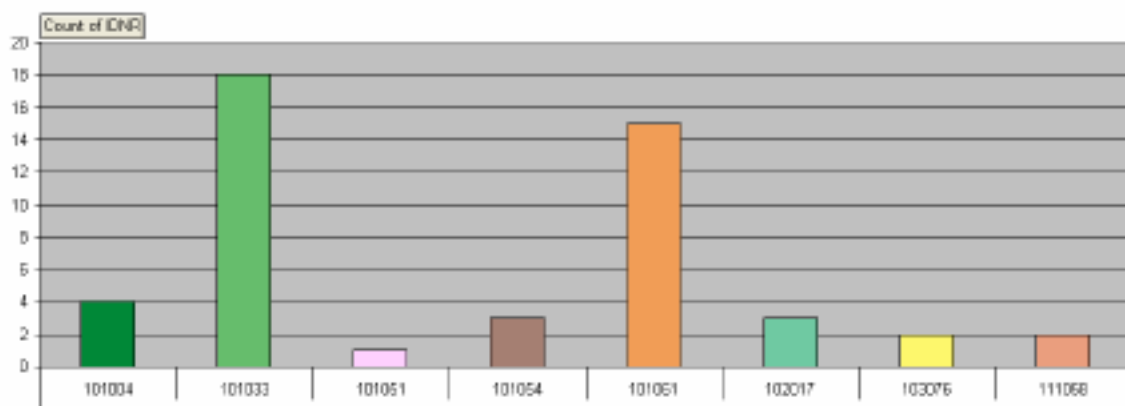
Rock domain 5

Number of outcrops composed solely of one rock type.
 Y-axis indicates total number of outcrops in the rock domain.

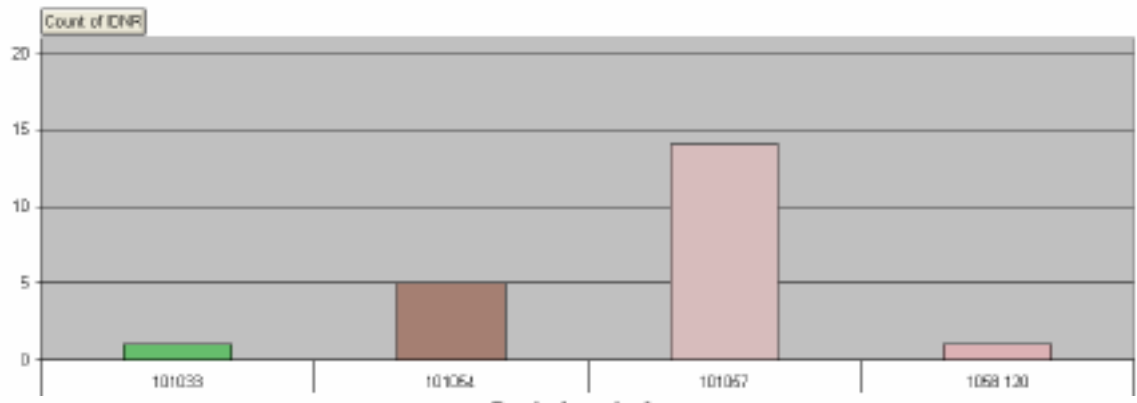


Rock domain 5

Number of occurrences of each rock type [N = 48]



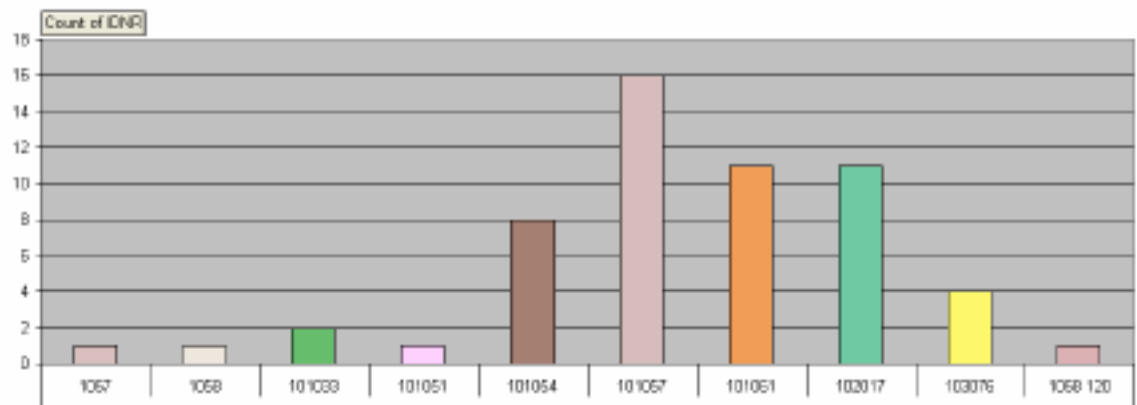
Rock domain 6
 Number of outcrops where each rock type is dominating.
 Y-axis indicates total number of outcrops in the rock domain. [N = 21]



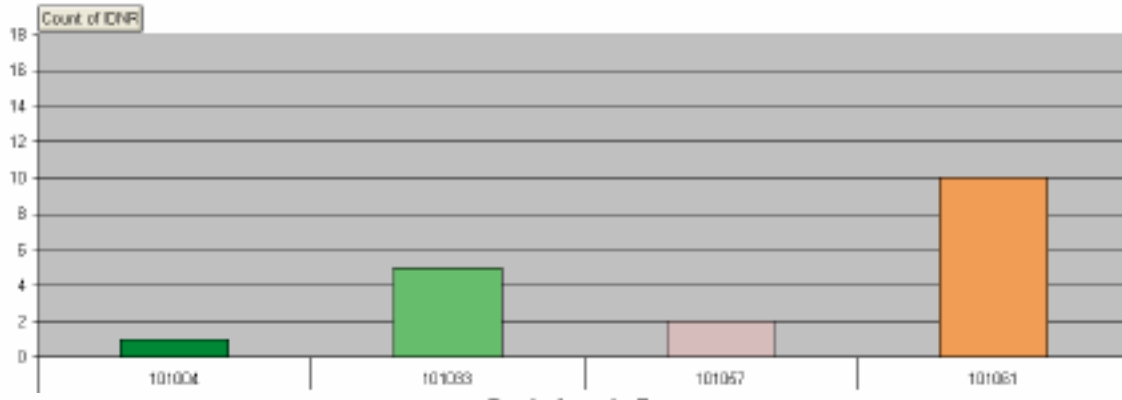
Rock domain 6
 Number of outcrops composed solely of one rock type.
 Y-axis indicates total number of outcrops in the rock domain.



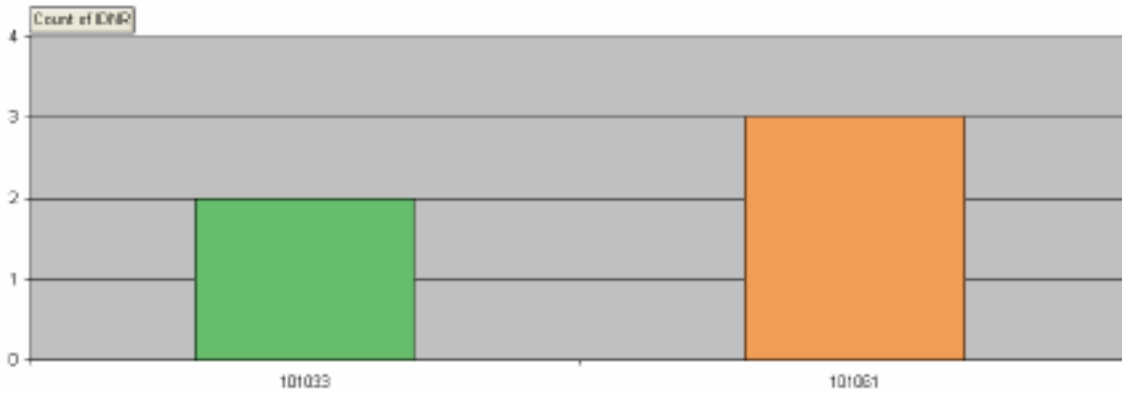
Rock domain 6
 Number of occurrences of each rock type [N = 56]



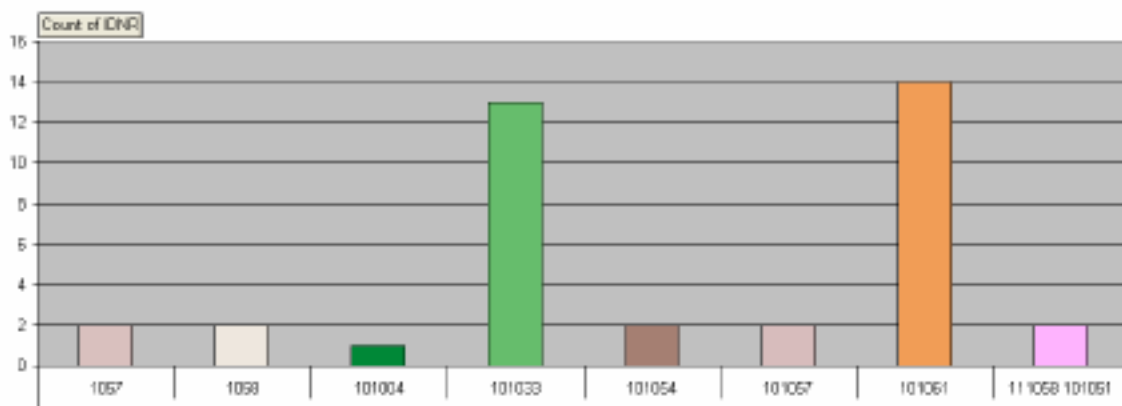
Rock domain 7
 Number of outcrops where each rock type is dominating.
 Y-axis indicates total number of outcrops in the rock domain. [N = 18]



Rock domain 7
 Number of outcrops composed solely of one rock type.
 Y-axis indicates total number of outcrops in the rock domain.

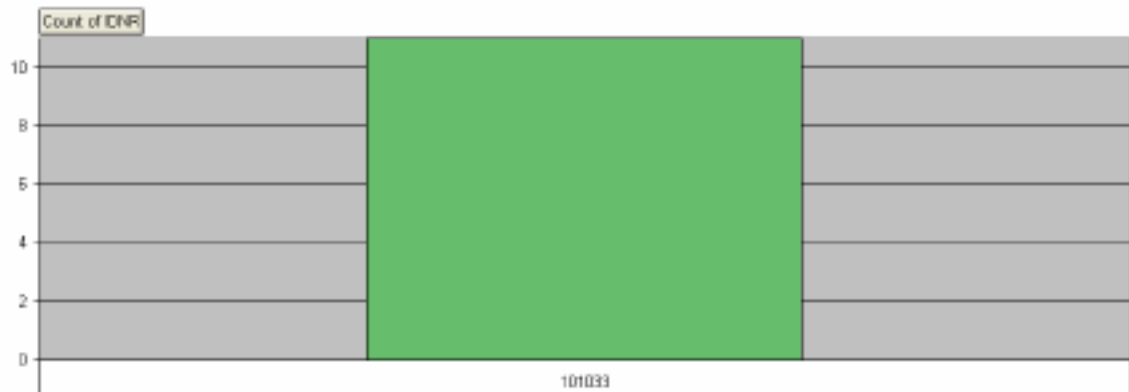


Rock domain 7
 Number of occurrences of each rock type [N = 38]



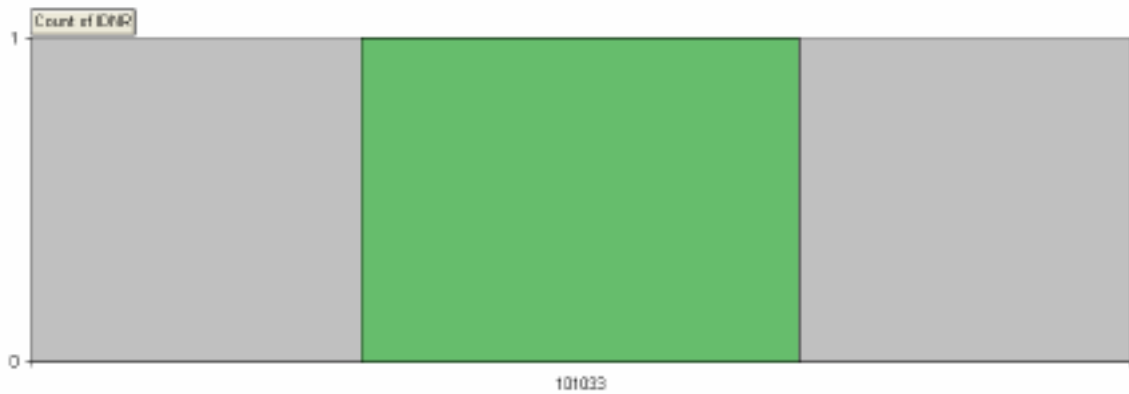
Rock domain 8

Number of outcrops where each rock type is dominating.
Y-axis indicates total number of outcrops in the rock domain. [N = 11]



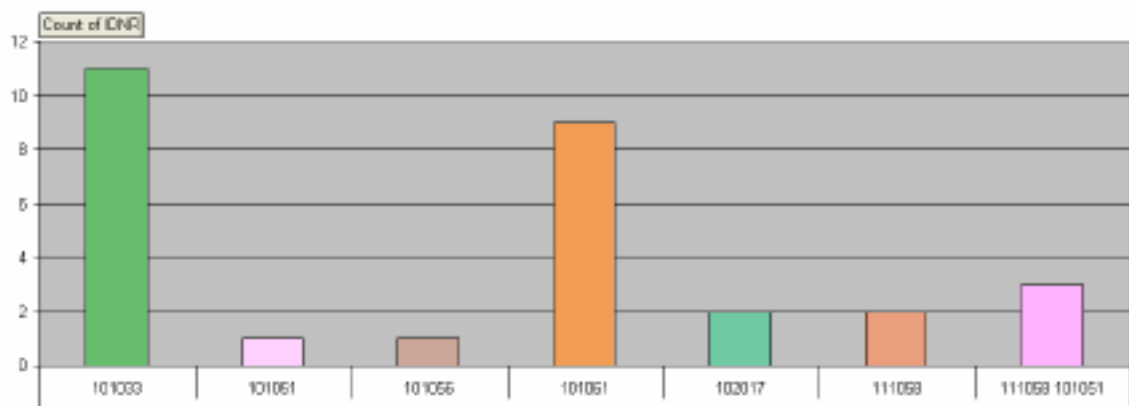
Rock domain 8

Number of outcrops composed solely of one rock type.
Y-axis indicates total number of outcrops in the rock domain.

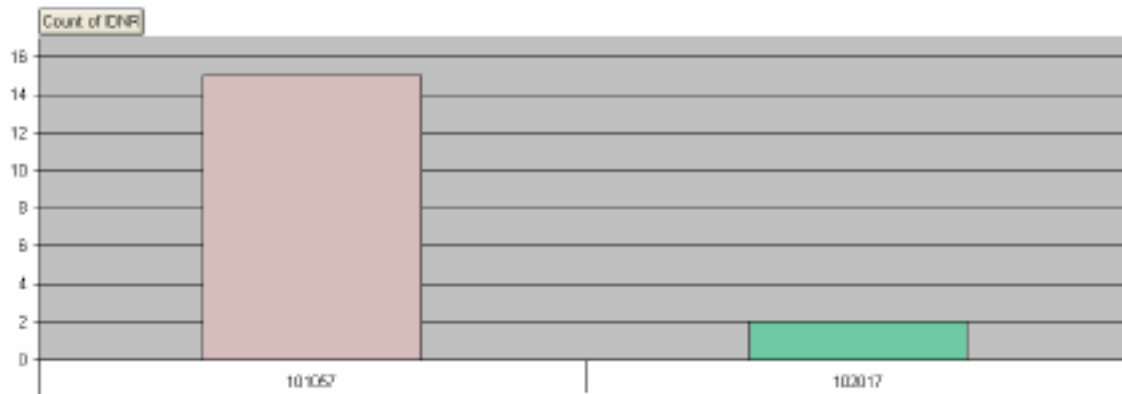


Rock domain 8

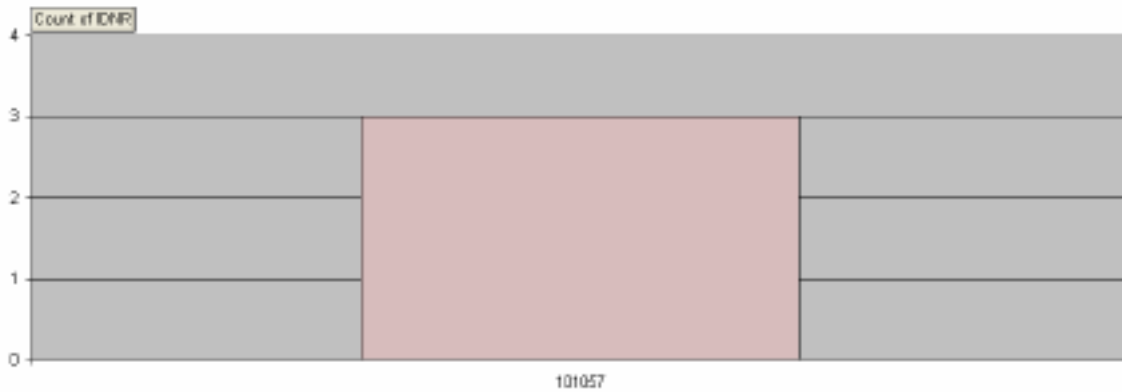
Number of occurrences of each rock type [N = 29]



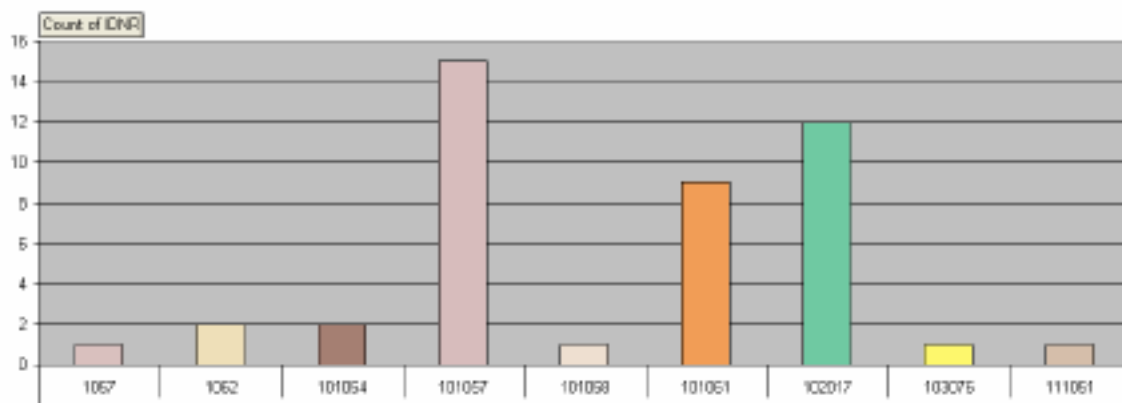
Rock domain 11
 Number of outcrops where each rock type is dominating.
 Y-axis indicates total number of outcrops in the rock domain. [N = 17]



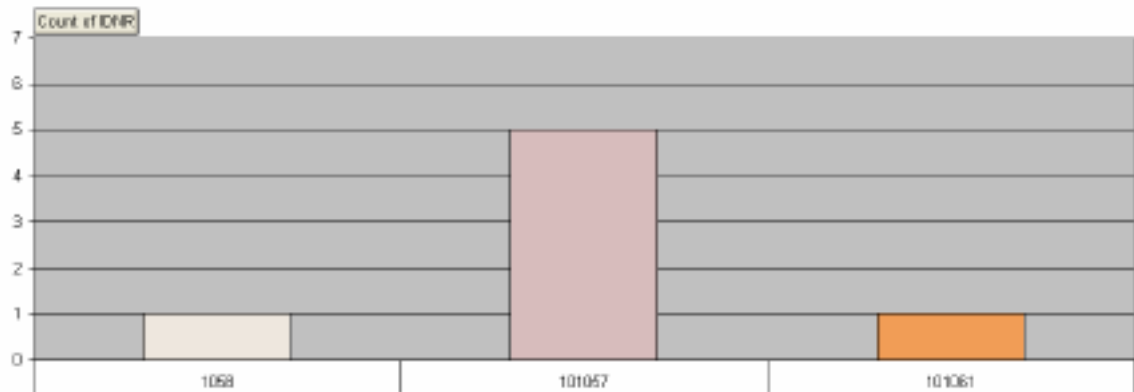
Rock domain 11
 Number of outcrops composed solely of one rock type.
 Y-axis indicates total number of outcrops in the rock domain.



Rock domain 11
 Number of occurrences of each rock type [N = 44]



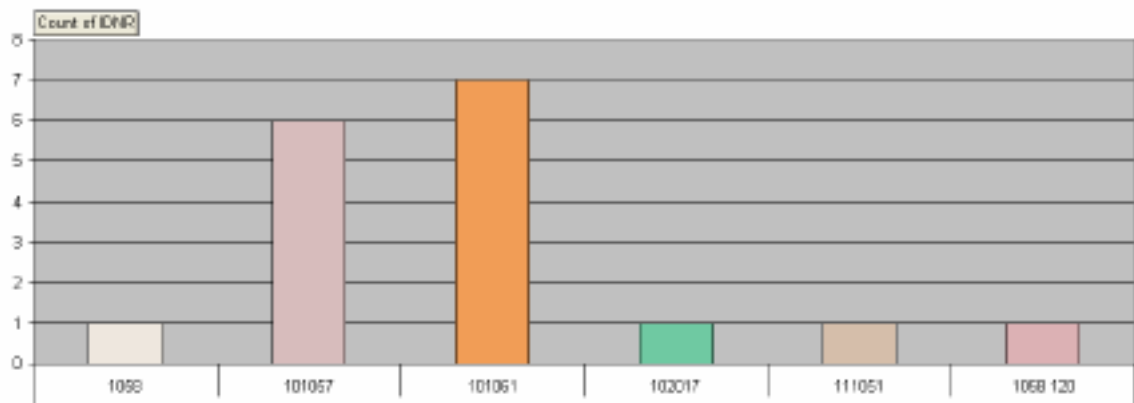
Rock domain 12
 Number of outcrops where each rock type is dominating.
 Y-axis indicates total number of outcrops in the rock domain. [N = 7]



Rock domain 12
 Number of outcrops composed solely of one rock type.
 Y-axis indicates total number of outcrops in the rock domain.

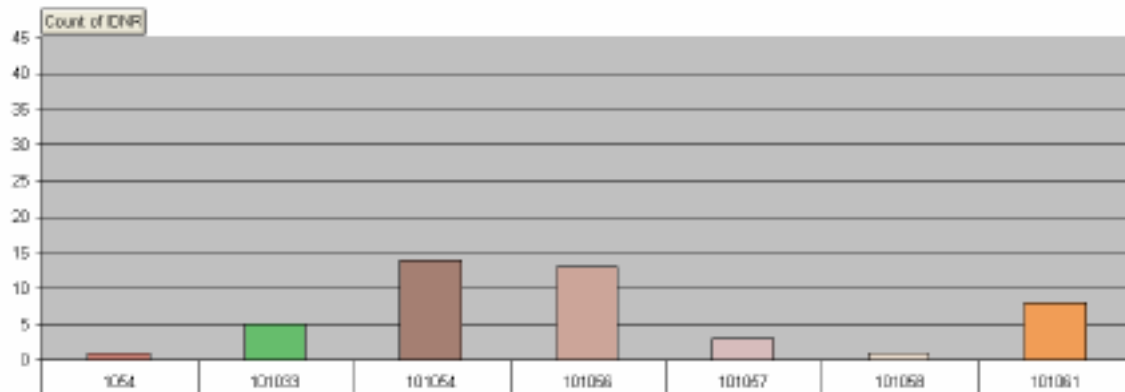


Rock domain 12
 Number of occurrences of each rock type [N = 17]



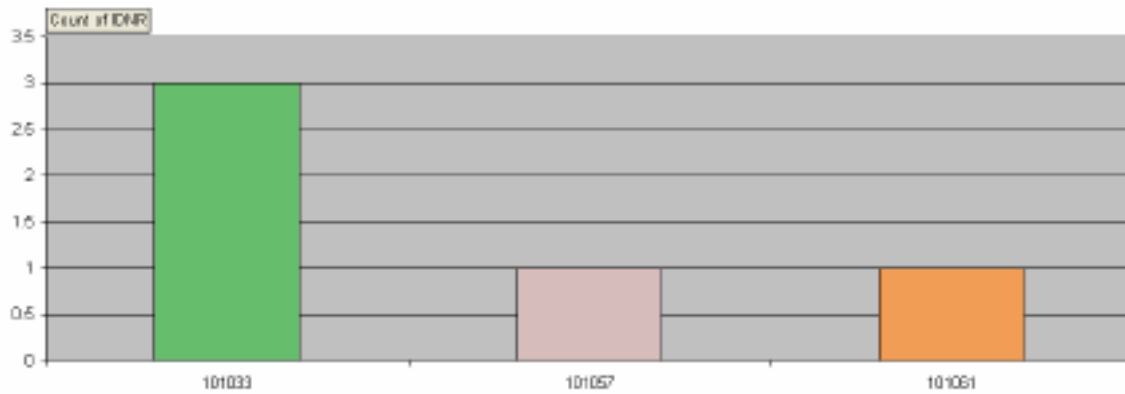
Rock domain 13

Number of outcrops where each rock type is dominating.
Y-axis indicates total number of outcrops in the rock domain. [N = 45]



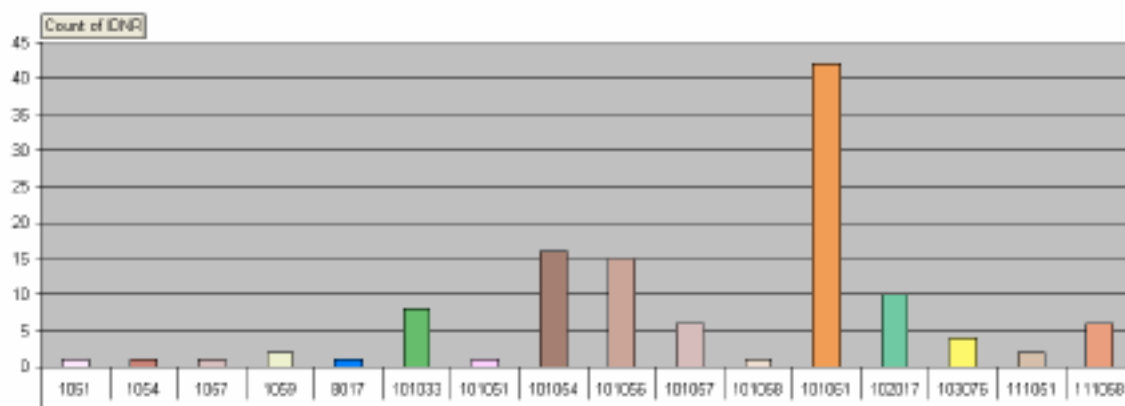
Rock domain 13

Number of outcrops composed solely of one rock type.
Y-axis indicates total number of outcrops in the rock domain.

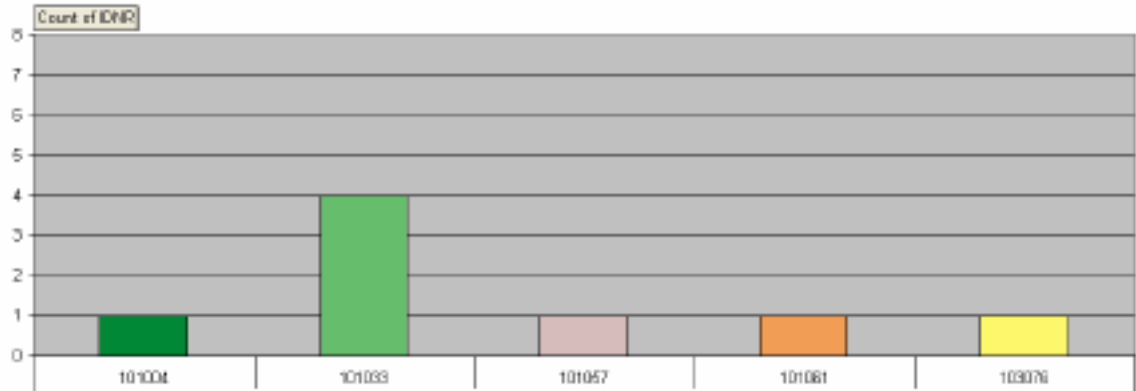


Rock domain 13

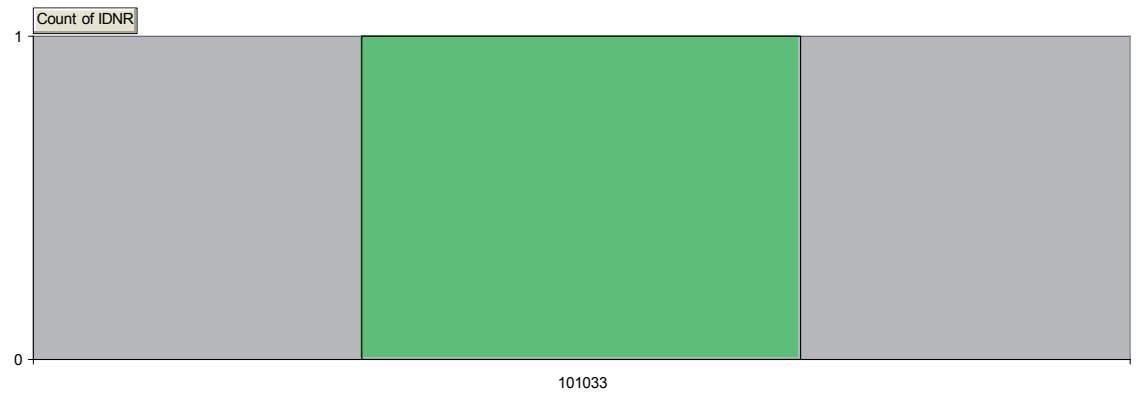
Number of occurrences of each rock type [N = 117]



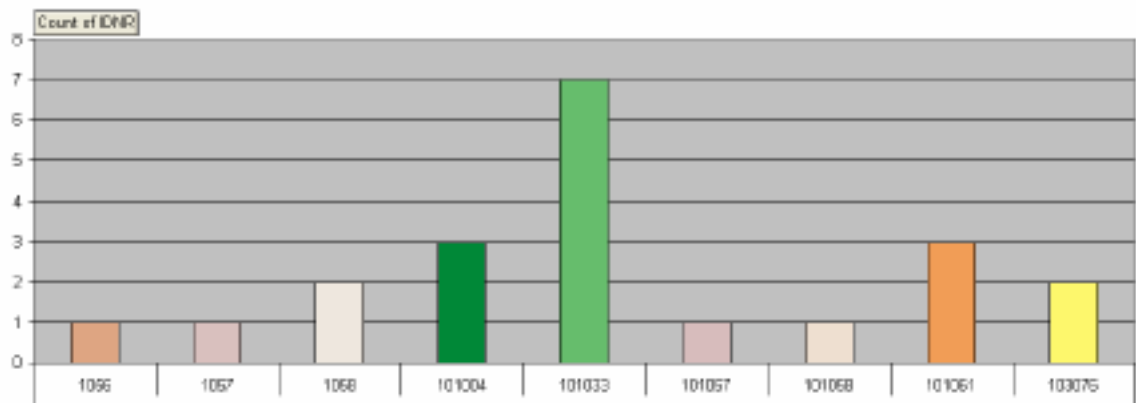
Rock domain 14
 Number of outcrops where each rock type is dominating.
 Y-axis indicates total number of outcrops in the rock domain. [N = 8]



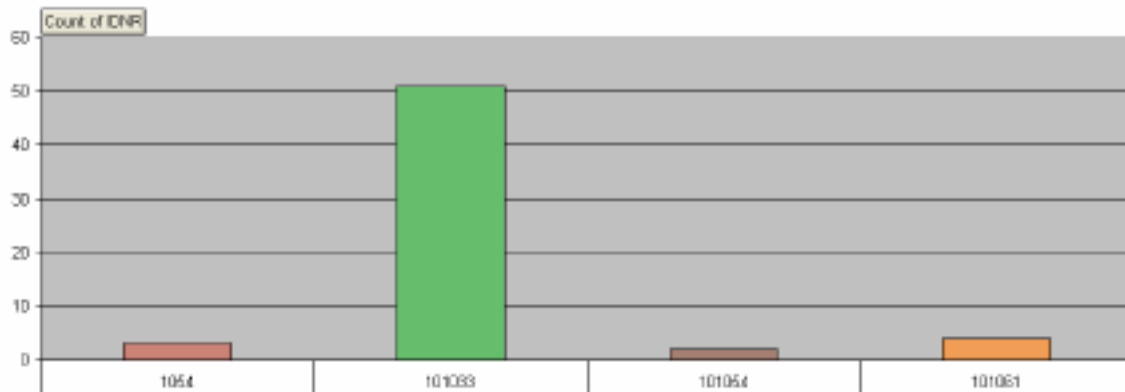
Rock domain 14
 Number of outcrops composed solely of one rock type.
 Y-axis indicates total number of outcrops in the rock domain.



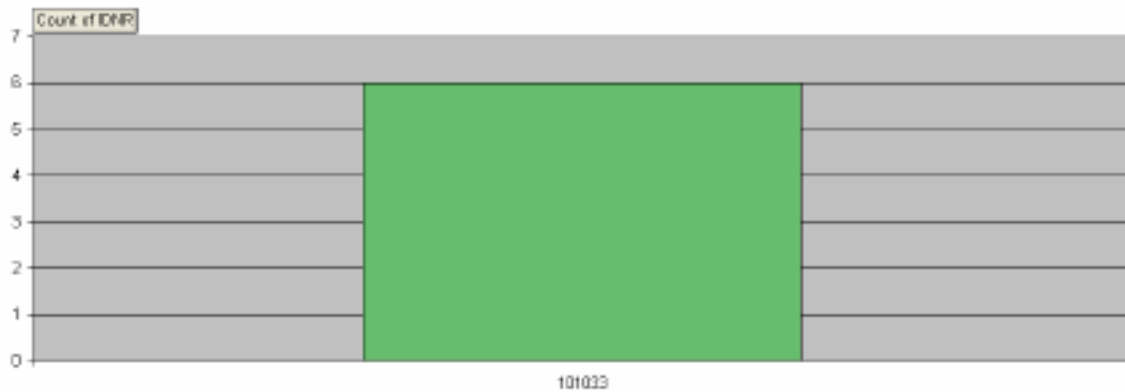
Rock domain 14
 Number of occurrences of each rock type [N = 21]



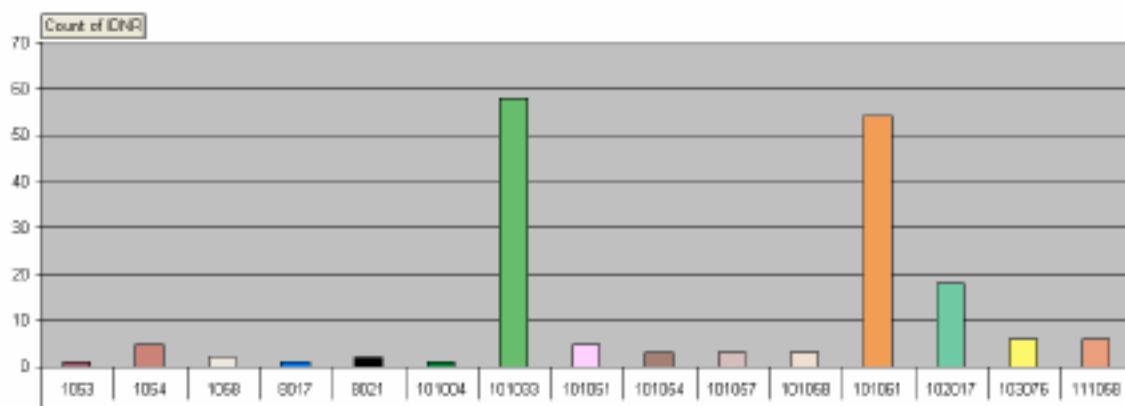
Rock domain 16
 Number of outcrops where each rock type is dominating.
 Y-axis indicates total number of outcrops in the rock domain. [N = 60]



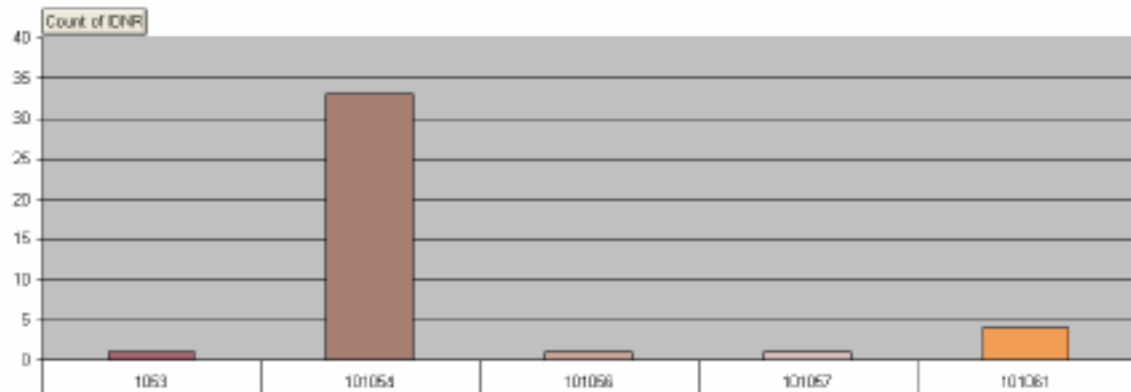
Rock domain 16
 Number of outcrops composed solely of one rock type.
 Y-axis indicates total number of outcrops in the rock domain.



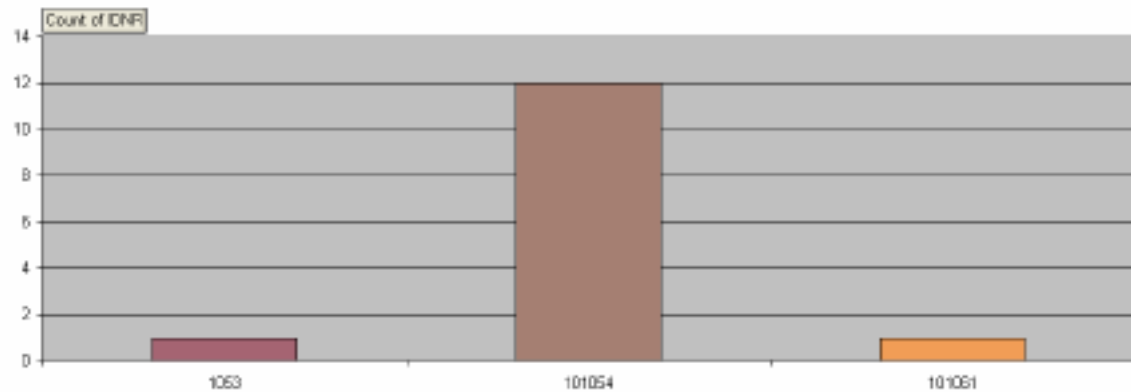
Rock domain 16
 Number of occurrences of each rock type [N = 168]



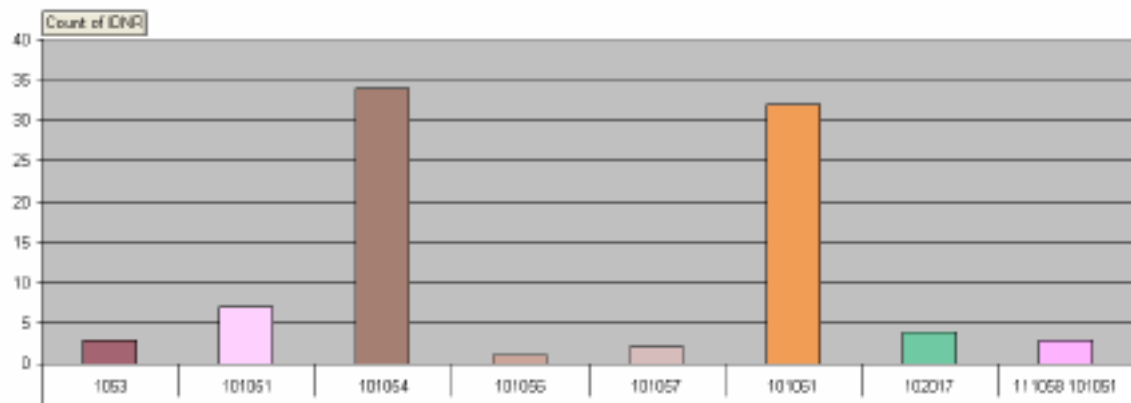
Rock domain 17
 Number of outcrops where each rock type is dominating.
 Y-axis indicates total number of outcrops in the rock domain. [N = 40]



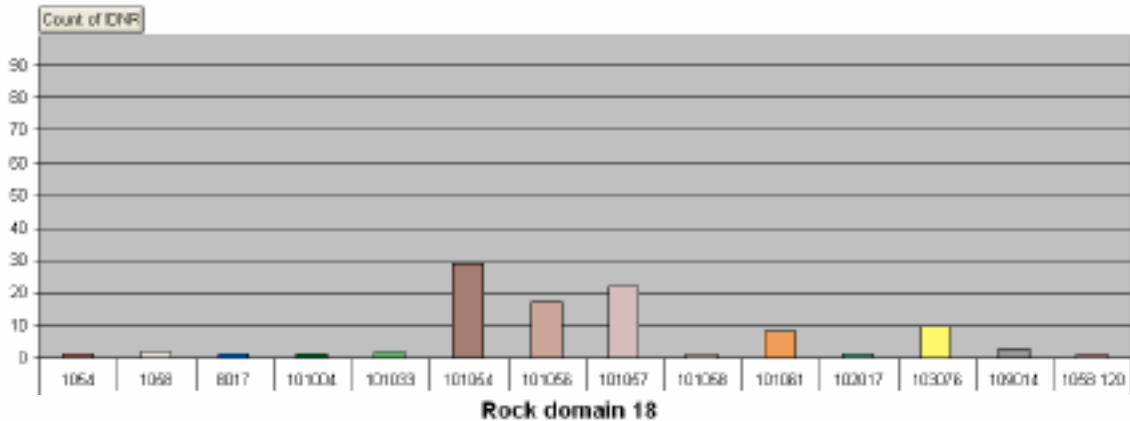
Rock domain 17
 Number of outcrops composed solely of one rock type.
 Y-axis indicates total number of outcrops in the rock domain.



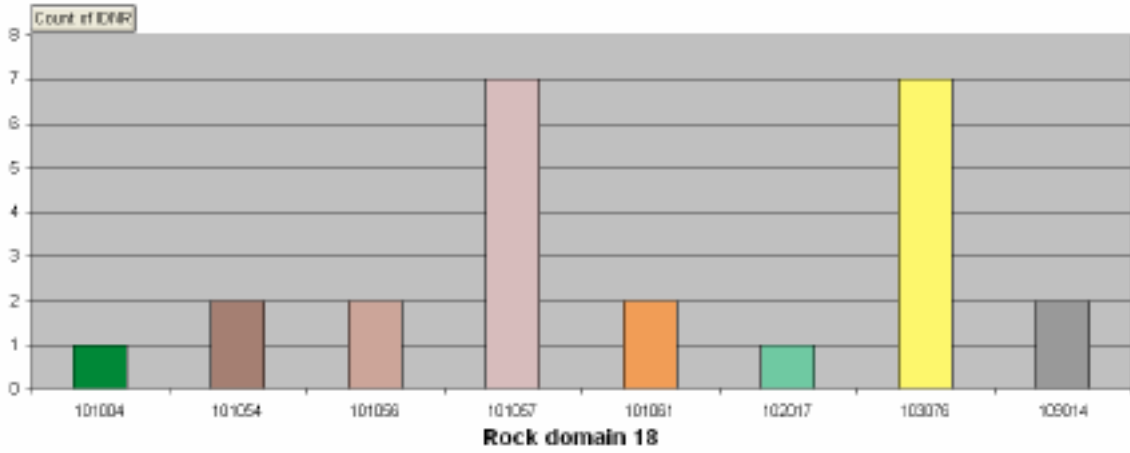
Rock domain 17
 Number of occurrences of each rock type [N = 86]



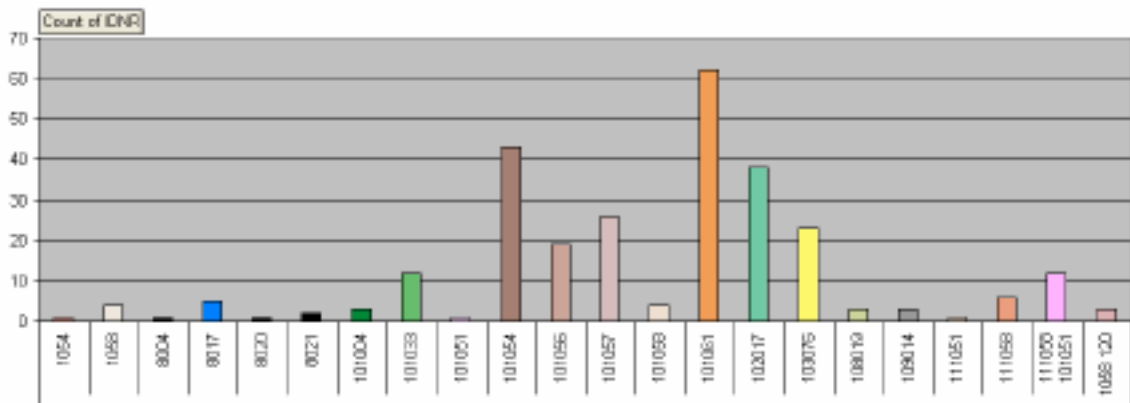
Rock domain 18
 Number of outcrops where each rock type is dominating.
 Y-axis indicates total number of outcrops in the rock domain. [N = 99]



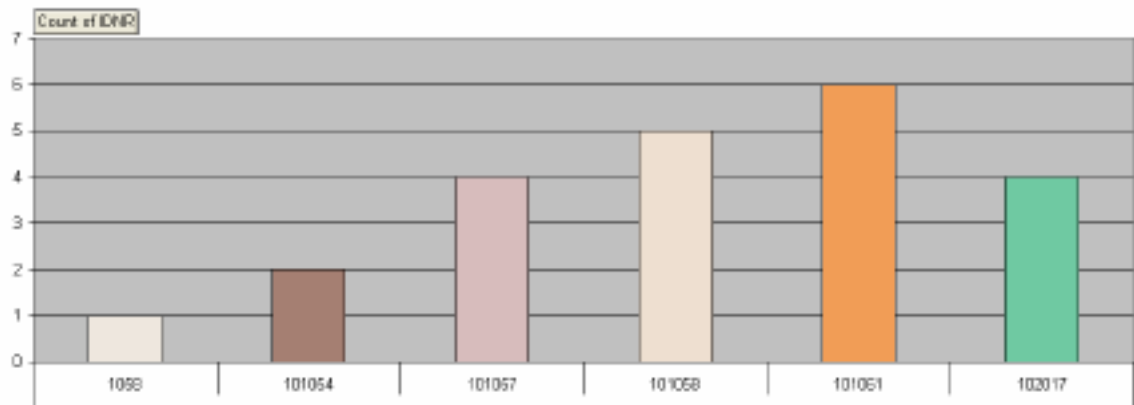
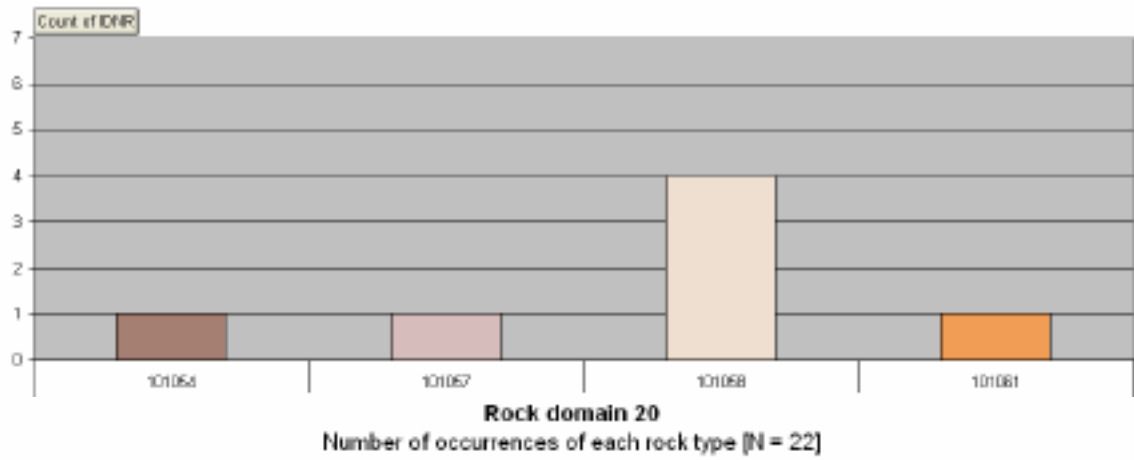
Rock domain 18
 Number of outcrops composed solely of one rock type.
 Y-axis indicates total number of outcrops in the rock domain.



Rock domain 18
 Number of occurrences of each rock type [N = 273]



Rock domain 20
 Number of outcrops where each rock type is dominating.
 Y-axis indicates total number of outcrops in the rock domain. [N = 7]



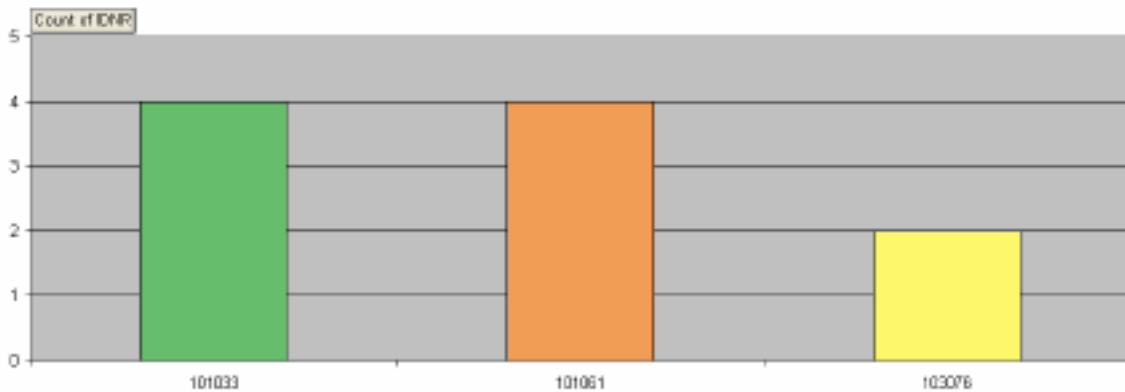
Rock domain 21

Number of outcrops where each rock type is dominating.
 Y-axis indicates total number of outcrops in the rock domain. [N = 98]



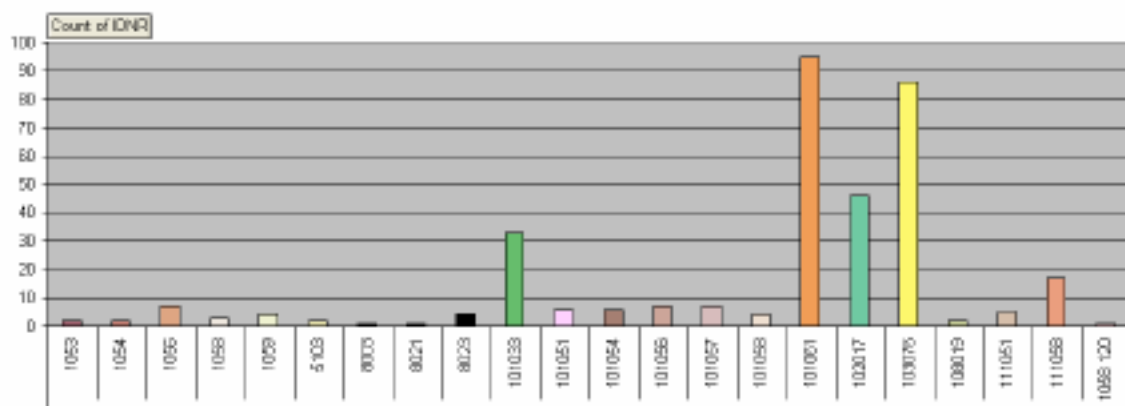
Rock domain 21

Number of outcrops composed solely of one rock type.
 Y-axis indicates total number of outcrops in the rock domain.



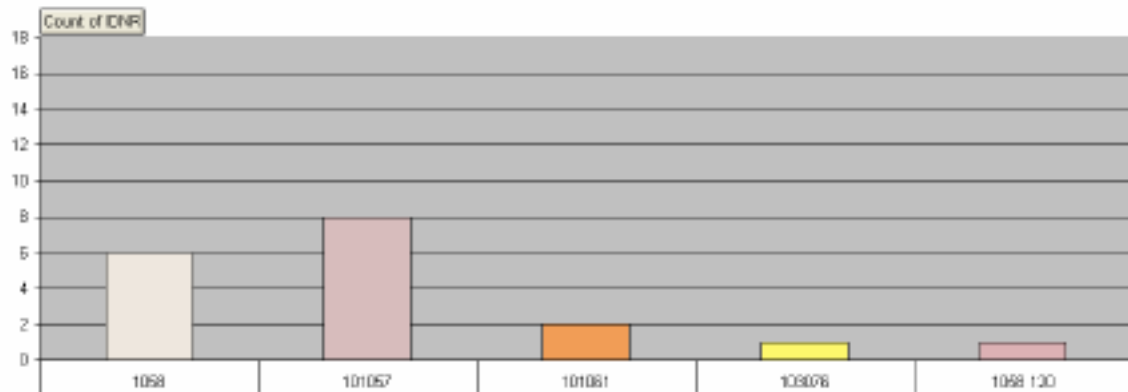
Rock domain 21

Number of occurrences of each rock type [N = 341]



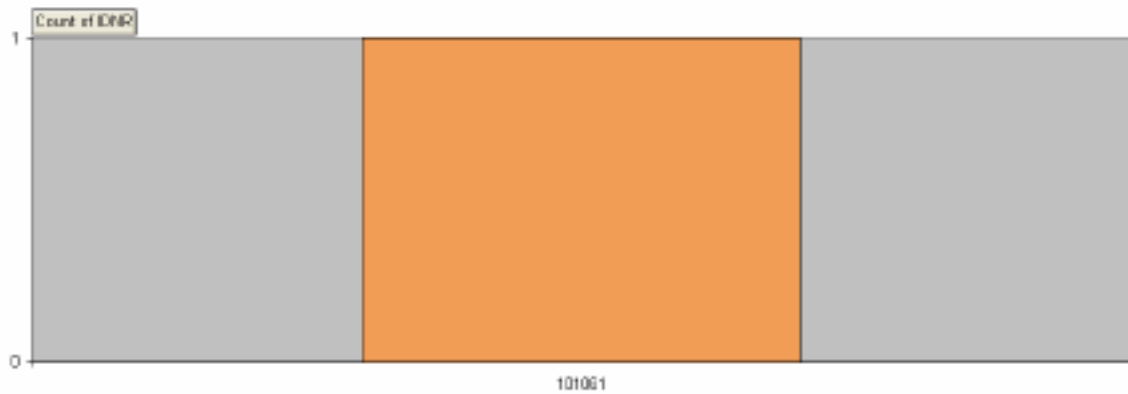
Rock domain 22

Number of outcrops where each rock type is dominating.
Y-axis indicates total number of outcrops in the rock domain. [N = 18]



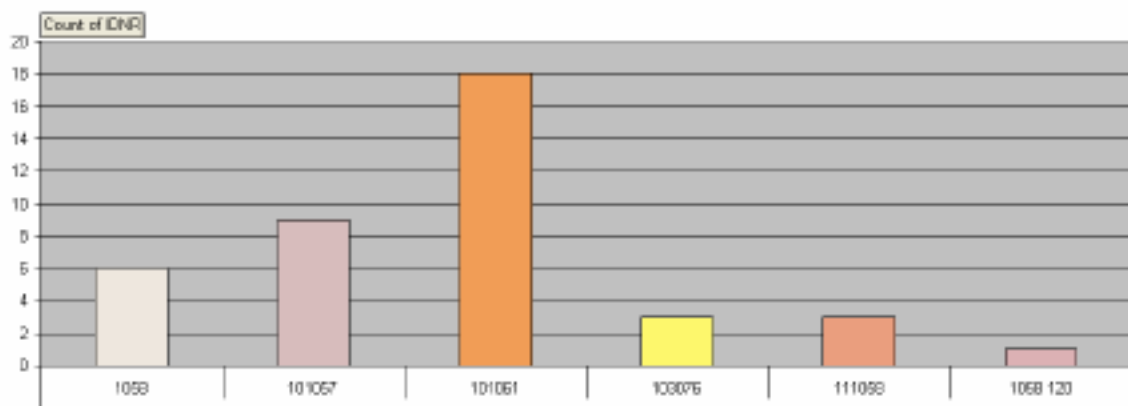
Rock domain 22

Number of outcrops composed solely of one rock type.
Y-axis indicates total number of outcrops in the rock domain.



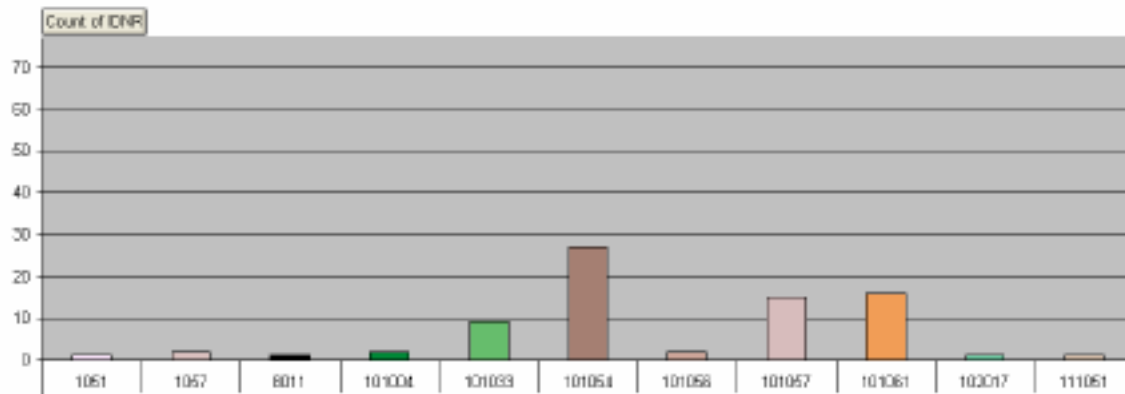
Rock domain 22

Number of occurrences of each rock type [N = 40]



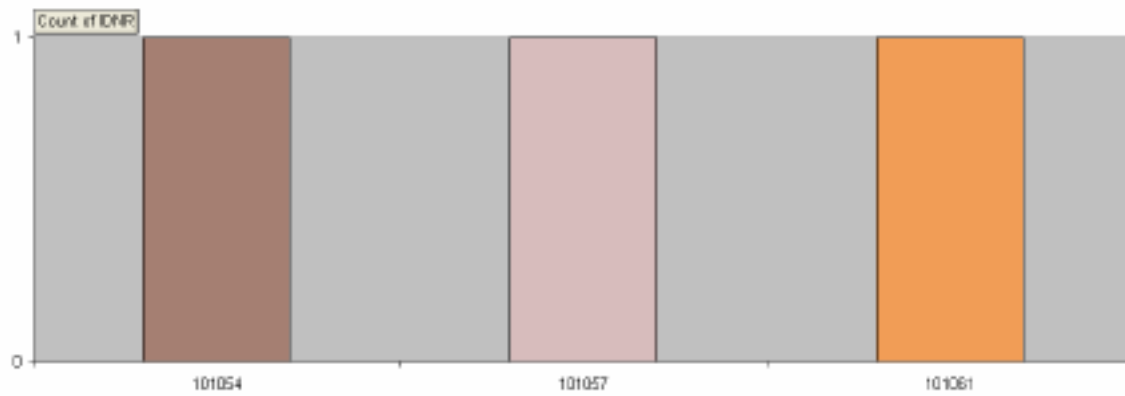
Rock domain 23

Number of outcrops where each rock type is dominating.
Y-axis indicates total number of outcrops in the rock domain. [N = 77]



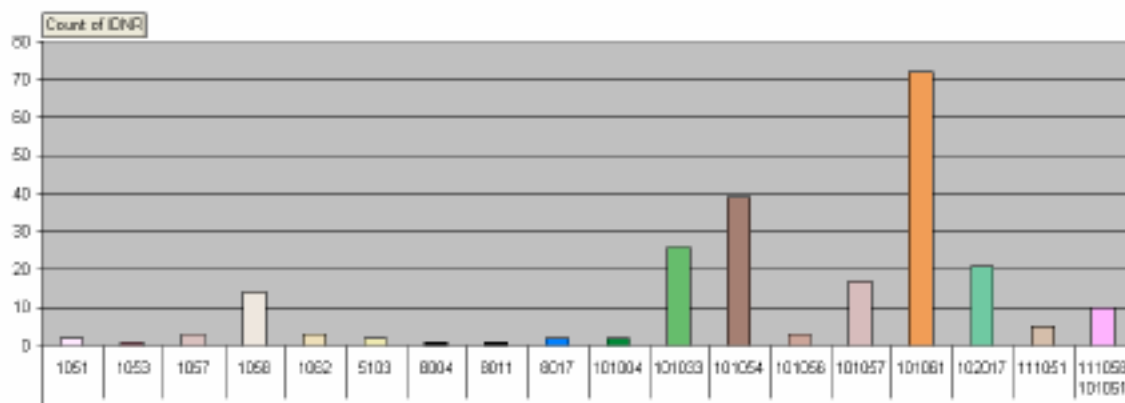
Rock domain 23

Number of outcrops composed solely of one rock type.
Y-axis indicates total number of outcrops in the rock domain.

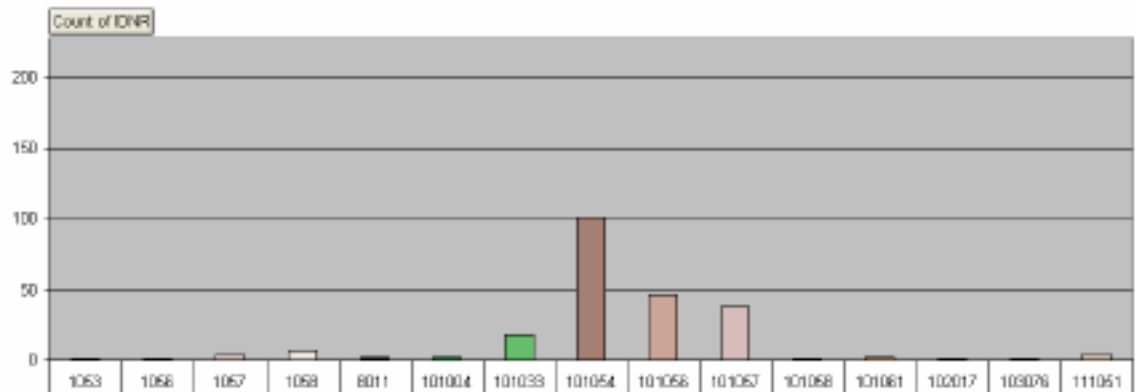


Rock domain 23

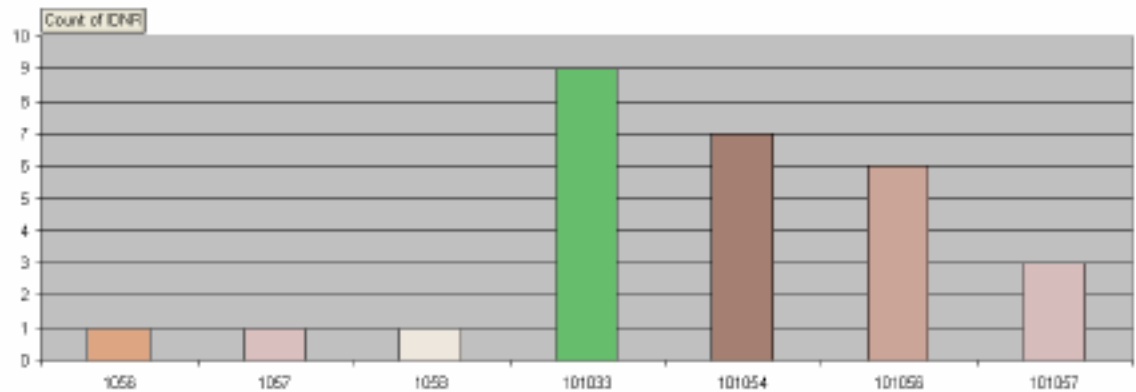
Number of occurrences of each rock type [N = 224]



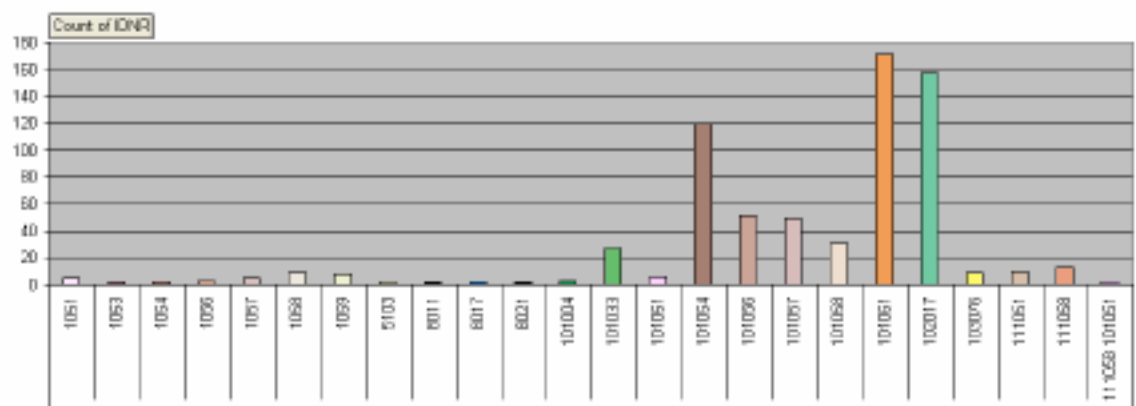
Rock domain 24
 Number of outcrops where each rock type is dominating.
 Y-axis indicates total number of outcrops in the rock domain. [N = 228]



Rock domain 24
 Number of outcrops composed solely of one rock type.
 Y-axis indicates total number of outcrops in the rock domain.

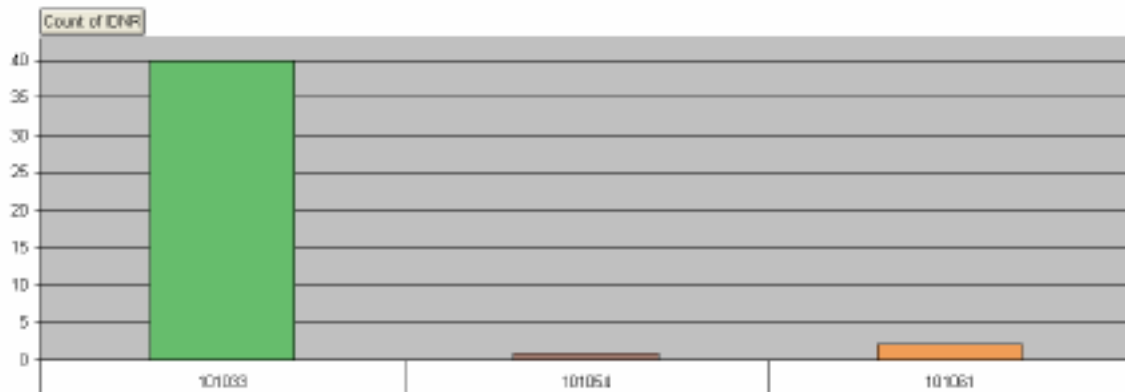


Rock domain 24
 Number of occurrences of each rock type [N = 691]



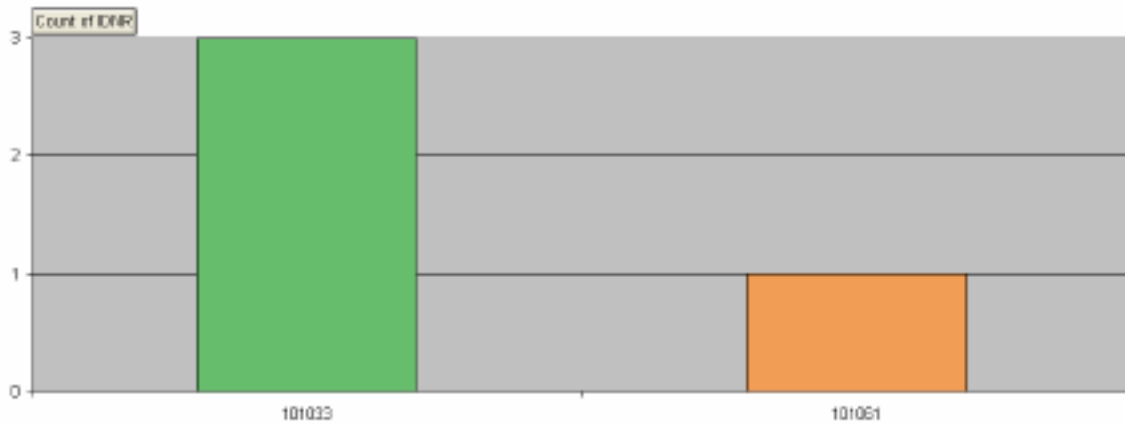
Rock domain 25

Number of outcrops where each rock type is dominating.
Y-axis indicates total number of outcrops in the rock domain. [N = 43]



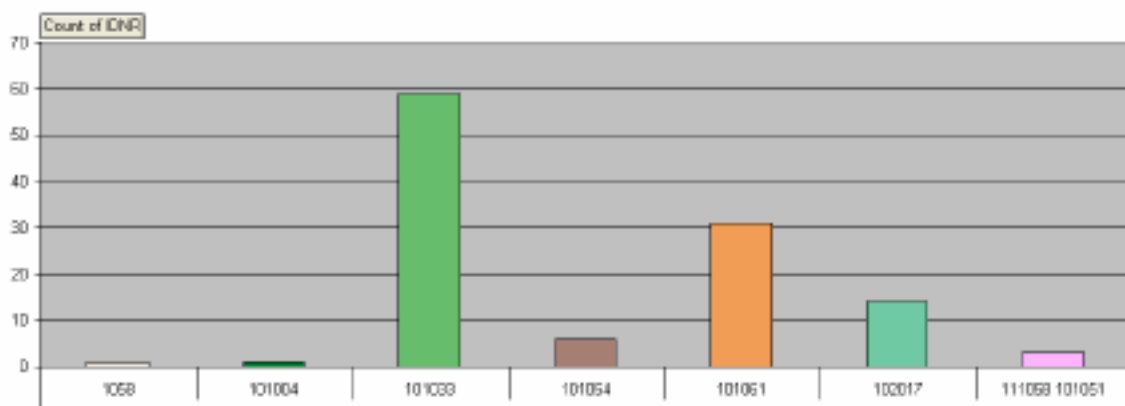
Rock domain 25

Number of outcrops composed solely of one rock type.
Y-axis indicates total number of outcrops in the rock domain.

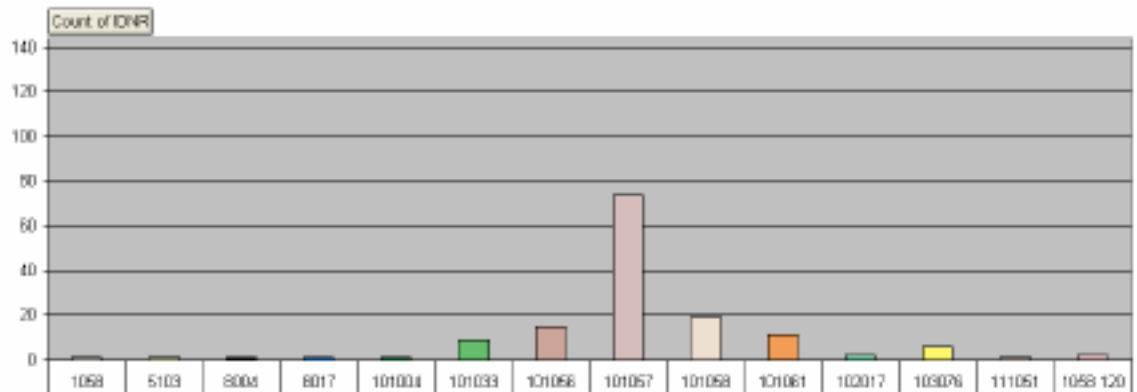


Rock domain 25

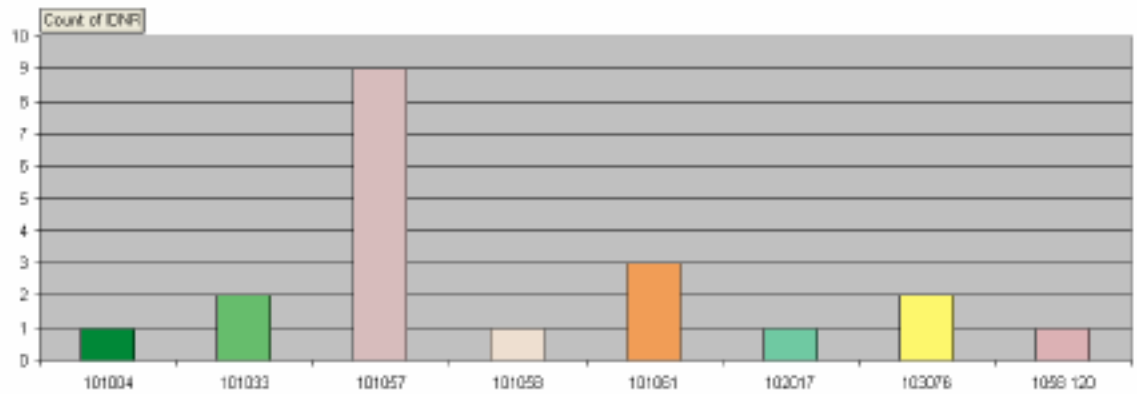
Number of occurrences of each rock type [N = 115]



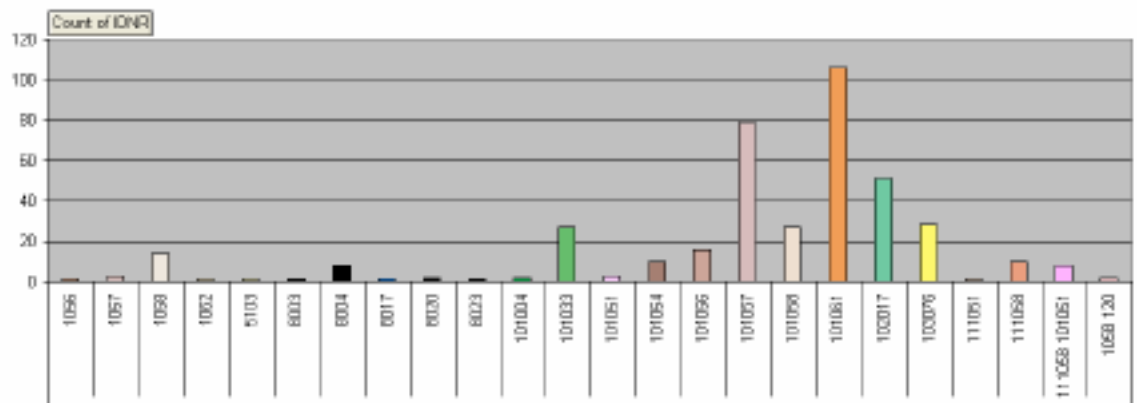
Rock domain 26
 Number of outcrops where each rock type is dominating.
 Y-axis indicates total number of outcrops in the rock domain. [N = 144]



Rock domain 26
 Number of outcrops composed solely of one rock type.
 Y-axis indicates total number of outcrops in the rock domain.

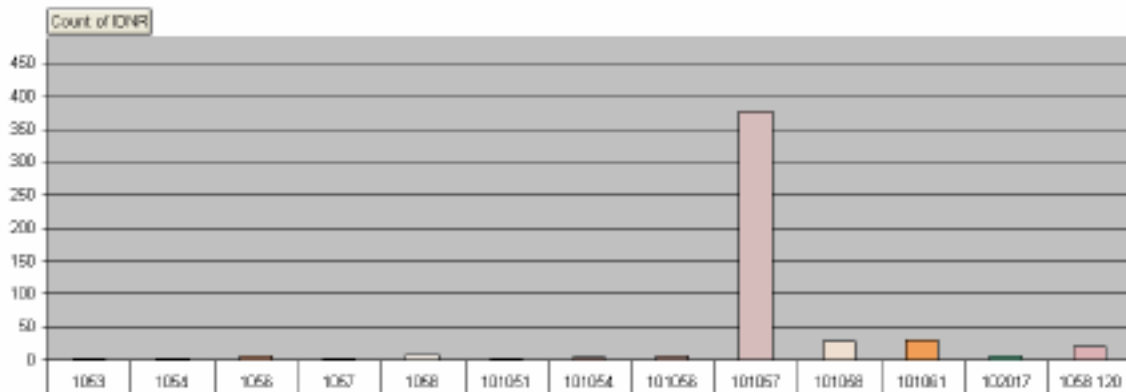


Rock domain 26
 Number of occurrences of each rock type [N = 403]



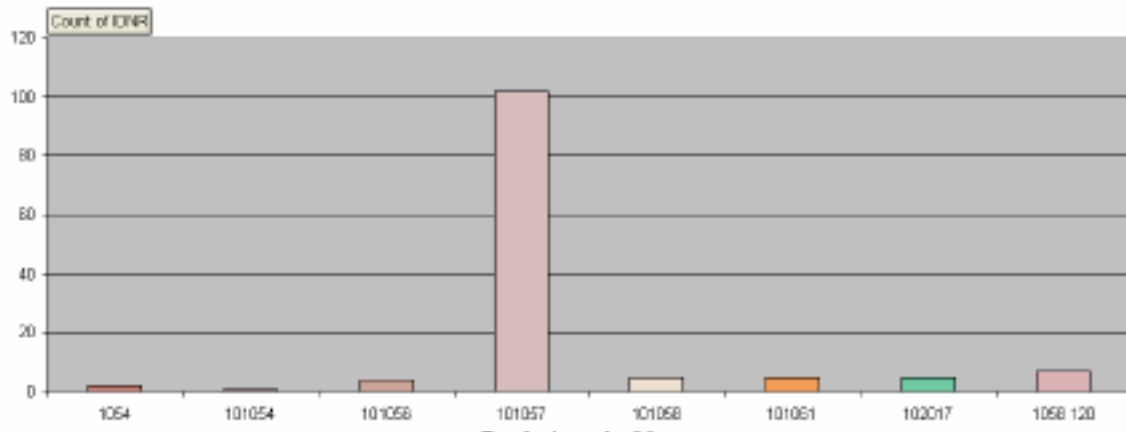
Rock domain 29

Number of outcrops where each rock type is dominating.
 Y-axis indicates total number of outcrops in the rock domain. [N = 488]



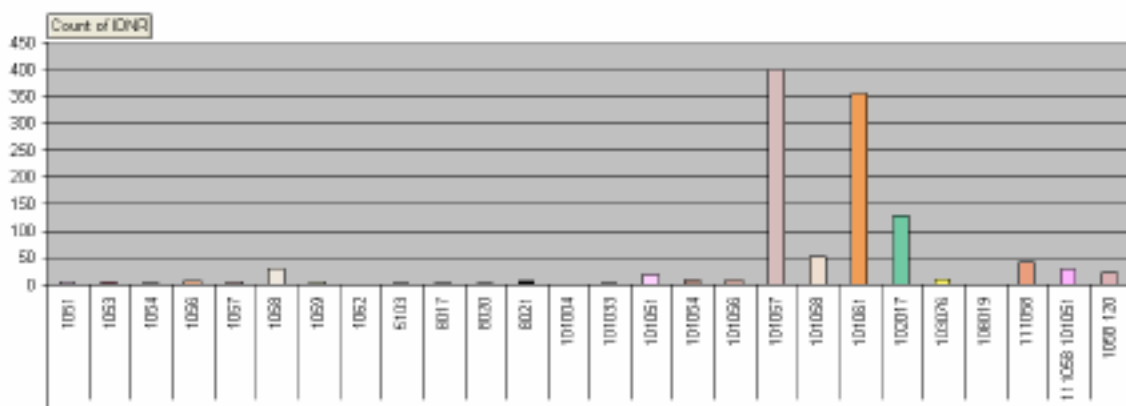
Rock domain 29

Number of outcrops composed solely of one rock type.
 Y-axis indicates total number of outcrops in the rock domain.

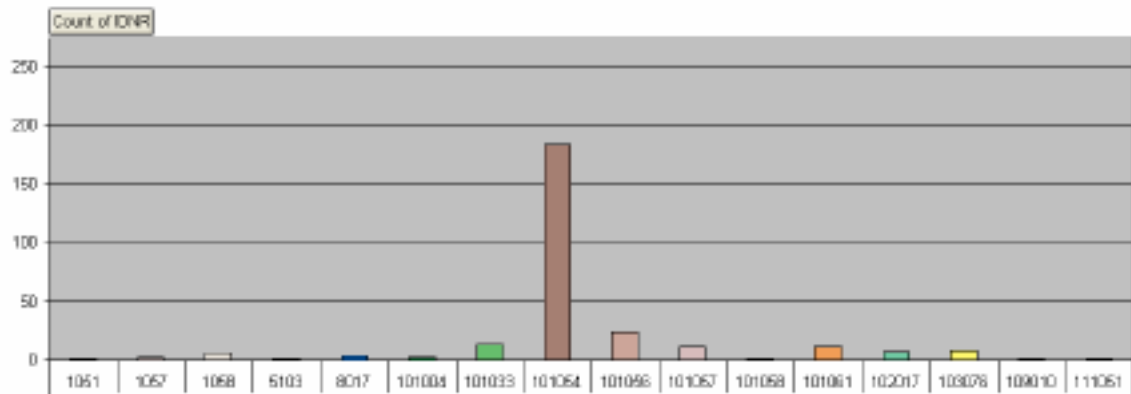


Rock domain 29

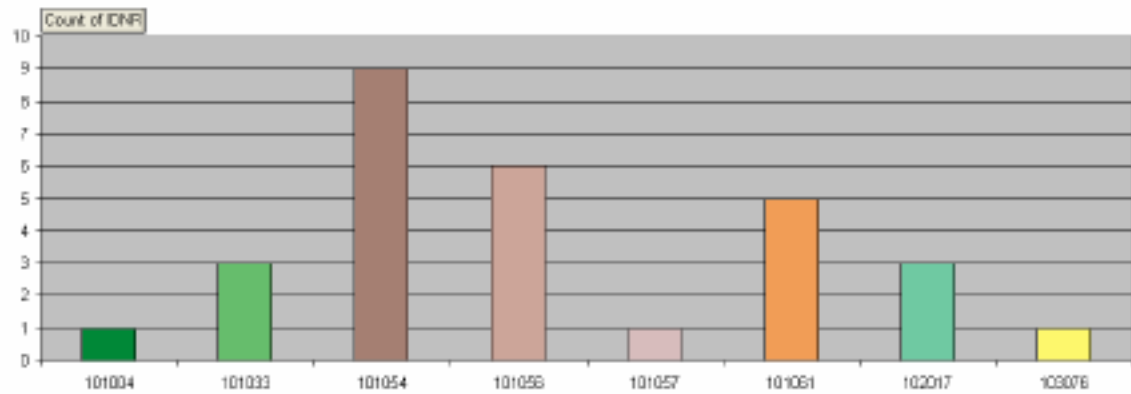
Number of occurrences of each rock type [N = 1154]



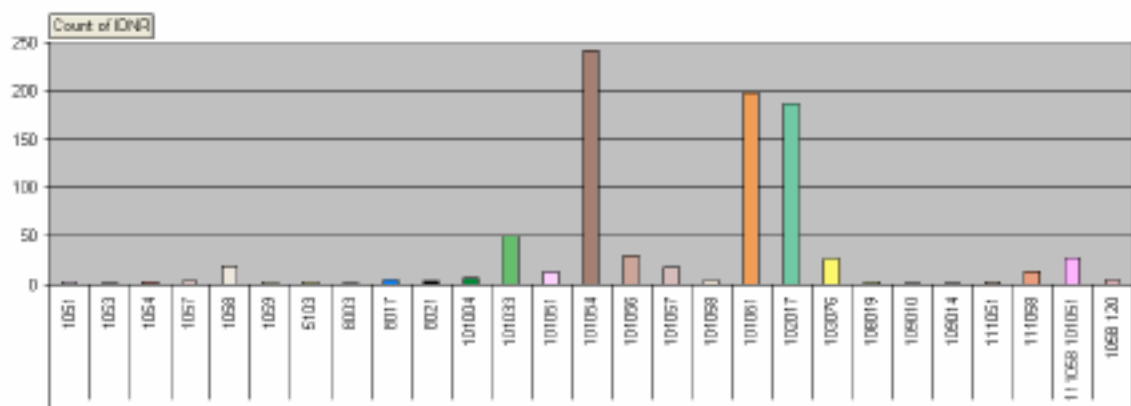
Rock domain 30
 Number of outcrops where each rock type is dominating.
 Y-axis indicates total number of outcrops in the rock domain. [N = 274]



Rock domain 30
 Number of outcrops composed solely of one rock type.
 Y-axis indicates total number of outcrops in the rock domain.

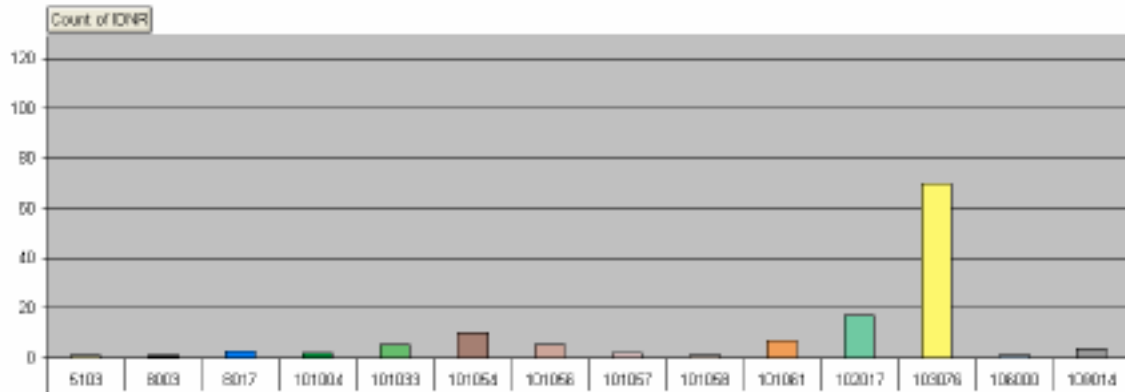


Rock domain 30
 Number of occurrences of each rock type [N = 876]



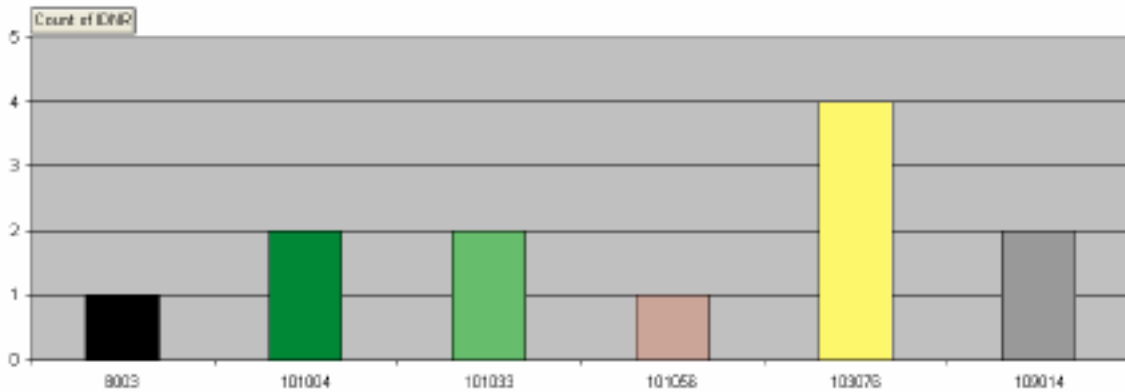
Rock domain 31

Number of outcrops where each rock type is dominating.
Y-axis indicates total number of outcrops in the rock domain. [N = 129]



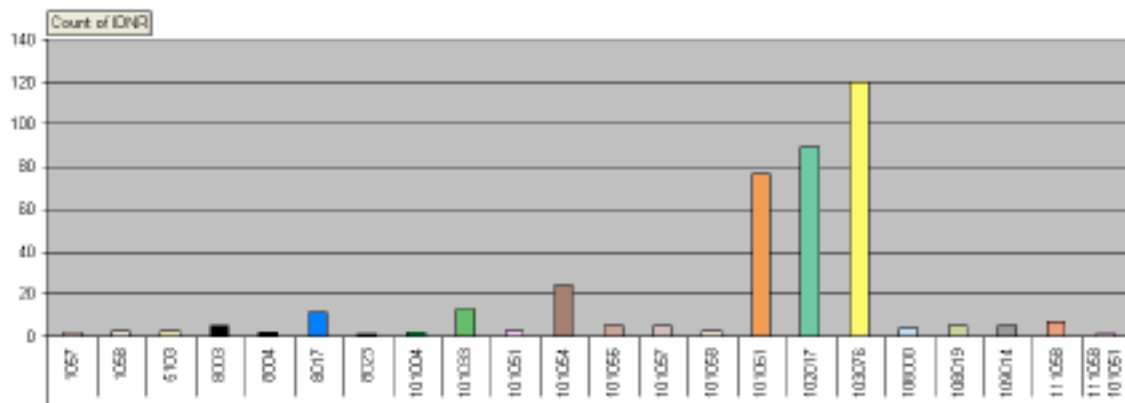
Rock domain 31

Number of outcrops composed solely of one rock type.
Y-axis indicates total number of outcrops in the rock domain.

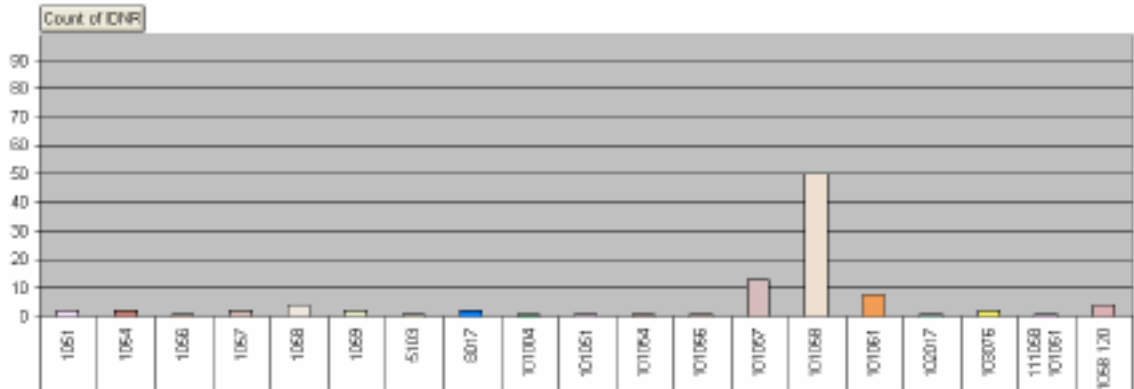


Rock domain 31

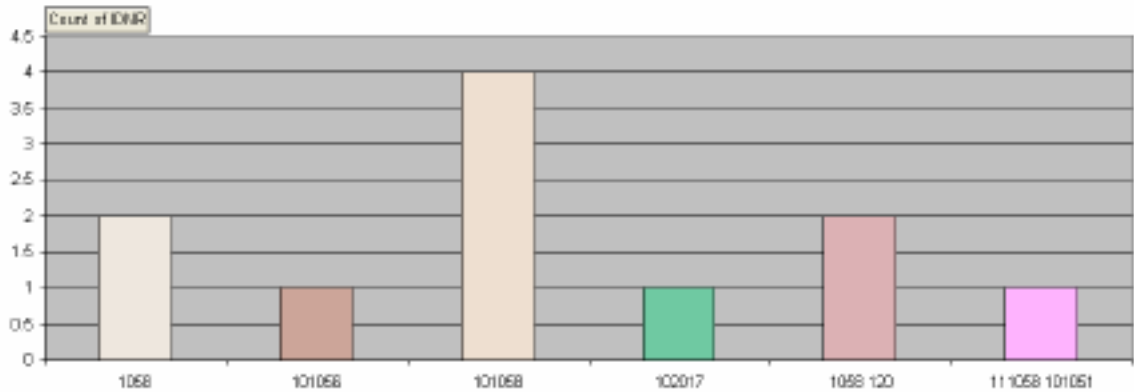
Number of occurrences of each rock type [N = 390]



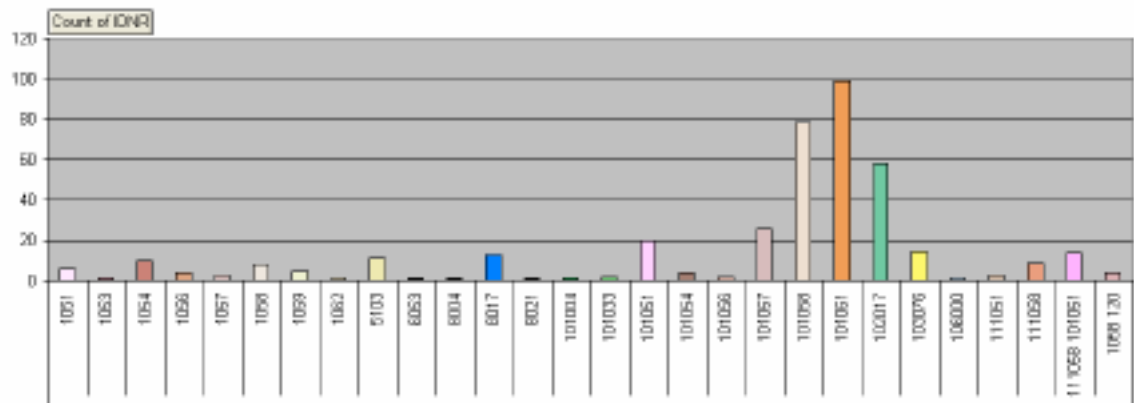
Rock domain 32
 Number of outcrops where each rock type is dominating.
 Y-axis indicates total number of outcrops in the rock domain. [N = 99]



Rock domain 32
 Number of outcrops composed solely of one rock type.
 Y-axis indicates total number of outcrops in the rock domain.

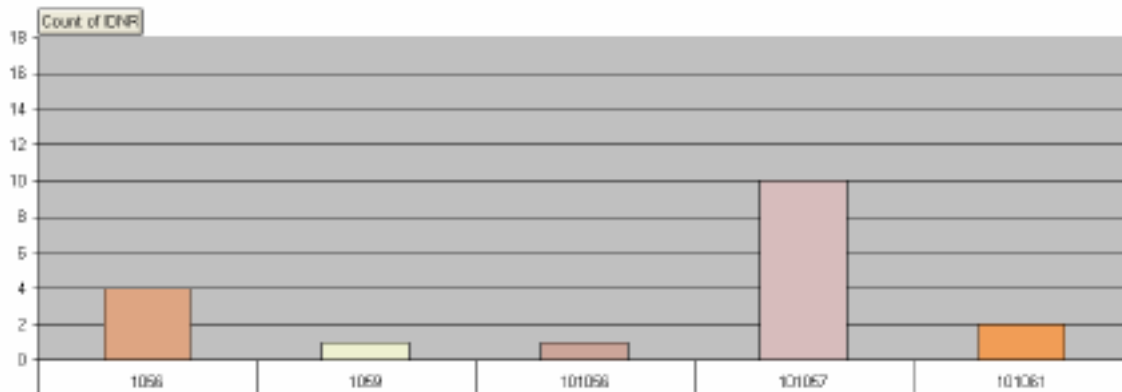


Rock domain 32
 Number of occurrences of each rock type [N = 401]



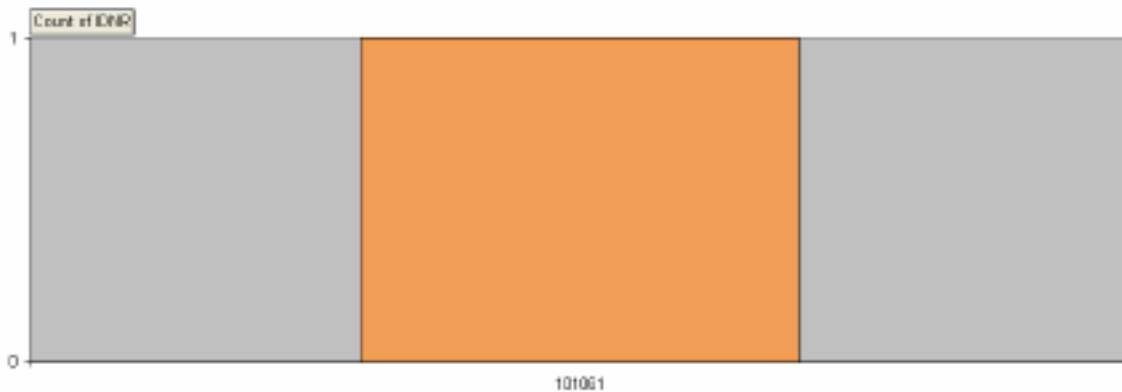
Rock domain 33

Number of outcrops where each rock type is dominating.
Y-axis indicates total number of outcrops in the rock domain. [N = 18]



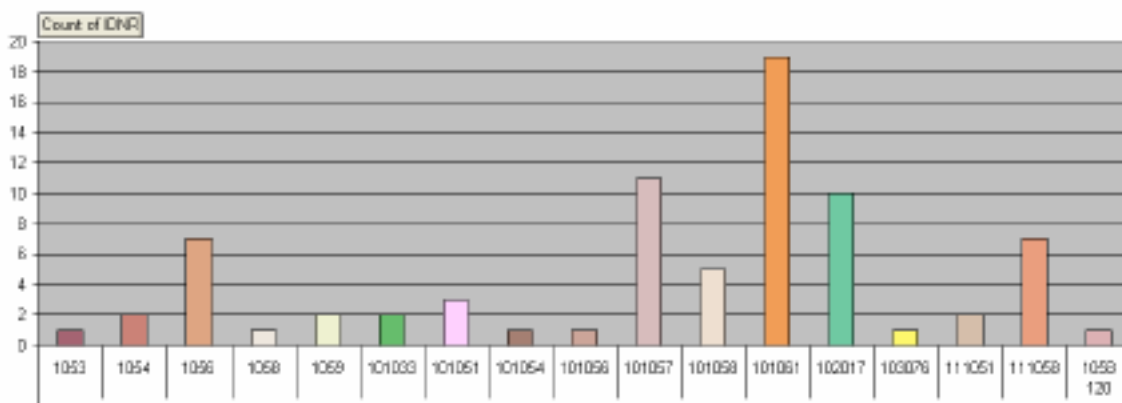
Rock domain 33

Number of outcrops composed solely of one rock type.
Y-axis indicates total number of outcrops in the rock domain.

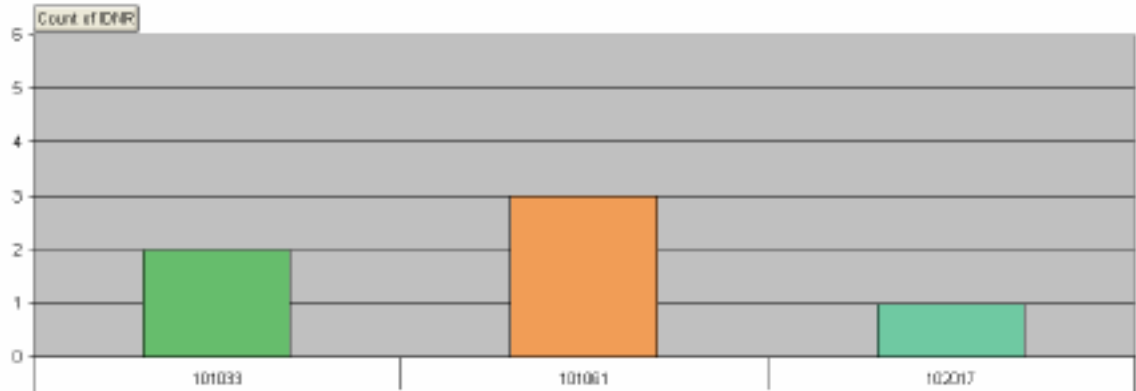


Rock domain 33

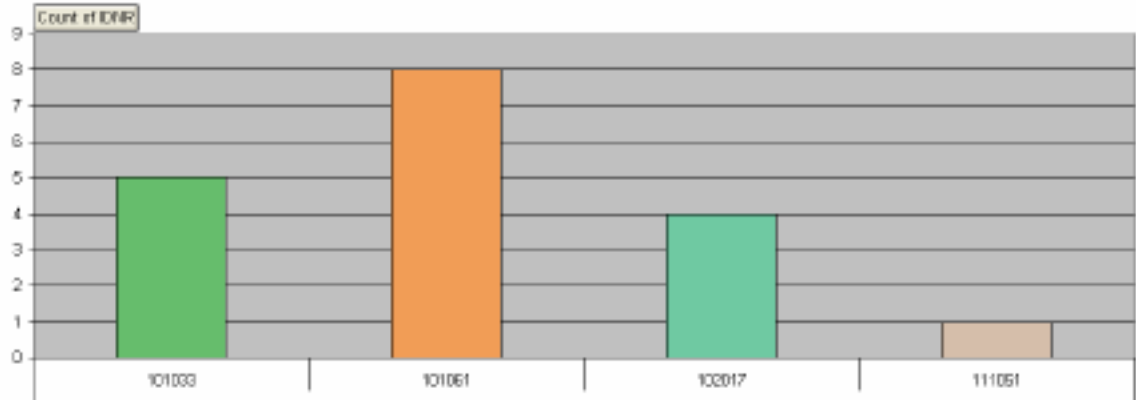
Number of occurrences of each rock type [N = 76]



Rock domain 35
 Number of outcrops where each rock type is dominating.
 Y-axis indicates total number of outcrops in the rock domain. [N = 6]

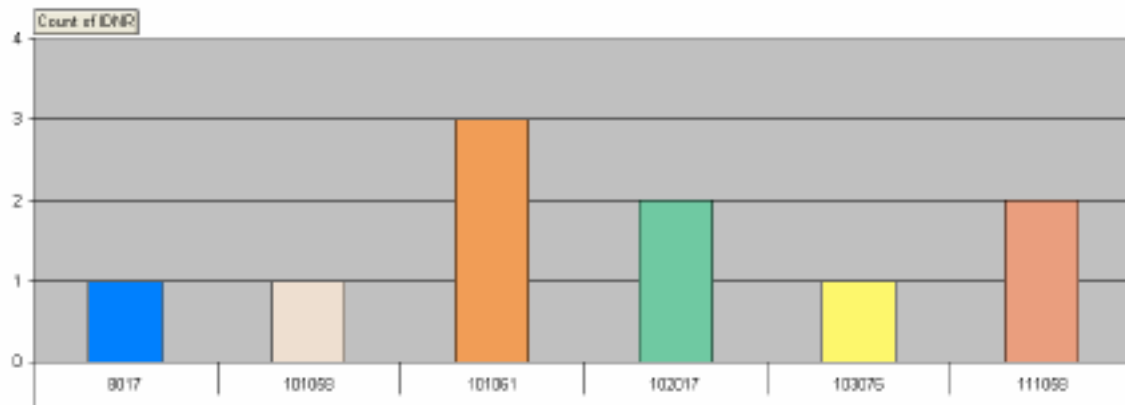
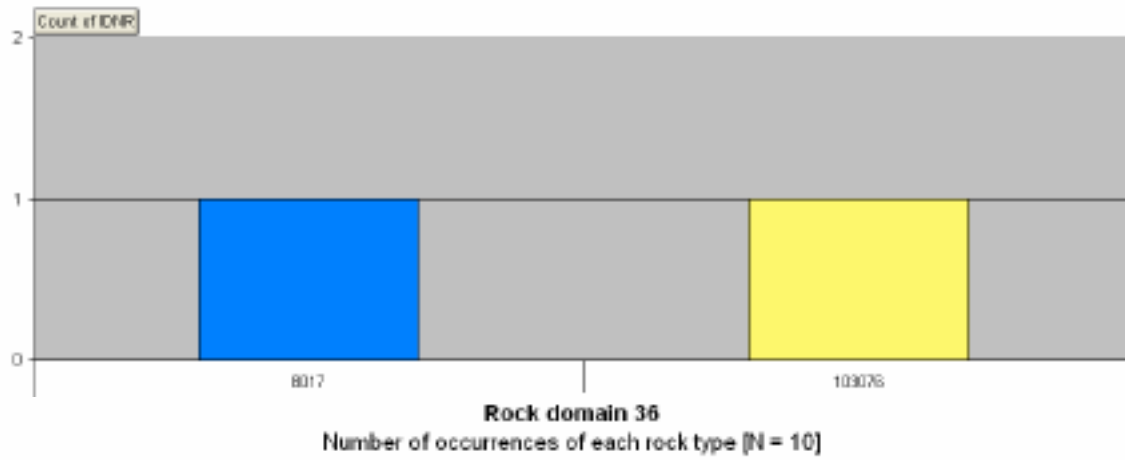


Rock domain 35
 Number of occurrences of each rock type [N = 18]



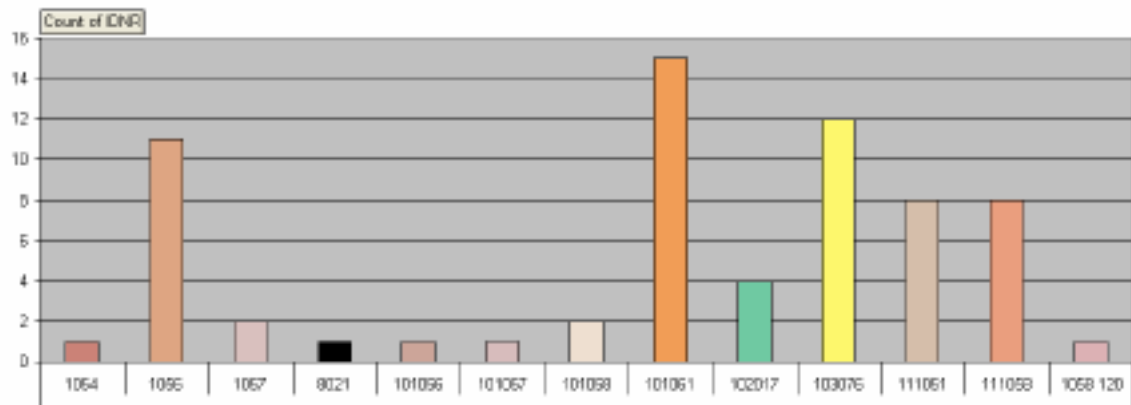
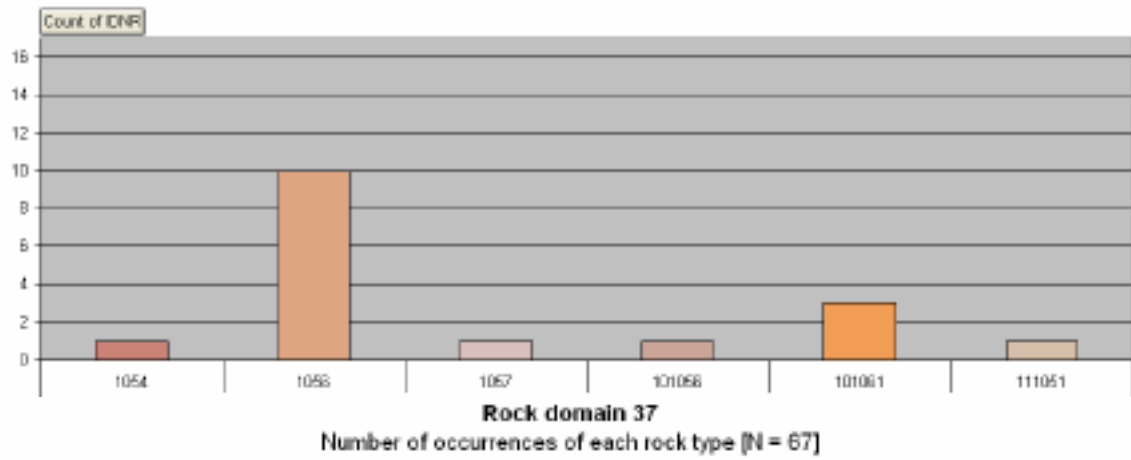
Rock domain 36

Number of outcrops where each rock type is dominating.
Y-axis indicates total number of outcrops in the rock domain. [N = 2]



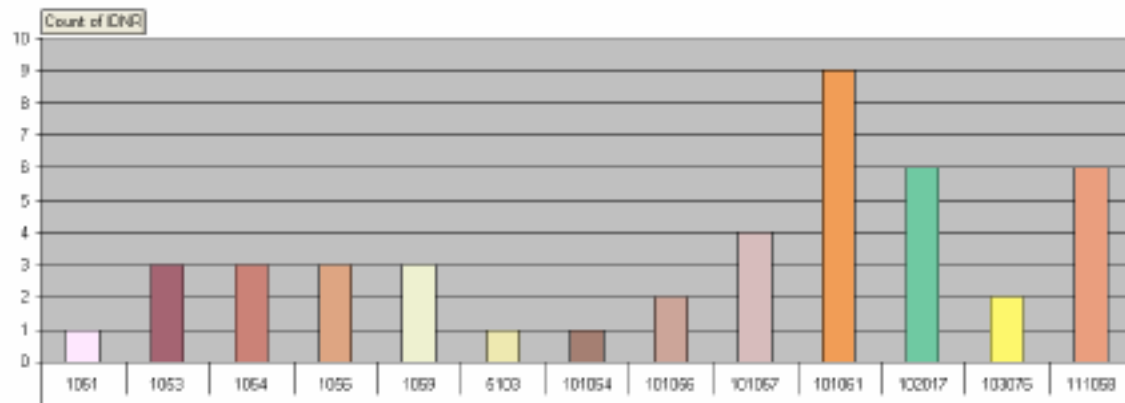
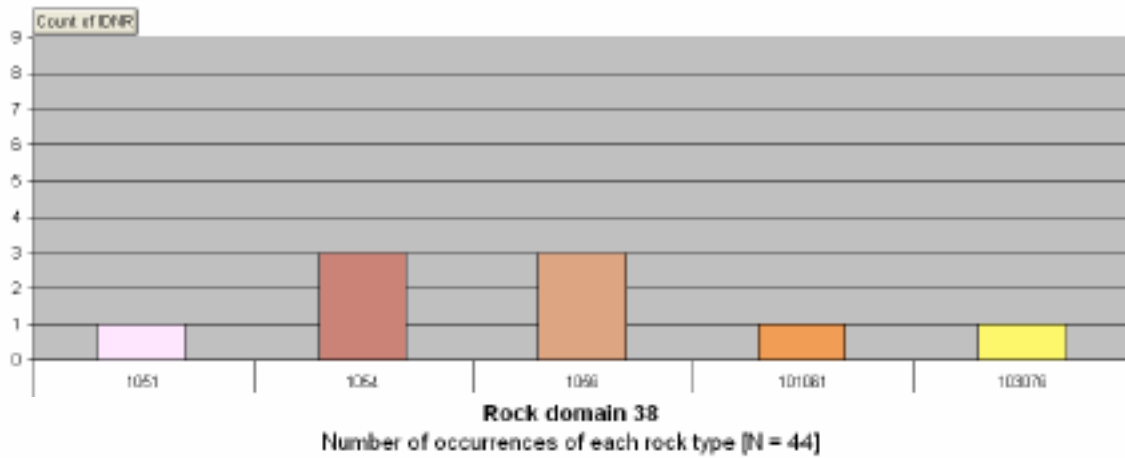
Rock domain 37

Number of outcrops where each rock type is dominating.
Y-axis indicates total number of outcrops in the rock domain. [N = 17]



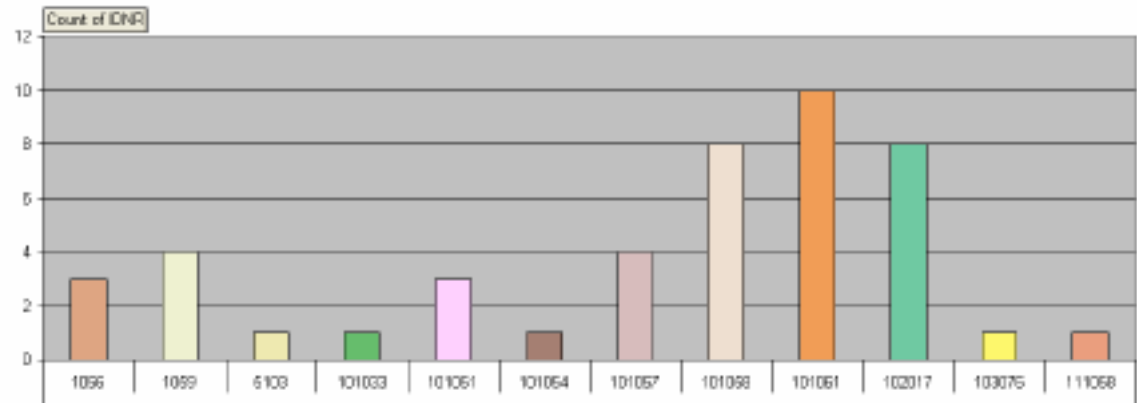
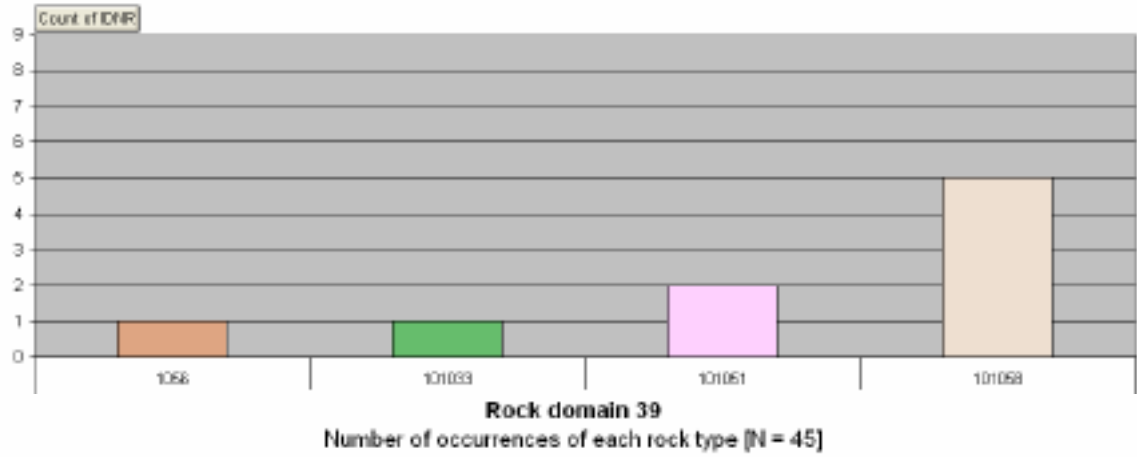
Rock domain 38

Number of outcrops where each rock type is dominating.
Y-axis indicates total number of outcrops in the rock domain. [N = 9]



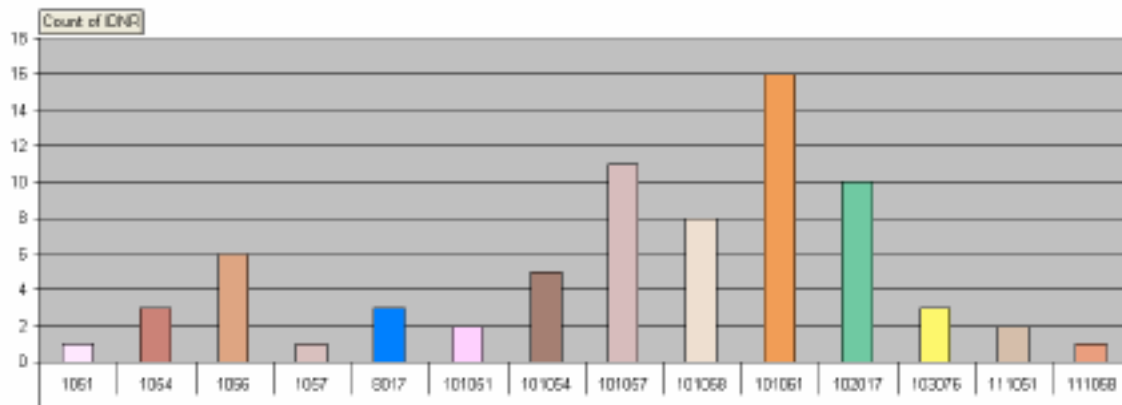
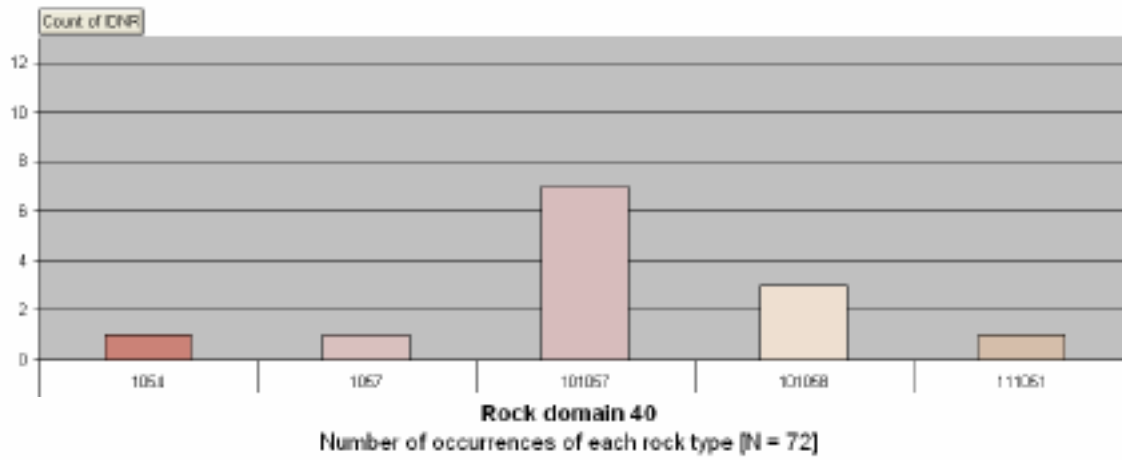
Rock domain 39

Number of outcrops where each rock type is dominating.
Y-axis indicates total number of outcrops in the rock domain. [N = 9]



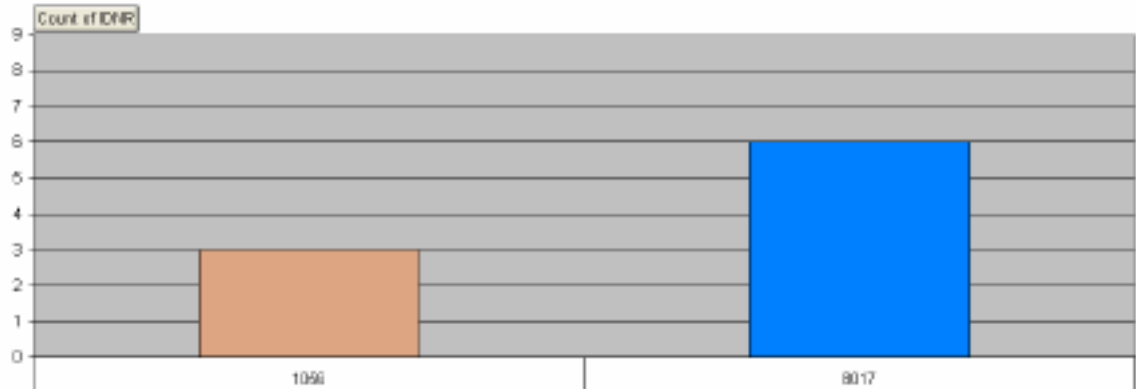
Rock domain 40

Number of outcrops where each rock type is dominating.
Y-axis indicates total number of outcrops in the rock domain. [N = 13]



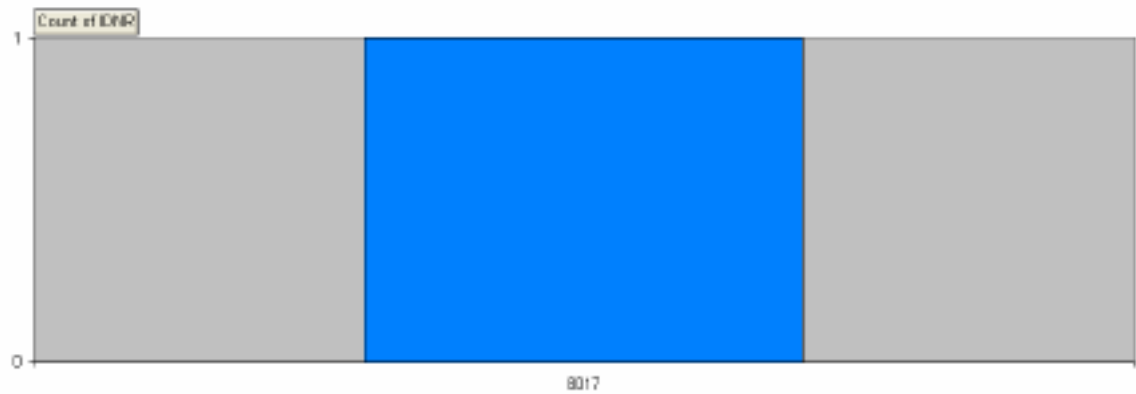
Rock domain 41

Number of outcrops where each rock type is dominating.
Y-axis indicates total number of outcrops in the rock domain. [N = 9]



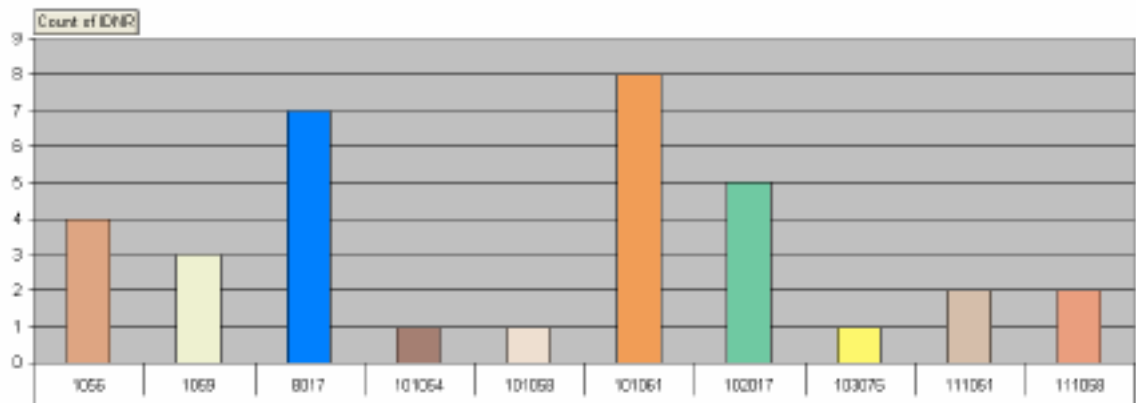
Rock domain 41

Number of outcrops composed solely of one rock type.
Y-axis indicates total number of outcrops in the rock domain.



Rock domain 41

Number of occurrences of each rock type [N = 34]



Orientation of ductile structures in rock domains

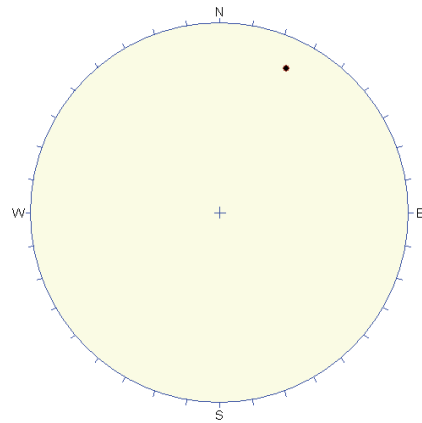
The orientations of ductile structures (fold axis, mineral stretching lineation, tectonic foliation/banding) in each rock domain are presented in the lower hemisphere of different stereographic projections. The data are predominantly from the surface. Data at depth from cored boreholes are only available for rock domains RFM012, RFM017, RFM018 and RFM029. These borehole data are specifically marked.

The number of measurements of each ductile structure in each domain is shown with the letter N. The Fisher mean value calculated for a linear structure (fold axis or mineral stretching lineation) refers to the trend and plunge of this structure. For example, the mean value of the mineral stretching lineation in rock domain RFM003 (136/40) plunges 40° in a direction S44E. All planar structures are plotted as poles to planes. The estimated trend and plunge for the Fisher mean orientation of the tectonic foliation/banding have been converted to a strike and dip notation (right-hand-rule). For example, the mean value of the tectonic foliation/banding presented for rock domain RFM003 (108/75) strikes N72W and dips 75° to the south-west. This corresponds to the mean orientation vector with trend and plunge 018/15°.

**Rock domain
RFM001**

Pole to tectonic
foliation

N = 1



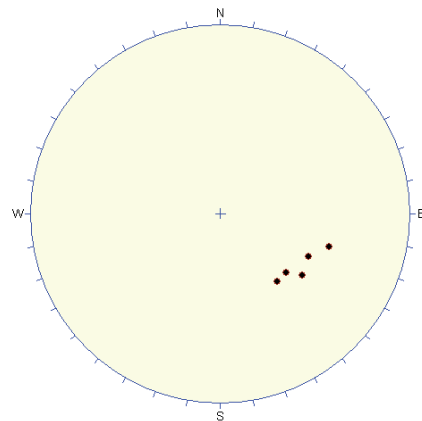
**Rock domain
RFM002**

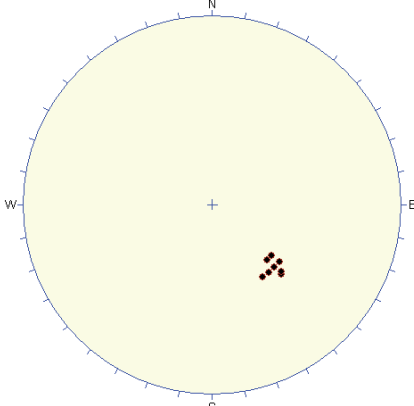
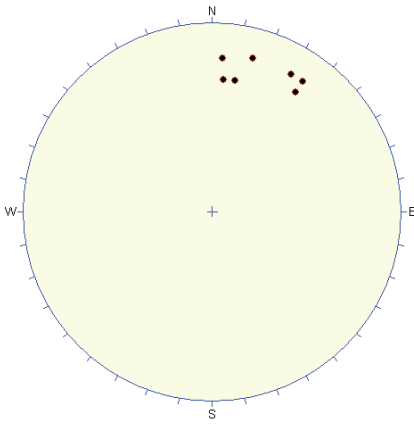
Mineral stretching
lineation

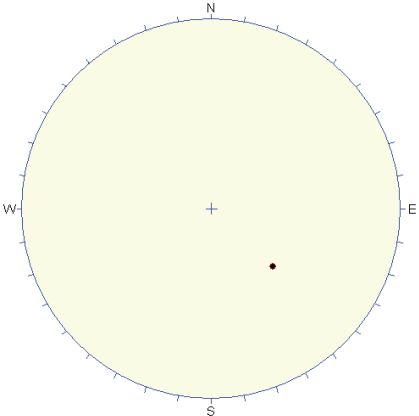
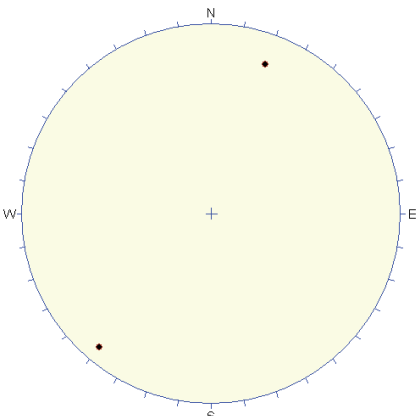
N = 5

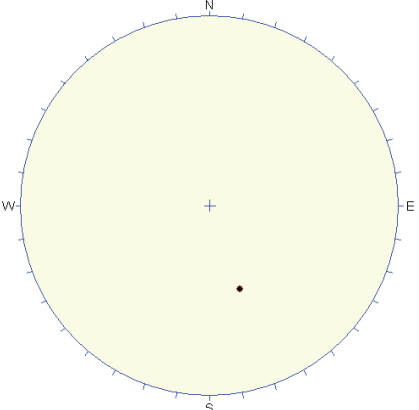
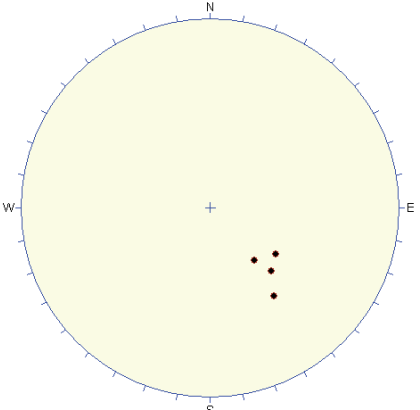
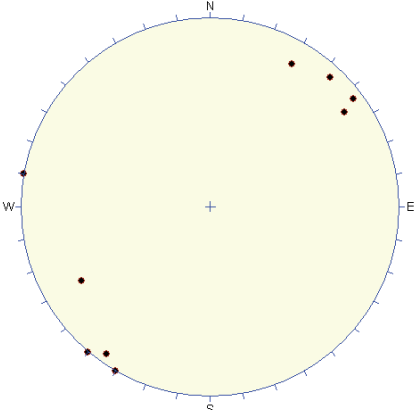
Fisher mean =
124/36

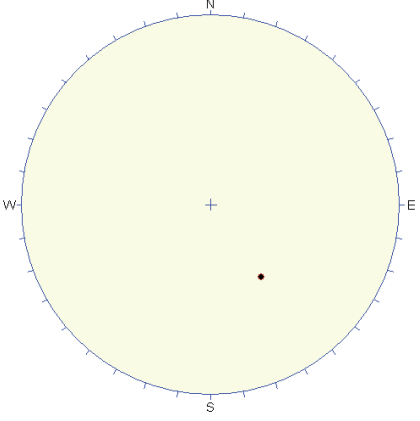
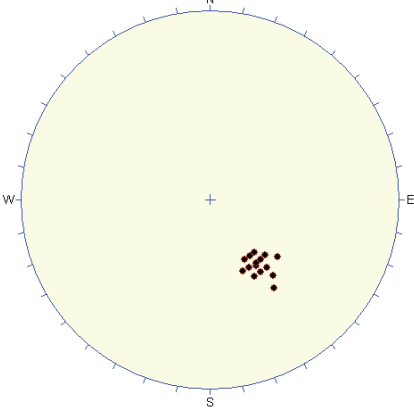
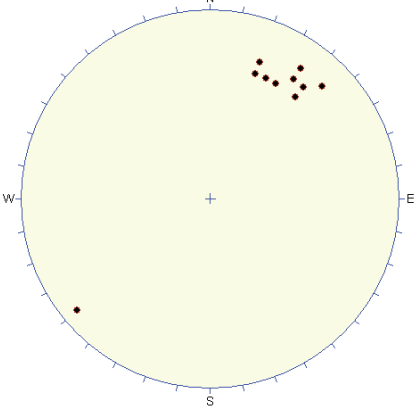
K value = 47

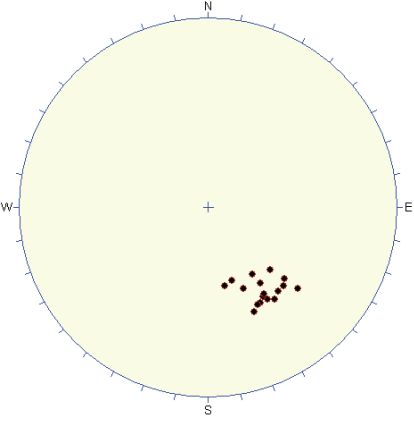
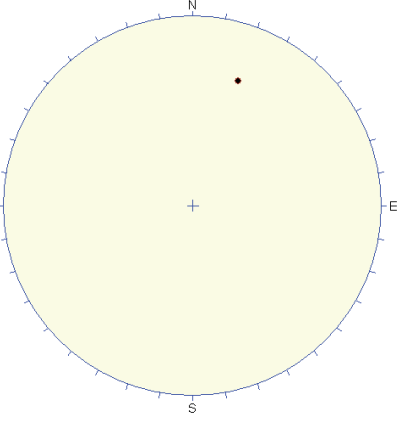


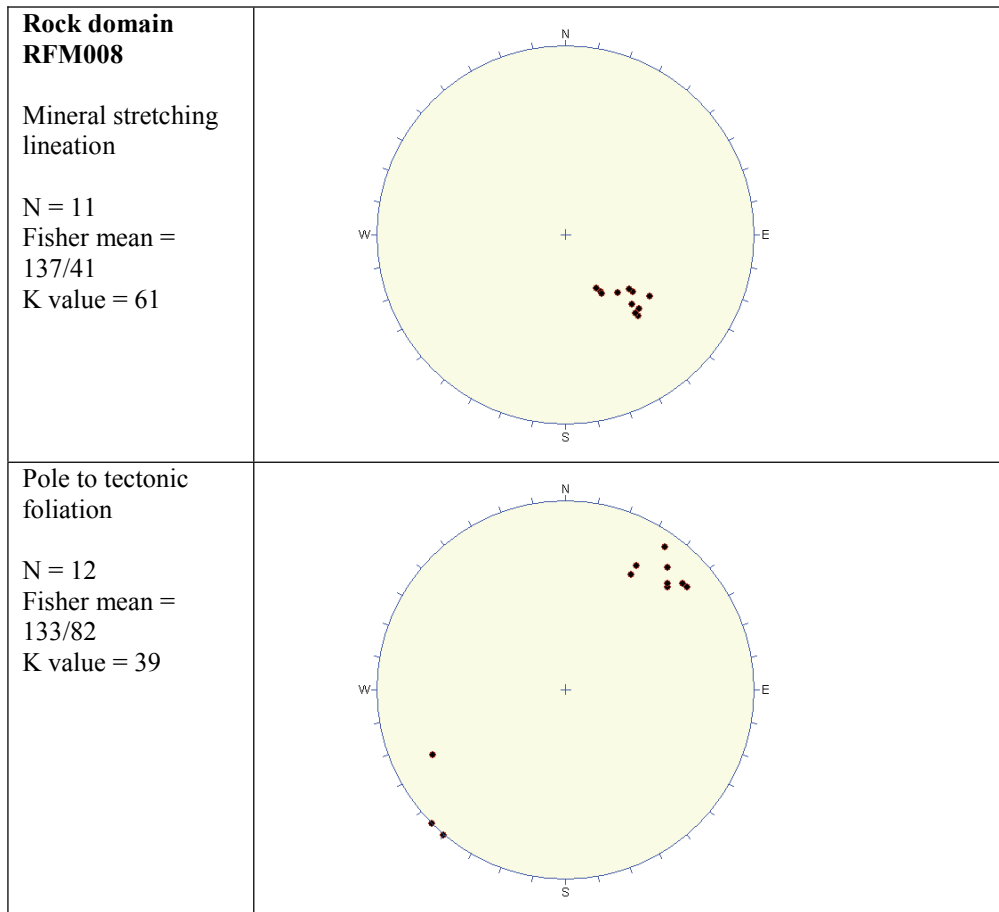
<p>Rock domain RFM003</p> <p>Mineral stretching lineation</p> <p>N = 8 Fisher mean = 136/40 K value = 240</p>	
<p>Pole to tectonic foliation/banding</p> <p>N=8 Fisher mean = 108/75 K value = 35</p>	

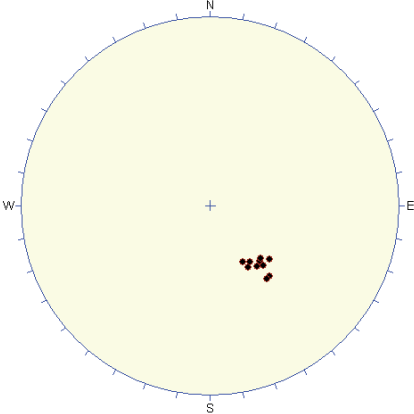
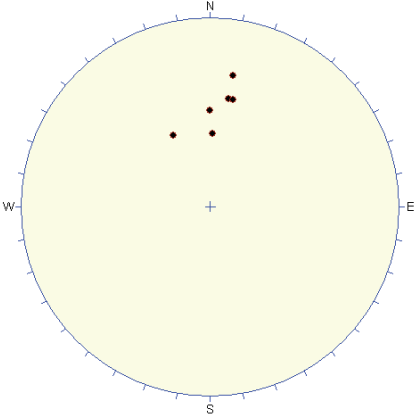
<p>Rock domain RFM004</p> <p>Mineral stretching lineation</p> <p>$N = 2$</p>	 <p>A circular Wulff net plot with a light yellow background. The plot is marked with cardinal directions: 'N' at the top, 'S' at the bottom, 'W' on the left, and 'E' on the right. A central crosshair is present. A single black dot is plotted in the lower-right quadrant, approximately at a dip of 30 degrees and an azimuth of 135 degrees.</p>
<p>Pole to tectonic foliation</p> <p>$N = 2$</p>	 <p>A circular Wulff net plot with a light yellow background, identical in layout to the one above. It features cardinal directions 'N', 'S', 'W', 'E' and a central crosshair. Two black dots are plotted: one in the upper-right quadrant (approximately 60 degrees dip, 135 degrees azimuth) and one in the lower-left quadrant (approximately 30 degrees dip, 225 degrees azimuth).</p>

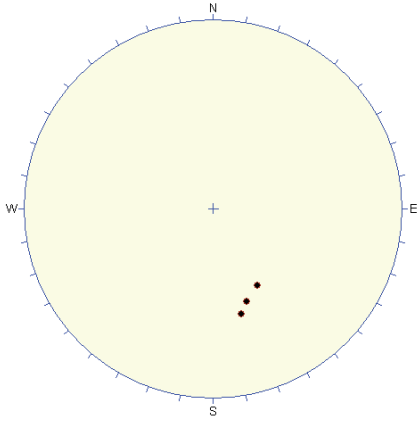
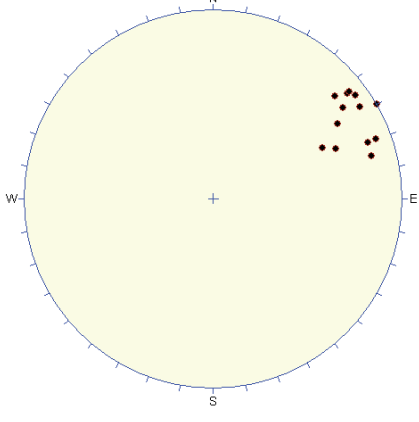
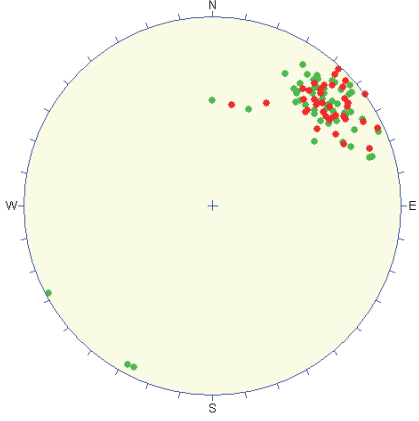
<p>Rock domain RFM005</p> <p>Fold axis</p> <p>N = 1</p>	 <p>A circular Wulff net plot with a central crosshair and tick marks around the perimeter. The cardinal directions are labeled: N at the top, S at the bottom, W on the left, and E on the right. A single black dot representing a data point is located in the lower-right quadrant, approximately at 130 degrees azimuth and 40 degrees plunge.</p>
<p>Mineral stretching lineation</p> <p>N = 4</p> <p>Fisher mean = 137/41</p> <p>K value = 60</p>	 <p>A circular Wulff net plot with a central crosshair and tick marks around the perimeter. The cardinal directions are labeled: N at the top, S at the bottom, W on the left, and E on the right. Four black dots representing data points are clustered together in the lower-right quadrant, approximately at 130 degrees azimuth and 40 degrees plunge, showing a tight distribution.</p>
<p>Pole to tectonic foliation</p> <p>N = 11</p> <p>Fisher mean = 136/89</p> <p>K value = 15</p>	 <p>A circular Wulff net plot with a central crosshair and tick marks around the perimeter. The cardinal directions are labeled: N at the top, S at the bottom, W on the left, and E on the right. Eleven black dots representing data points are scattered across the plot. One point is on the left edge (W), one is in the lower-left quadrant, and the remaining eight are clustered in the upper-right quadrant, indicating a bimodal distribution.</p>

<p>Rock domain RFM006</p> <p>Fold axis</p> <p>N = 1</p>	
<p>Mineral stretching lineation</p> <p>N = 17</p> <p>Fisher mean = 143/44</p> <p>K value = 128</p>	
<p>Pole to tectonic foliation</p> <p>N = 13</p> <p>Fisher mean = 127/77</p> <p>K value = 37</p>	

<p>Rock domain RFM007</p> <p>Mineral stretching lineation</p> <p>N = 17 Fisher mean = 147/34 K value = 61</p>	
<p>Pole to tectonic foliation</p> <p>N = 1</p>	



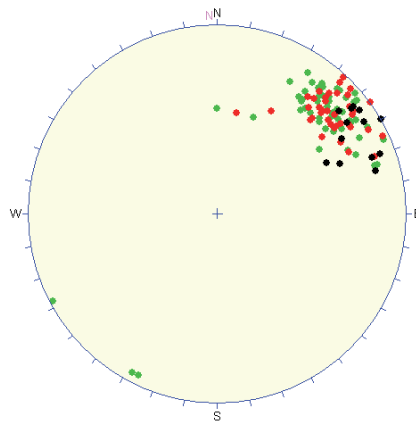
<p>Rock domain RFM011</p> <p>Mineral stretching lineation</p> <p>N = 10 Fisher mean = 141/46 K value = 185</p>	
<p>Pole to tectonic foliation</p> <p>N = 6</p>	

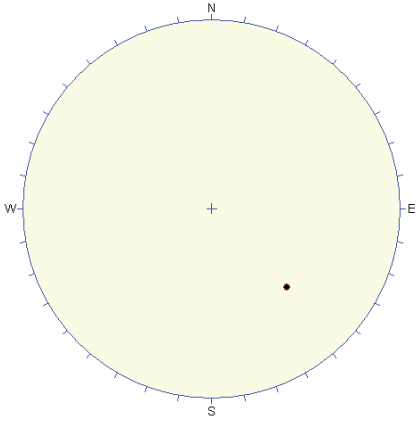
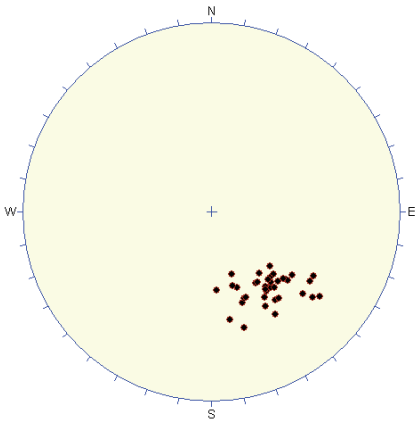
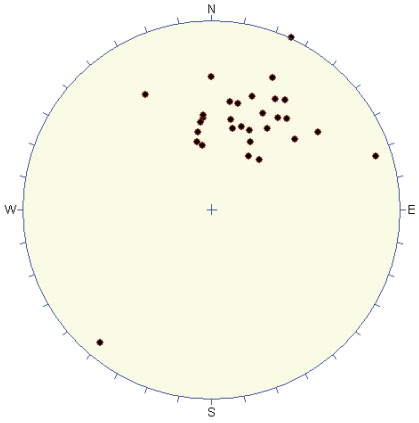
<p>Rock domain RFM012</p> <p>Mineral stretching lineation</p> <p>N = 5 Fisher mean = 155/37 K value = 125</p>	
<p>Pole to tectonic foliation</p> <p>N = 13 Fisher mean = 151/81 K value = 58</p>	
<p>Pole to tectonic foliation (red dots) and ductile or ductile-brittle deformation zones (green dots) along borehole length 177-500 m in KFM04A</p> <p>N = 95 Fisher mean = 138/78 K value = 38</p>	

**Rock domain
RFM012**

Pole to all ductile
planar structures.
Combined surface
(black dots) and
KFM04A (red and
green dots) data

N = 108
Fisher mean =
139/79
K value = 36

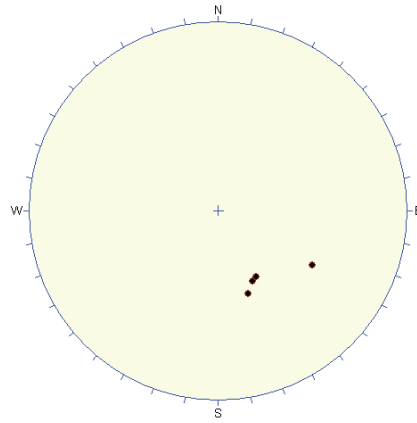


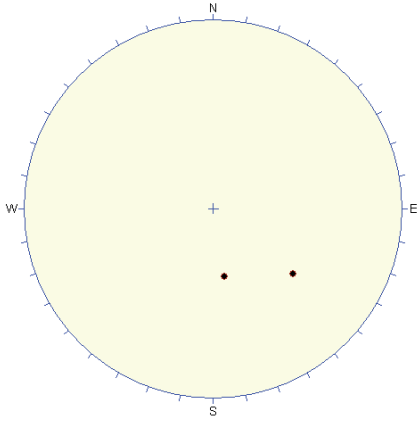
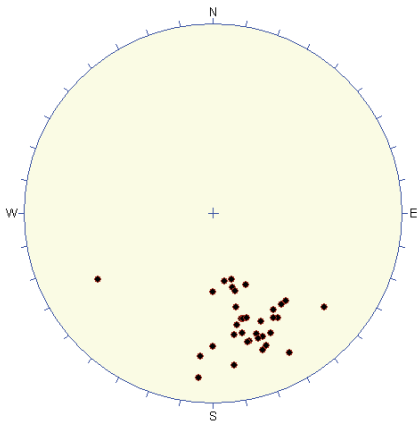
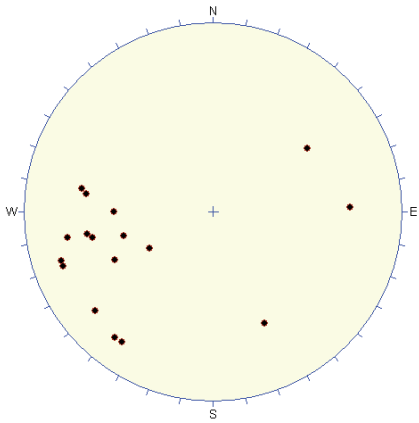
<p>Rock domain RFM013</p> <p>Fold axis</p> <p>N = 1</p>	
<p>Mineral stretching lineation</p> <p>N = 41</p> <p>Fisher mean = 144/36</p> <p>K value = 39</p>	
<p>Pole to tectonic foliation/banding</p> <p>N = 31</p> <p>Fisher mean = 112/57</p> <p>K value = 12</p>	

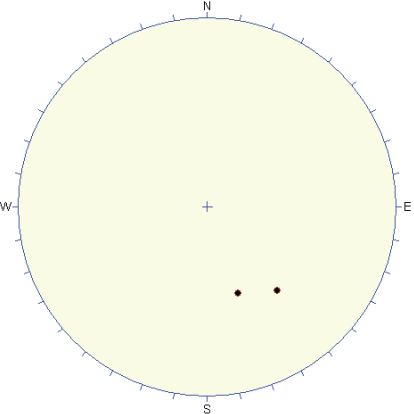
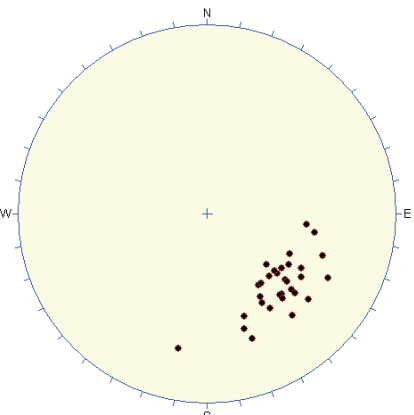
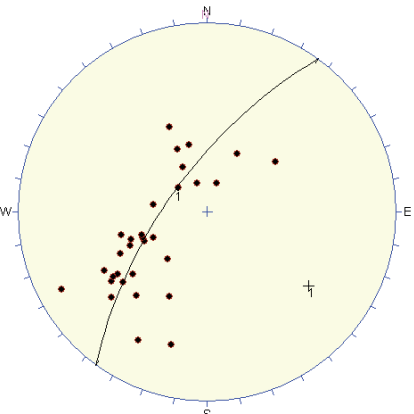
**Rock domain
RFM014**

Mineral stretching
lineation

N = 4
Fisher mean =
145/41
K value = 26



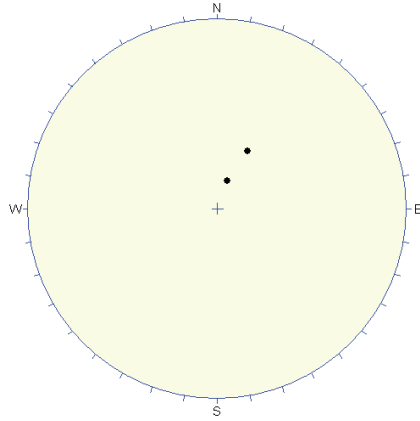
<p>Rock domain RFM016</p> <p>Fold axis</p> <p>N = 2</p>	
<p>Mineral stretching lineation</p> <p>N = 36 Fisher mean = 163/27 K value = 18</p>	
<p>Pole to tectonic foliation</p> <p>N = 17 Fisher mean = 334/74 K value = 6</p>	

<p>Rock domain RFM017</p> <p>Fold axis</p> <p>N = 2</p>	
<p>Mineral stretching lineation</p> <p>N = 31</p> <p>Fisher mean = 134/32</p> <p>K value = 21</p>	
<p>Pole to tectonic foliation</p> <p>N = 31</p> <p>Pole to best-fit great circle = 122/27</p>	

**Rock domain
RFM017**

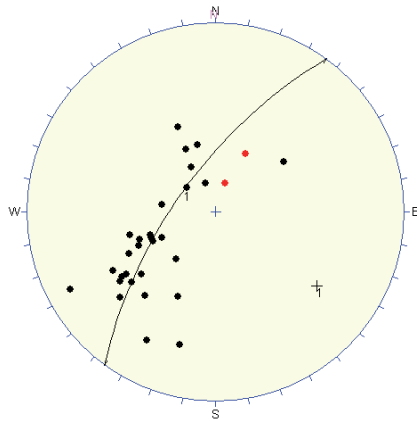
Pole to tectonic
foliation along
borehole length
220-293 m in
KFM03A

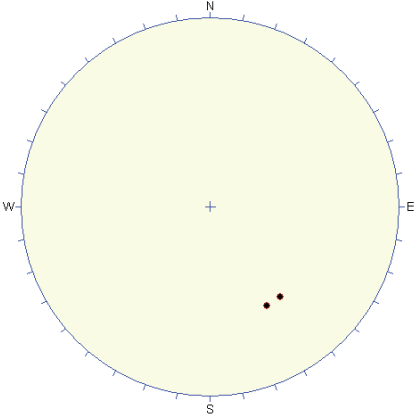
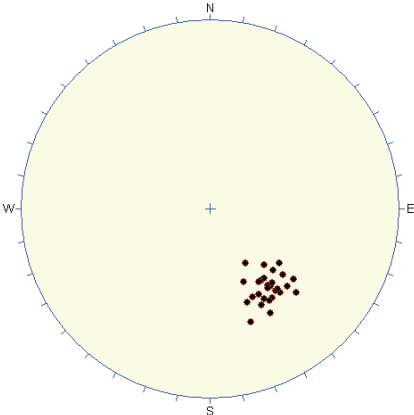
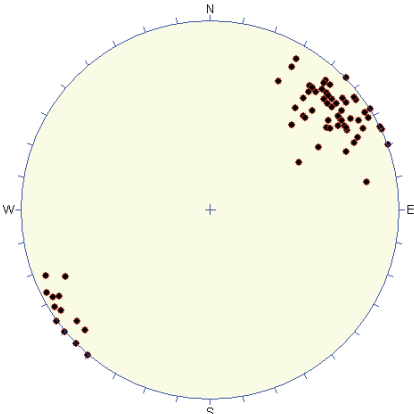
N = 2



Pole to tectonic
foliation. Combined
surface (black dots)
and KFM03A (red
dots) data

N = 33
Pole to best-fit
great circle =
126/23

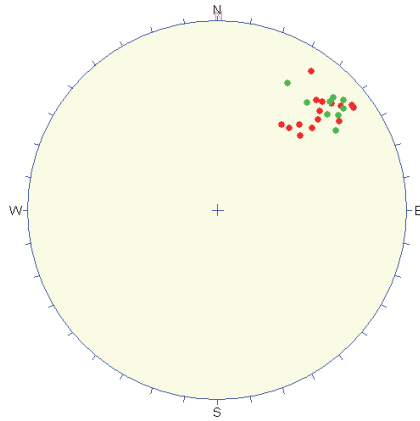


<p>Rock domain RFM018</p> <p>Fold axis</p> <p>N = 2</p>	 <p>A circular Wulff net plot with a central cross and tick marks around the perimeter. The cardinal directions are labeled: N at the top, S at the bottom, W on the left, and E on the right. Two small black dots are plotted in the lower right quadrant, approximately at 135 degrees and 30 degrees from the center.</p>
<p>Mineral stretching lineation</p> <p>N = 33</p> <p>Fisher mean = 143/35</p> <p>K value = 84</p>	 <p>A circular Wulff net plot with a central cross and tick marks around the perimeter. The cardinal directions are labeled: N at the top, S at the bottom, W on the left, and E on the right. A cluster of approximately 33 small black dots is plotted in the lower right quadrant, centered around 143 degrees and 35 degrees from the center.</p>
<p>Pole to tectonic foliation/banding</p> <p>N = 87</p> <p>Fisher mean = 142/ 83</p> <p>K value = 45</p>	 <p>A circular Wulff net plot with a central cross and tick marks around the perimeter. The cardinal directions are labeled: N at the top, S at the bottom, W on the left, and E on the right. Two distinct clusters of small black dots are plotted: one in the upper right quadrant (around 142 degrees and 83 degrees) and another in the lower left quadrant (around 222 degrees and 83 degrees).</p>

**Rock domain
RFM018**

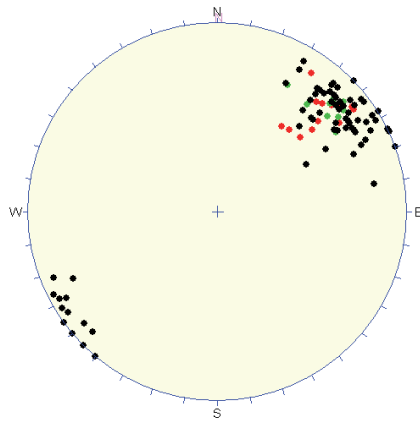
Pole to tectonic foliation (red dots) and ductile or ductile-brittle deformation zones (green dots) along borehole length 12-177 m in KFM04A

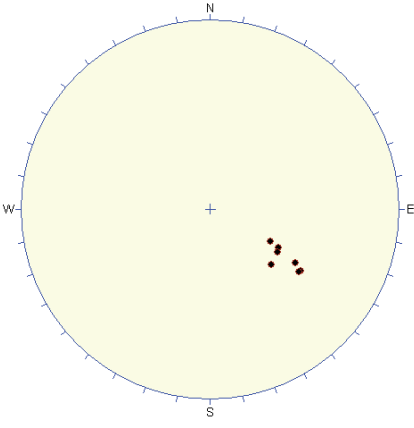
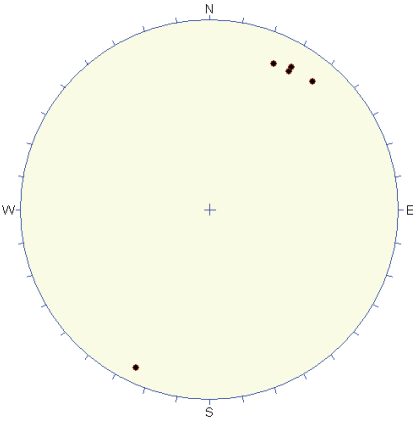
N = 26
Fisher mean = 136/75
K value = 72

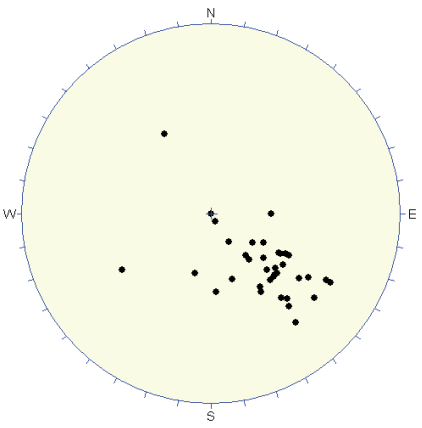
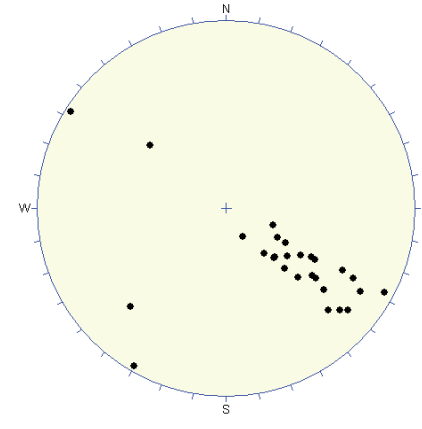
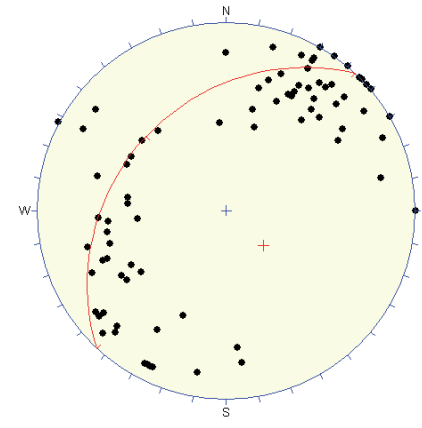


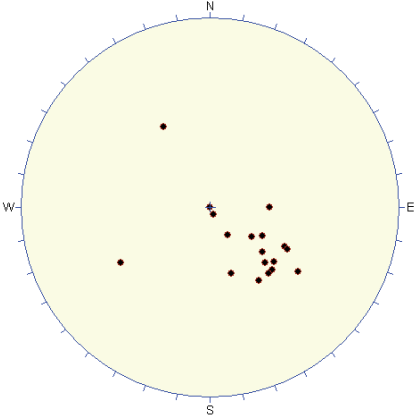
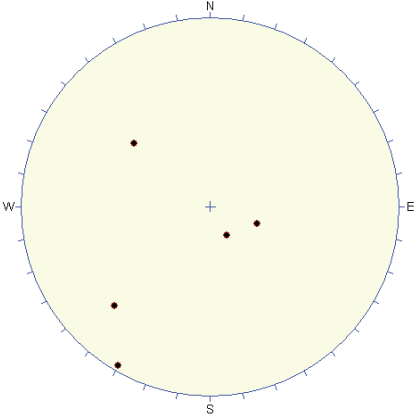
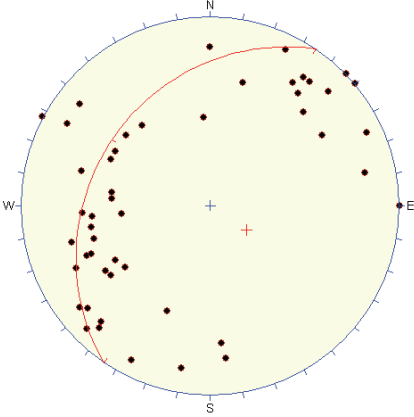
Pole to all ductile planar structures. Combined surface (black dots) and KFM04A (red and green dots) data

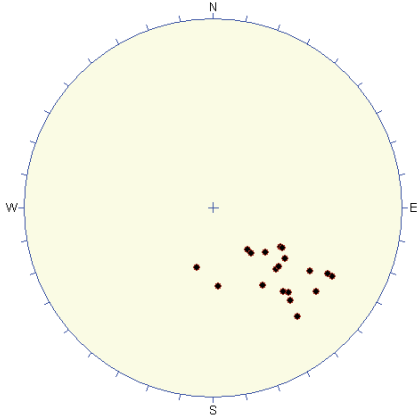
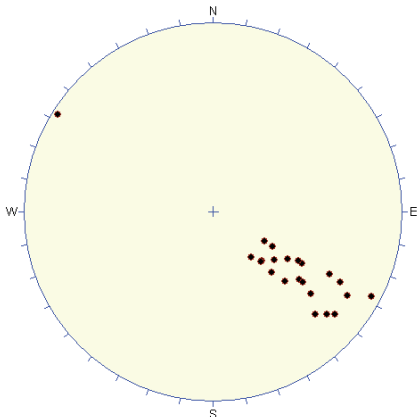
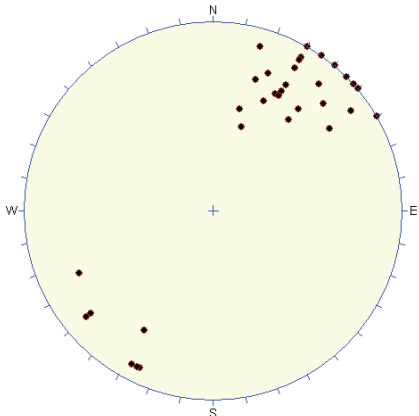
N = 113
Fisher mean = 141/81
K value = 44

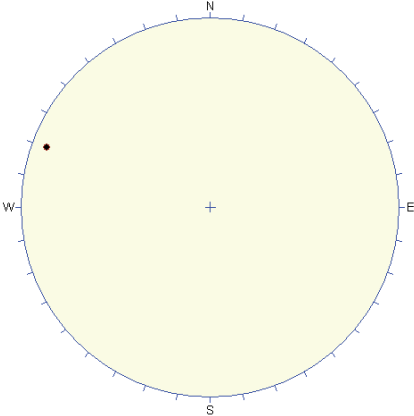
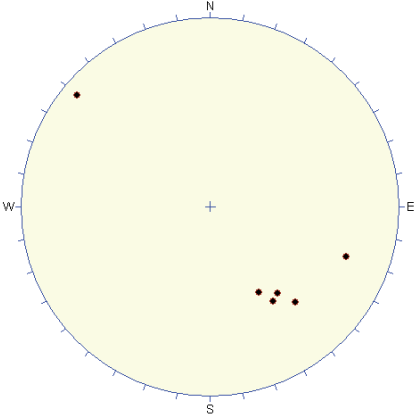
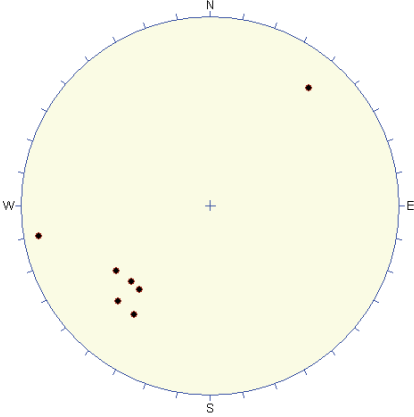


<p>Rock domain RFM020</p> <p>Mineral stretching lineation</p> <p>N = 7 Fisher mean = 123/40 K value = 87</p>	
<p>Pole to tectonic foliation/banding</p> <p>N = 5 Fisher mean = 120/84 K value = 88</p>	

<p>Rock domain RFM021</p> <p>Fold axis</p> <p>N = 38 Fisher mean = 135/47 K value = 9</p>	 <p>A Wulff stereonet plot showing the distribution of fold axis data points. The plot is circular with a light yellow background and a blue border. The cardinal directions are labeled: N (North) at the top, S (South) at the bottom, W (West) on the left, and E (East) on the right. The data points are represented by small black dots, with a central crosshair (+) indicating the Fisher mean. The points are clustered in the SE quadrant, indicating a fold axis orientation towards the southeast.</p>
<p>Mineral stretching lineation</p> <p>N = 27 Fisher mean = 132/31 K value = 7</p>	 <p>A Wulff stereonet plot showing the distribution of mineral stretching lineation data points. The plot is circular with a light yellow background and a blue border. The cardinal directions are labeled: N (North) at the top, S (South) at the bottom, W (West) on the left, and E (East) on the right. The data points are represented by small black dots, with a central crosshair (+) indicating the Fisher mean. The points are clustered in the SE quadrant, indicating a mineral stretching lineation orientation towards the southeast.</p>
<p>Pole to tectonic foliation/banding</p> <p>N = 87 Pole to best-fit great circle 133/60</p>	 <p>A Wulff stereonet plot showing the distribution of pole to tectonic foliation/banding data points. The plot is circular with a light yellow background and a blue border. The cardinal directions are labeled: N (North) at the top, S (South) at the bottom, W (West) on the left, and E (East) on the right. The data points are represented by small black dots, with a central crosshair (+) indicating the pole to the best-fit great circle. A red arc is drawn through the data points, representing the best-fit great circle. The points form a semi-circular arc centered on the N-S axis, indicating a tectonic foliation/banding orientation.</p>

<p>Rock domain RFM021, north- west of SFR</p> <p>Fold axis</p> <p>N = 18 Fisher mean = 134/58 K value = 7</p>	
<p>Mineral stretching lineation</p> <p>N = 5</p>	
<p>Pole to tectonic foliation/banding</p> <p>N = 52 Pole to best-fit great circle 124/64</p>	

<p>Rock domain RFM021, south- east of SFR</p> <p>Fold axis</p> <p>N = 20 Fisher mean = 136/37 K value = 19</p>	
<p>Mineral stretching lineation</p> <p>N = 22 Fisher mean = 127/30 K value = 19</p>	
<p>Pole to tectonic foliation/banding</p> <p>N = 35 Fisher mean = 127/83 K value = 20</p>	

<p>Rock domain RFM022</p> <p>Fold axis</p> <p>N = 1</p>	
<p>Mineral stretching lineation</p> <p>N = 7</p> <p>Fisher mean = 137/22</p> <p>K value = 19</p>	
<p>Pole to tectonic foliation</p> <p>N = 7</p> <p>Fisher mean = 319/72</p> <p>K value = 15</p>	

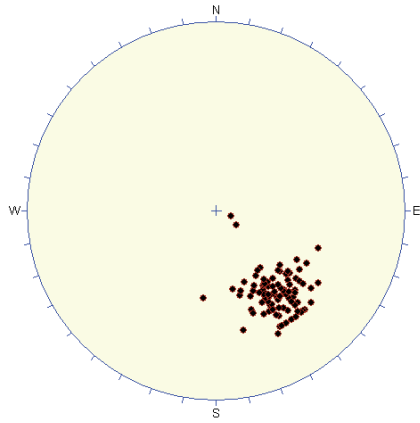
**Rock domain
RFM023**

Mineral stretching
lineation

N = 97

Fisher mean =
144/33

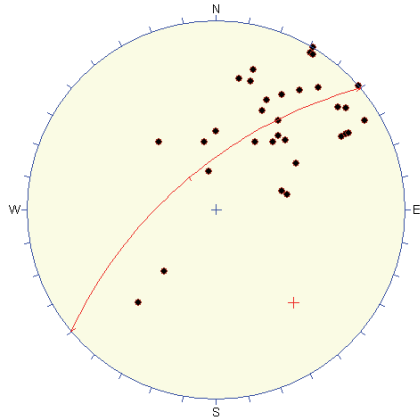
K value = 36

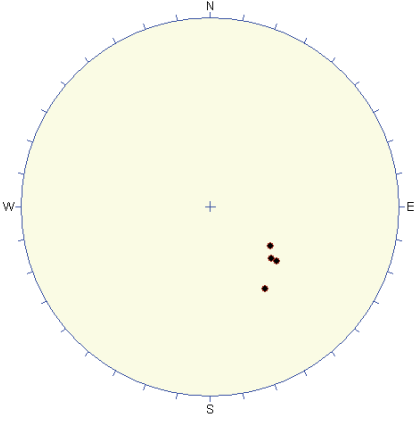
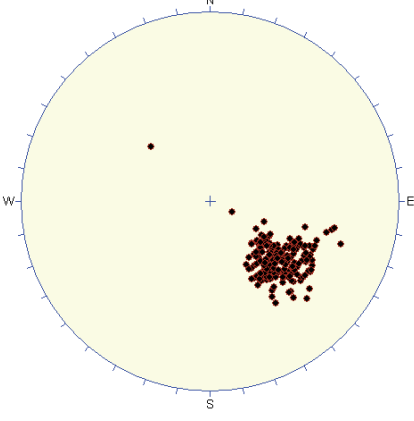
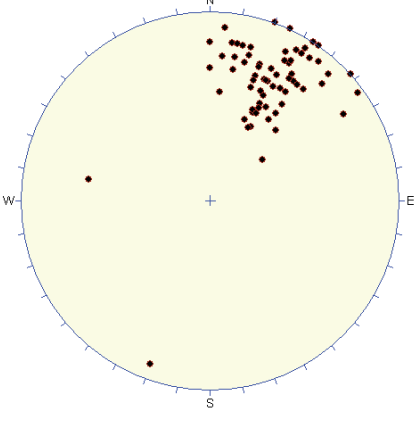


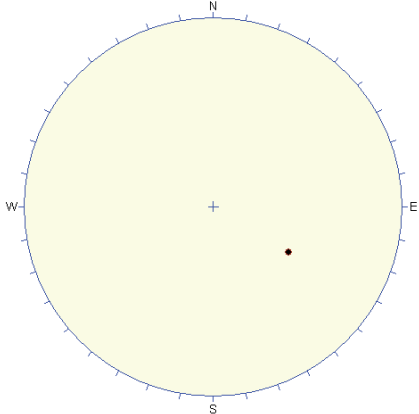
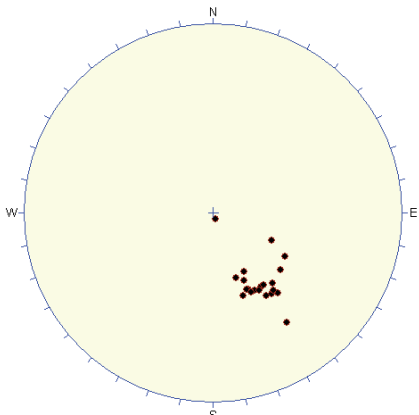
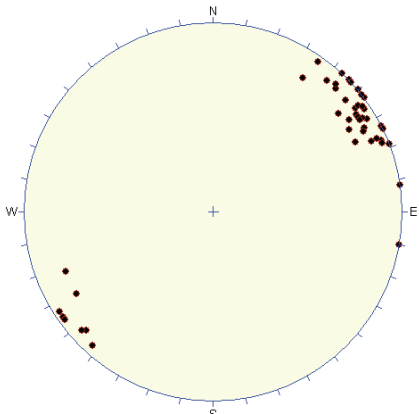
Pole to tectonic
foliation

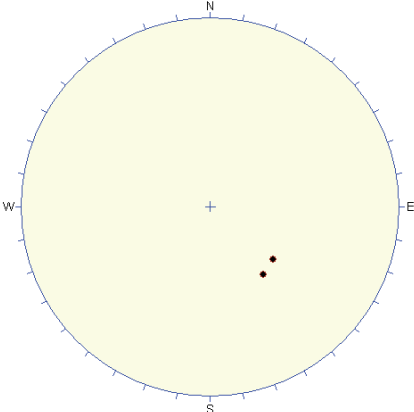
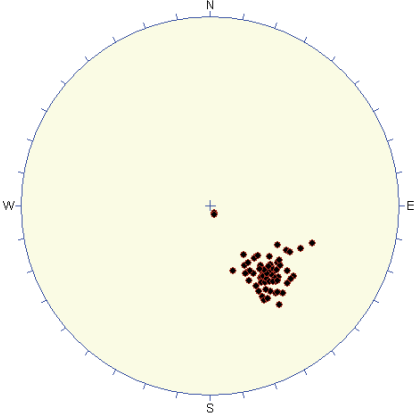
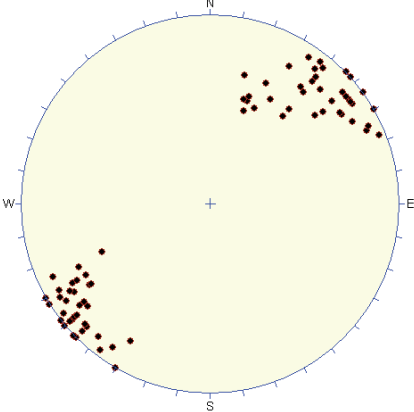
N = 34

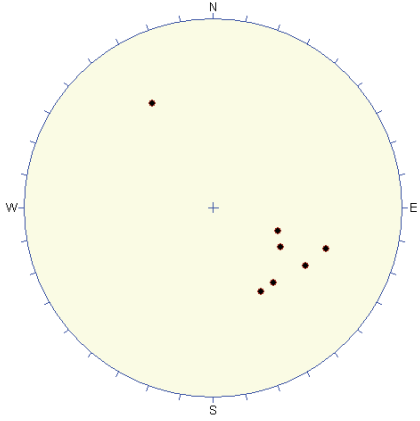
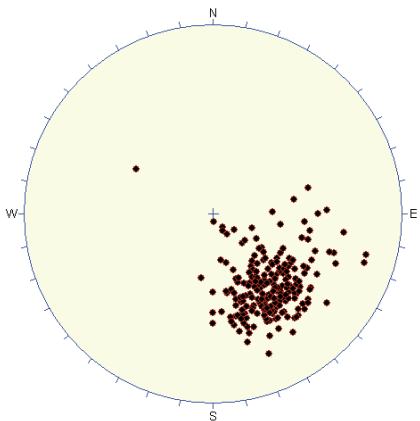
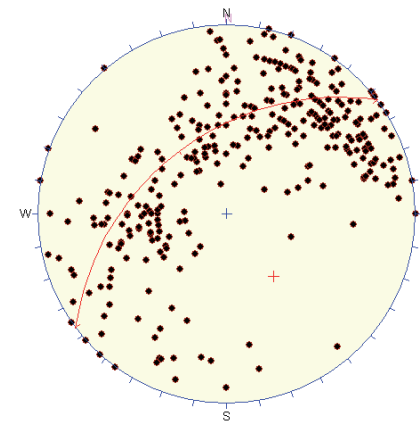
Pole to best-fit
great circle =
140/25

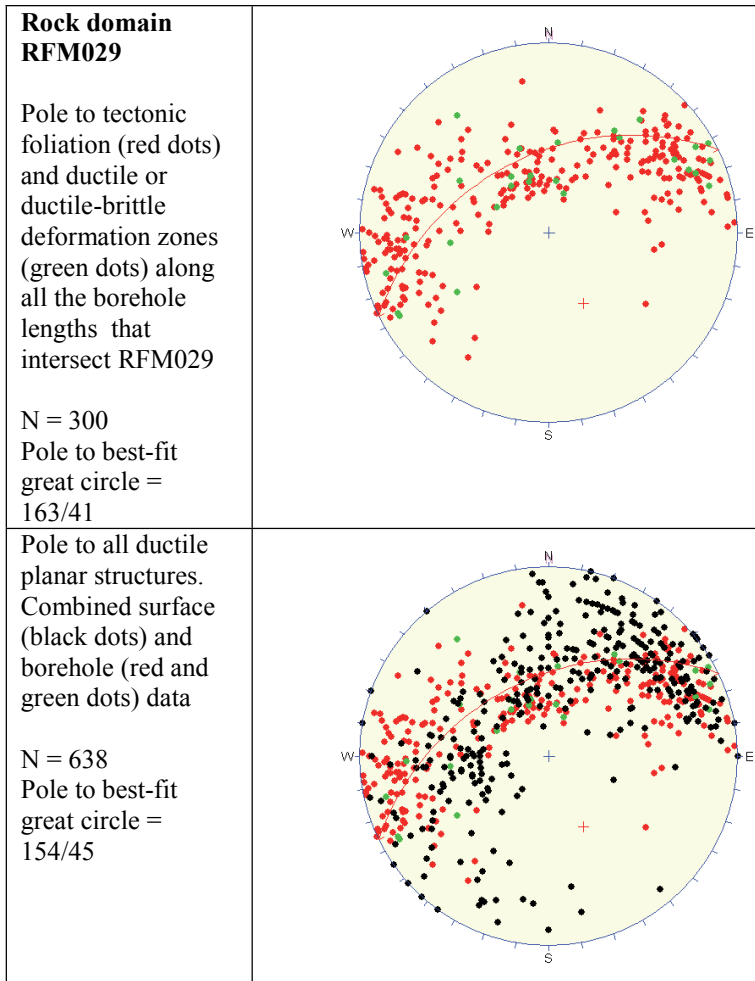


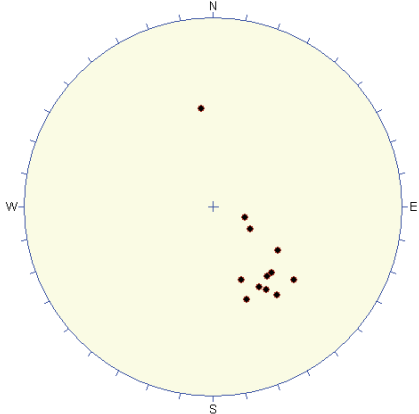
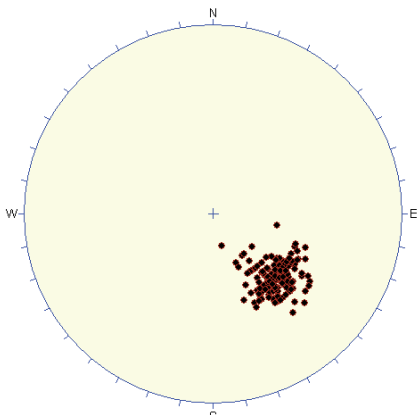
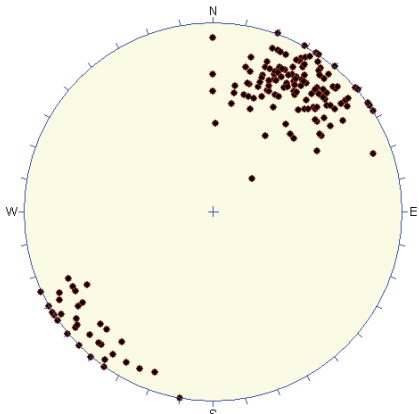
<p>Rock domain RFM024</p> <p>Fold axis</p> <p>N = 5 Fisher mean = 132/42 K value = 100</p>	
<p>Mineral stretching lineation</p> <p>N = 247 Fisher mean = 131/38 K value = 45</p>	
<p>Pole to tectonic foliation</p> <p>N = 69 Fisher mean = 118/73 K value = 18</p>	

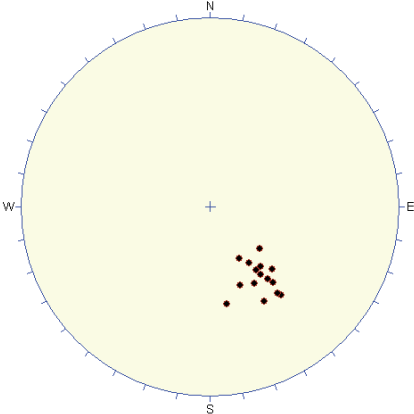
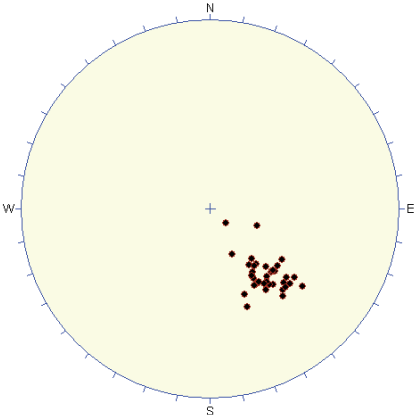
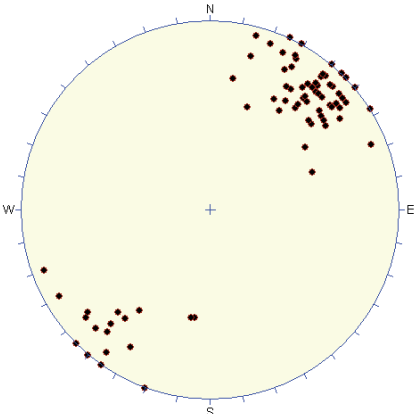
<p>Rock domain RFM025</p> <p>Fold axis</p> <p>N = 1</p>	
<p>Mineral stretching lineation</p> <p>N = 23</p> <p>Fisher mean = 145/42</p> <p>K value = 33</p>	
<p>Pole to tectonic foliation</p> <p>N = 47</p> <p>Fisher mean = 146/88</p> <p>K value = 44</p>	

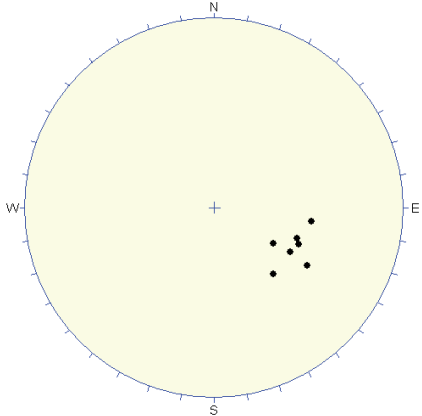
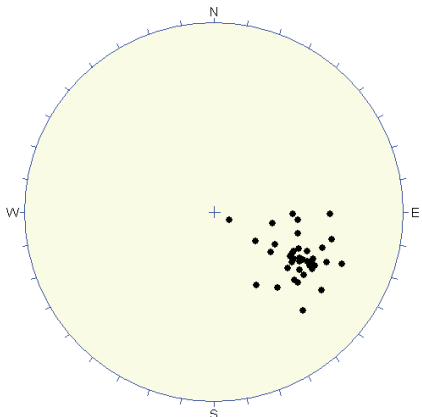
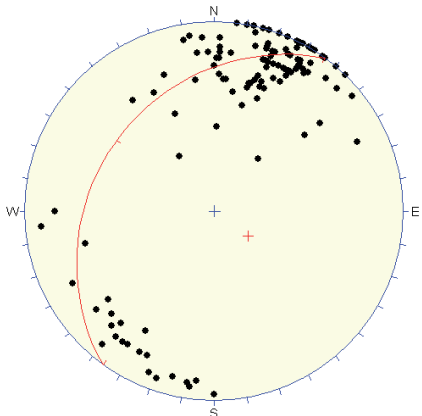
<p>Rock domain RFM026</p> <p>Fold axis</p> <p>N = 2</p>	
<p>Mineral stretching lineation</p> <p>N = 83</p> <p>Fisher mean = 139/41</p> <p>K value = 50</p>	
<p>Pole to tectonic foliation</p> <p>N = 91</p> <p>Fisher mean = 138/87</p> <p>K value = 23</p>	

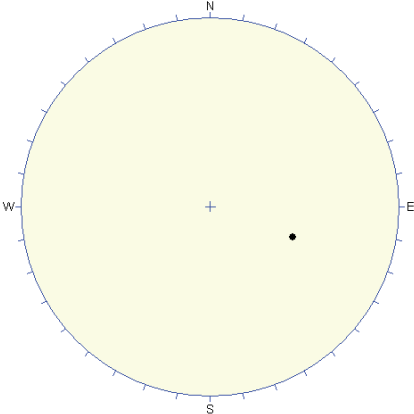
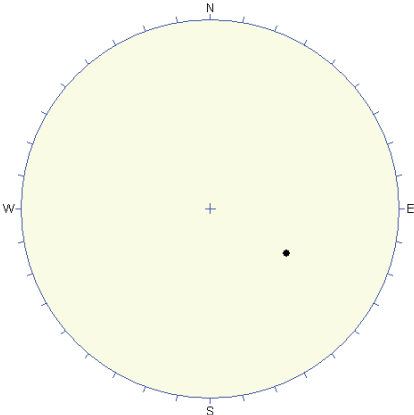
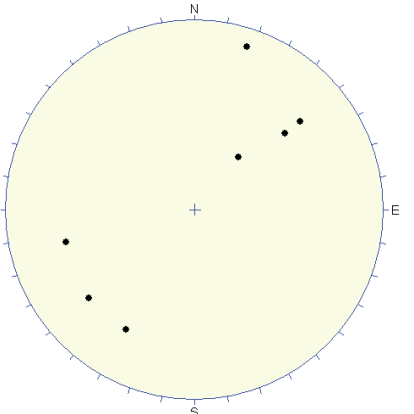
<p>Rock domain RFM029</p> <p>Fold axis</p> <p>N = 7 Fisher mean = 120/47 K value = 4</p> <p>Excluding one value that plunges to the NW</p> <p>N = 6 Fisher mean = 126/38 K value = 26</p>	
<p>Mineral stretching lineation</p> <p>N = 248 Fisher mean = 142/38 K value = 18</p>	
<p>Pole to tectonic foliation</p> <p>N = 338 Pole to best-fit great circle = 143/45</p>	

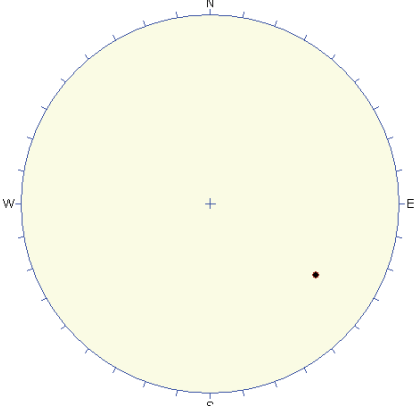
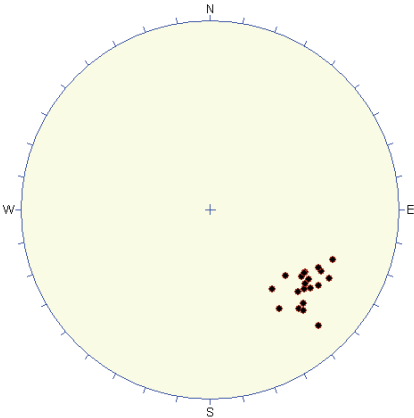
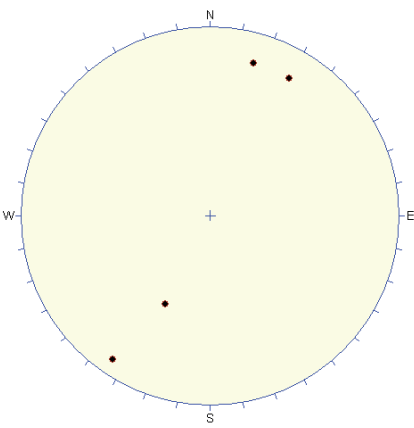


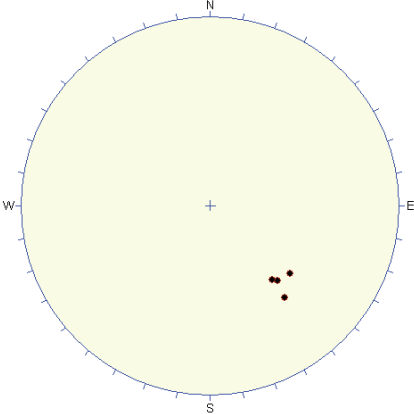
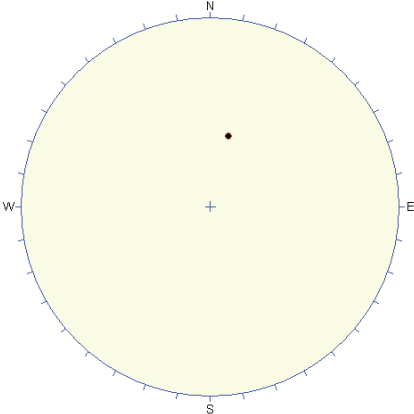
<p>Rock domain RFM030</p> <p>Fold axis</p> <p>N = 12 Fisher mean = 144/39 K value = 9</p>	
<p>Mineral stretching lineation</p> <p>N = 194 Fisher mean = 136/40 K value = 62</p>	
<p>Pole to tectonic foliation/banding</p> <p>N = 217 Fisher mean = 126/81 K value = 24</p>	

<p>Rock domain RFM031</p> <p>Fold axis</p> <p>N = 16 Fisher mean = 146/41 K value = 59</p>	
<p>Mineral stretching lineation</p> <p>N = 44 Fisher mean = 139/41 K value = 51</p>	
<p>Pole to tectonic foliation/banding</p> <p>N = 94 Fisher mean = 131/85 K value = 24</p>	

<p>Rock domain RFM032</p> <p>Fold axis</p> <p>N = 8 Fisher mean = 116/40 K value = 57</p>	 <p>A circular Wulff stereonet with a light yellow background. The perimeter is marked with tick marks and labeled with 'N' at the top, 'S' at the bottom, 'W' on the left, and 'E' on the right. A black crosshair is centered at the origin. Eight black dots representing data points are clustered in the eastern quadrant, roughly between 0 and 90 degrees longitude and 0 and 30 degrees latitude.</p>
<p>Mineral stretching lineation</p> <p>N = 45 Fisher mean = 118/37 K value = 51</p>	 <p>A circular Wulff stereonet with a light yellow background. The perimeter is marked with tick marks and labeled with 'N' at the top, 'S' at the bottom, 'W' on the left, and 'E' on the right. A black crosshair is centered at the origin. Forty-five black dots representing data points are clustered in the eastern quadrant, roughly between 0 and 90 degrees longitude and 0 and 30 degrees latitude, showing a slightly wider spread than the rock domain data.</p>
<p>Pole to tectonic foliation/banding</p> <p>N = 124 Pole to best-fit great circle = 126/65</p>	 <p>A circular Wulff stereonet with a light yellow background. The perimeter is marked with tick marks and labeled with 'N' at the top, 'S' at the bottom, 'W' on the left, and 'E' on the right. A black crosshair is centered at the origin. One hundred and twenty-four black dots representing data points are distributed along a great circle arc that passes through the center. A red line is drawn along this arc, representing the best-fit great circle. The arc is roughly oriented from the northwest to the southeast.</p>

<p>Rock domain RFM032 east of 1638000</p> <p>Fold axis</p> <p>N = 2</p>	
<p>Mineral stretching lineation</p> <p>N = 1</p>	
<p>Pole to tectonic foliation/banding</p> <p>N = 7 Fisher mean = 135/84 K value = 6</p>	

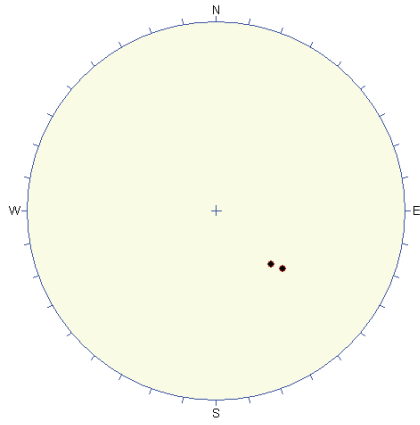
<p>Rock domain RFM033</p> <p>Fold axis</p> <p>N = 1</p>	
<p>Mineral stretching lineation</p> <p>N = 22</p> <p>Fisher mean = 129/24</p> <p>K value = 71</p>	
<p>Pole to tectonic foliation</p> <p>N = 4</p>	

<p>Rock domain RFM035</p> <p>Mineral stretching lineation</p> <p>N = 4 Fisher mean = 137/32 K value = 179</p>	
<p>Pole to tectonic foliation</p> <p>N = 1</p>	

Rock domain
RFM036

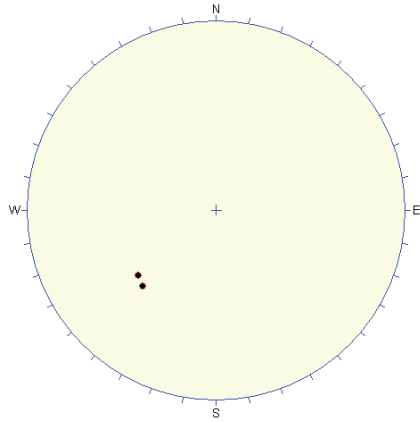
Fold axis

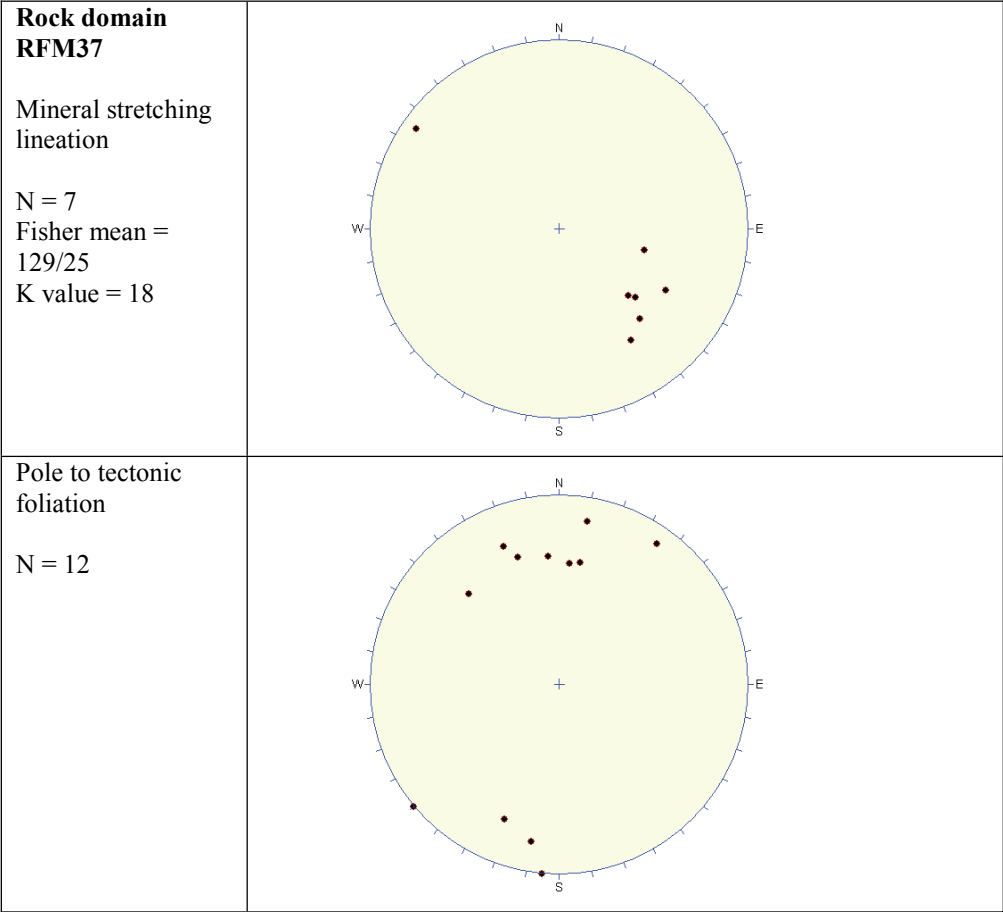
N = 2

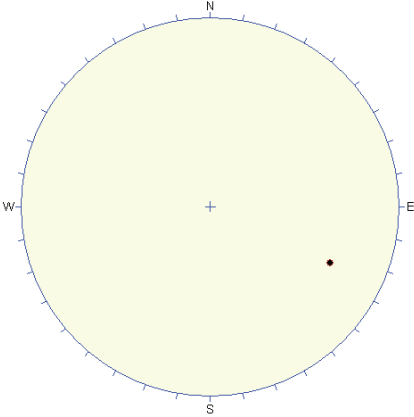
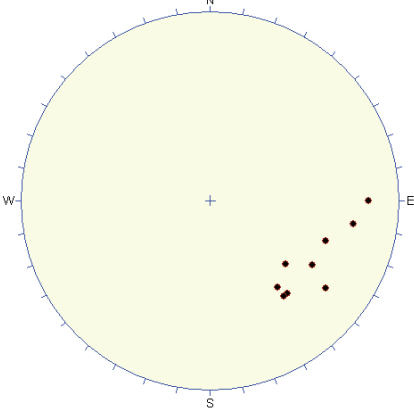
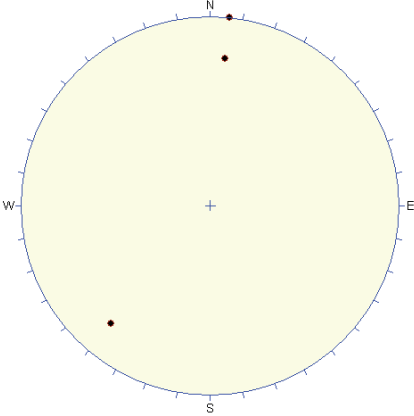


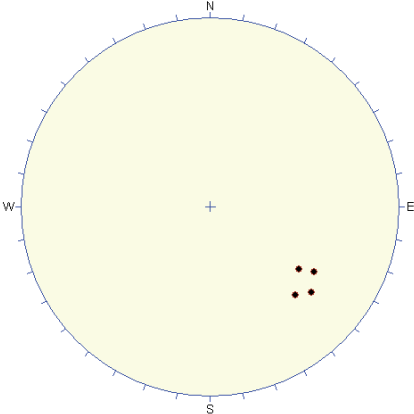
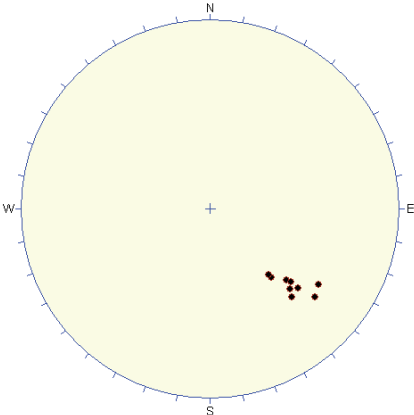
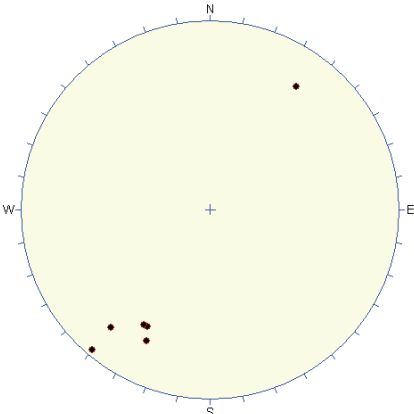
Pole to tectonic
foliation/banding

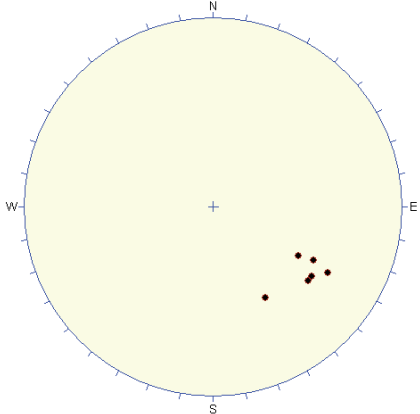
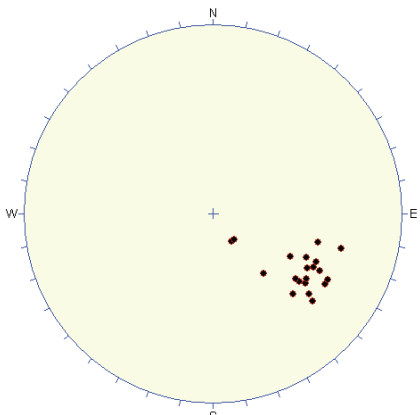
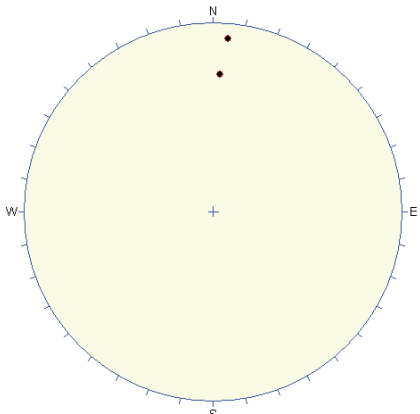
N = 2

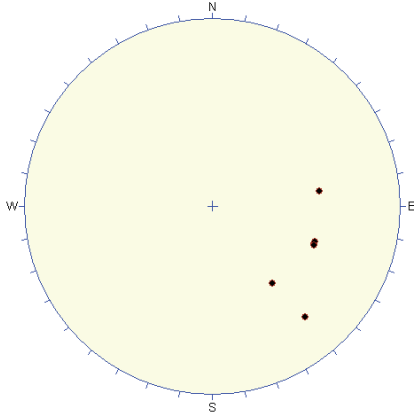
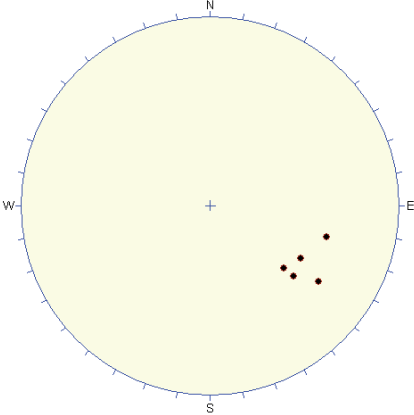
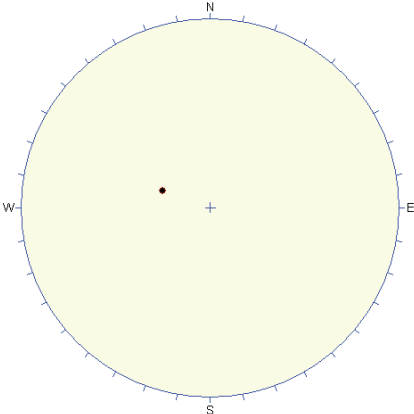




<p>Rock domain RFM038</p> <p>Fold axis</p> <p>N = 1</p>	 <p>A circular Wulff net plot with a central cross and tick marks around the perimeter. The cardinal directions are labeled: N at the top, S at the bottom, W on the left, and E on the right. A single black dot representing a data point is located in the ESE quadrant, approximately at 30 degrees from the E axis and 30 degrees from the S axis.</p>
<p>Mineral stretching lineation</p> <p>N = 11</p> <p>Fisher mean = 126/24</p> <p>K value = 19</p>	 <p>A circular Wulff net plot with a central cross and tick marks around the perimeter. The cardinal directions are labeled: N at the top, S at the bottom, W on the left, and E on the right. Eleven black dots representing data points are clustered in the ESE quadrant, roughly between 15 and 45 degrees from the E axis and 15 and 45 degrees from the S axis.</p>
<p>Pole to tectonic foliation</p> <p>N = 3</p>	 <p>A circular Wulff net plot with a central cross and tick marks around the perimeter. The cardinal directions are labeled: N at the top, S at the bottom, W on the left, and E on the right. Three black dots representing data points are located: one near the N axis (top), one near the E axis (right), and one near the W axis (left).</p>

<p>Rock domain RFM039</p> <p>Fold axis</p> <p>N = 4 Fisher mean = 128/26 K value = 151</p>	
<p>Mineral stretching lineation</p> <p>N = 9 Fisher mean = 133/29 K value = 96</p>	
<p>Pole to tectonic foliation</p> <p>N = 6 Fisher mean = 303/81 K value = 33</p>	

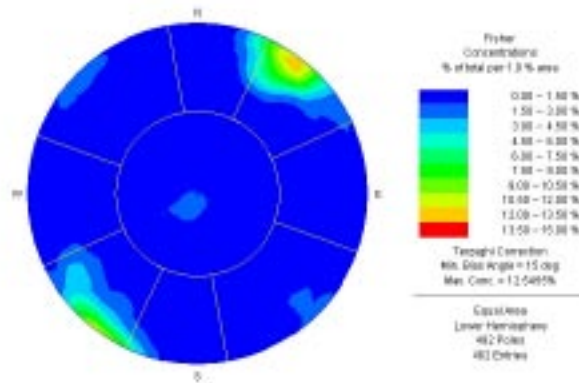
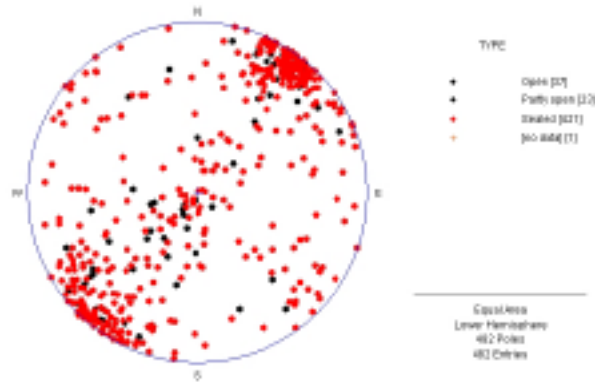
<p>Rock domain RFM040</p> <p>Fold axis</p> <p>N = 7 Fisher mean = 126/27 K value = 52</p>	
<p>Mineral stretching lineation</p> <p>N = 21 Fisher mean = 123/32 K value = 25</p>	
<p>Pole to tectonic foliation/banding</p> <p>N = 2</p>	

<p>Rock domain RFM041</p> <p>Fold axis</p> <p>N = 6 Fisher mean = 116/30 K value = 15</p>	 <p>A circular Wulff net plot with a light yellow background and a blue border. The plot is marked with cardinal directions: N at the top, S at the bottom, W on the left, and E on the right. A central crosshair is present. Six dark red data points are plotted, clustered in the eastern-southern quadrant, indicating a fold axis orientation.</p>
<p>Mineral stretching lineation</p> <p>N = 5 Fisher mean = 122/29 K value = 54</p>	 <p>A circular Wulff net plot with a light yellow background and a blue border. The plot is marked with cardinal directions: N at the top, S at the bottom, W on the left, and E on the right. A central crosshair is present. Five dark red data points are plotted, clustered in the eastern-southern quadrant, indicating a mineral stretching lineation orientation.</p>
<p>Pole to tectonic foliation/banding</p> <p>N = 1</p>	 <p>A circular Wulff net plot with a light yellow background and a blue border. The plot is marked with cardinal directions: N at the top, S at the bottom, W on the left, and E on the right. A central crosshair is present. One dark red data point is plotted in the western-southern quadrant, representing the pole to tectonic foliation/banding.</p>

Orientation of fractures in deterministic deformation zones

The orientations of fractures (open, partly open and sealed) in each deterministic deformation zone are presented as poles to planes in the lower hemisphere of an equal area stereographic projection. The total number of oriented fractures (poles) along each zone is indicated. The number of poles in an identified fracture set and both the Fisher mean value and the K value for the poles in the identified set are also provided. Fracture sets have been identified in a contoured stereographic plot, according to the procedure described in the main text of this report (Section 3.1). For some zones, alternative boundaries between fracture sets have been chosen and are shown in different contoured stereographic plots.

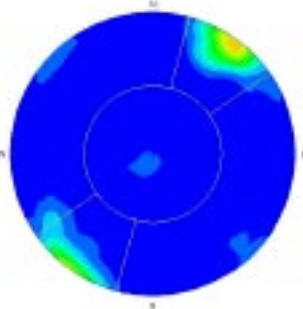
ZFMNW003 A-F



NW fracture set in the contoured stereographic plot above:
 276 poles
 K value = 17
 Mean pole = 040/02

Gently-dipping fracture set in the contoured stereographic plot above:
 77 poles
 K value = 12
 Mean pole = 209/86

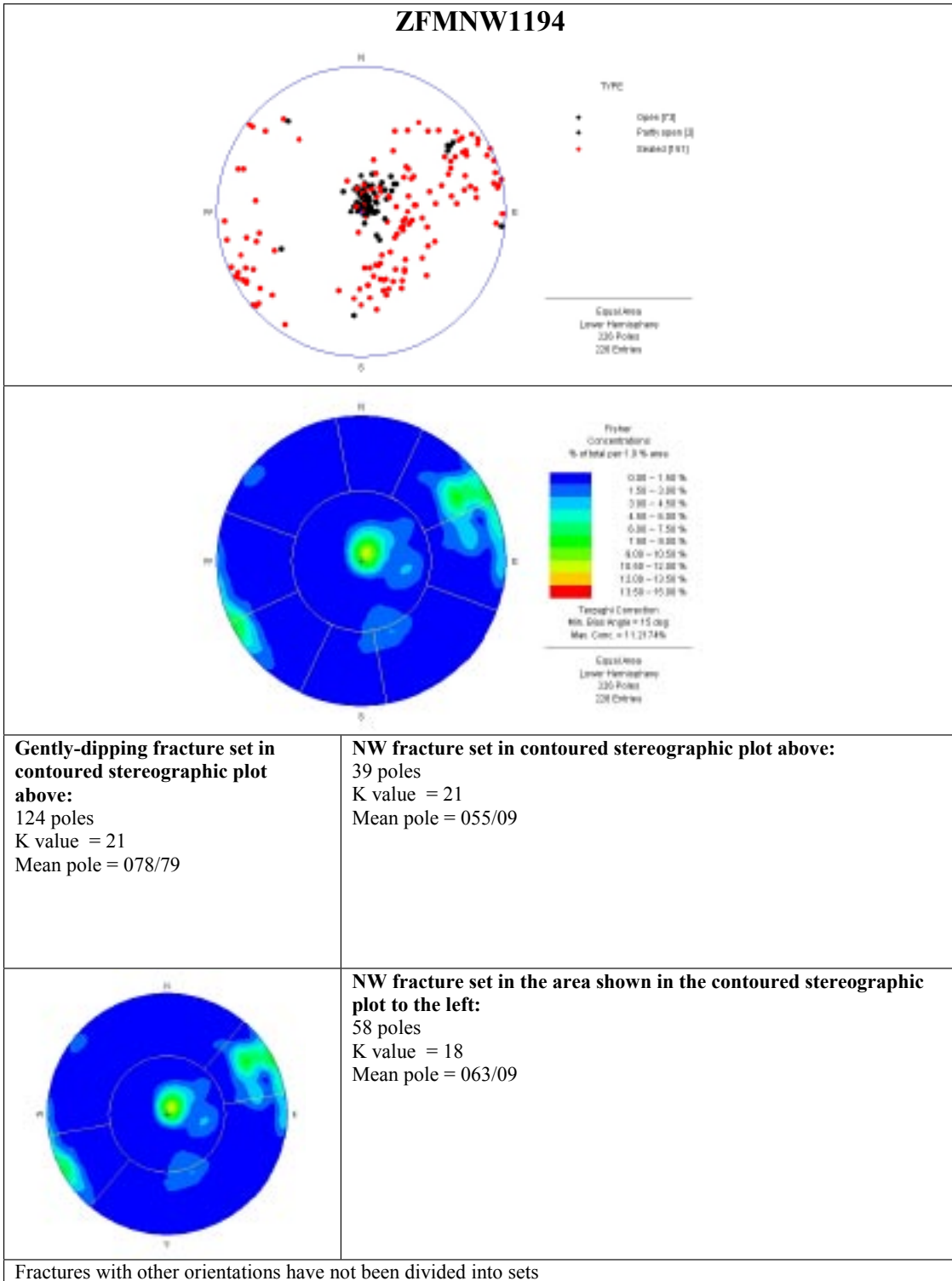
NE fracture set in the contoured stereographic plot above:
 52 poles
 K value = 10
 Mean pole = 137/01



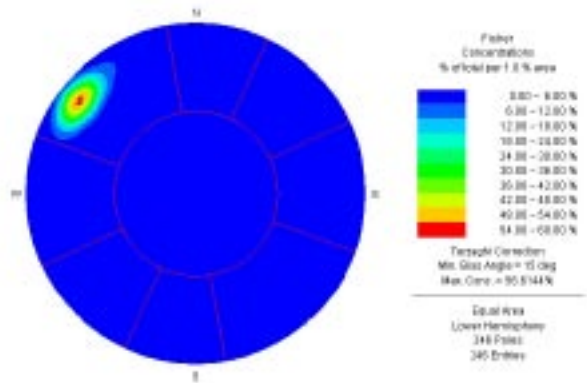
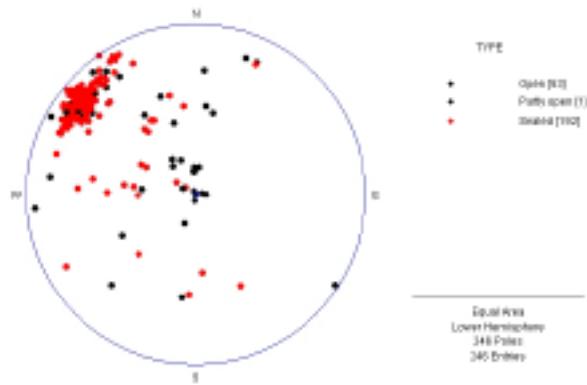
NW fracture set in the area shown in the contoured stereographic plot to the left:
 273 poles
 K value = 20
 Mean pole = 036/03

Fractures with other orientations have not been divided into sets

ZFMNW1194



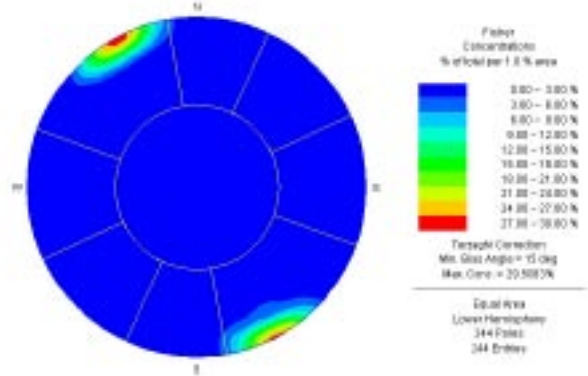
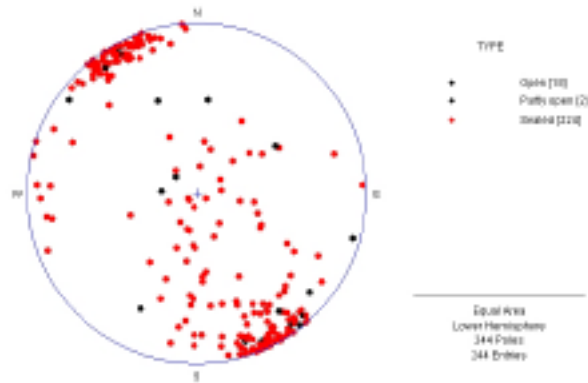
ZFMNE0061



NE fracture set:
197 poles
K value = 69
Mean pole = 310/14

Fractures with other orientations have not been divided into sets

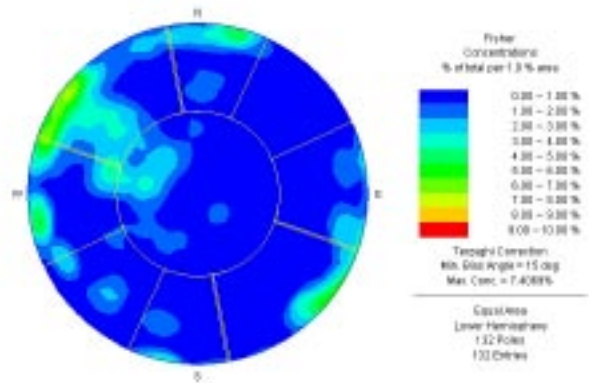
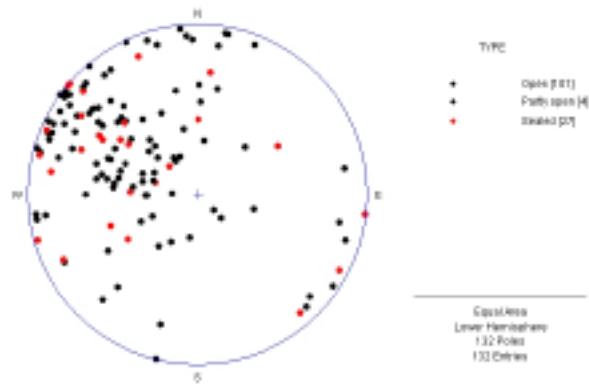
ZFMNE0062A, B



NE fracture set:
176 poles
K value = 33
Mean pole = 151/0

Fractures with other orientations have not been divided into sets

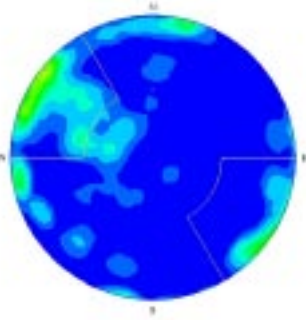
ZFMNE0065



NE fracture set in the contoured stereographic plot above:
 55 poles
 K value = 14
 Mean pole = 311/14

NS fracture set in the contoured stereographic plot above:
 24 poles
 K value = 13
 Mean pole = 274/09

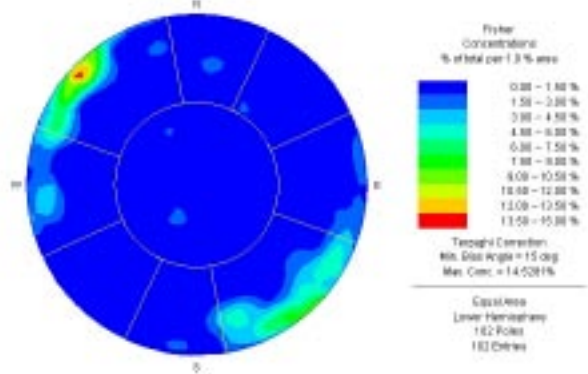
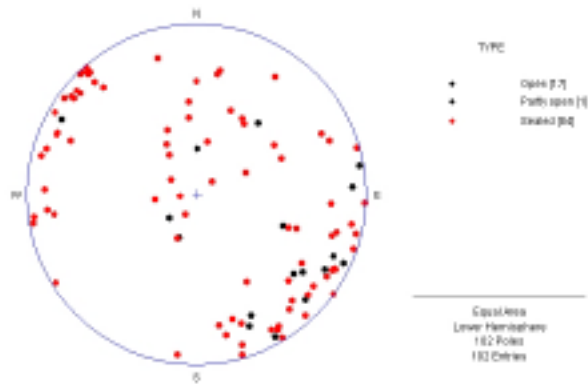
EW fracture set in the contoured stereographic plot above:
 13 poles
 K value = 18
 Mean pole = 009/07



NE fracture set in the area shown in the contoured stereographic plot to the left:
 66 poles
 K value = 13
 Mean pole = 300/13

Fractures with other orientations have not been divided into sets

ZFMNE103A, B



NE fracture set:

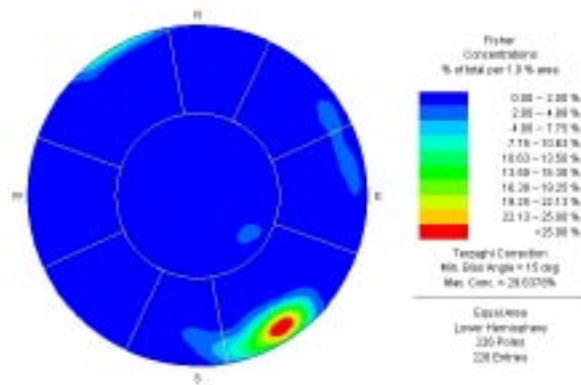
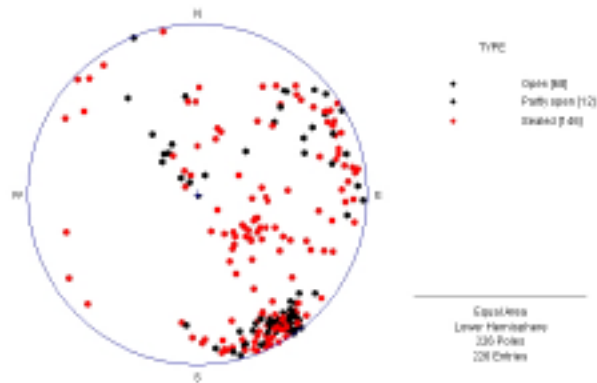
54 poles
 K value = 15
 Mean pole = 137/03

NS fracture set:

22 poles
 K value = 15
 Mean pole = 092/03

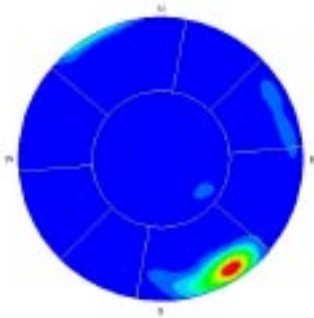
Fractures with other orientations have not been divided into sets

ZFMNE0401



NE fracture set in contoured stereographic plot above:

115 poles
K value = 33
Mean pole = 149/09



NE fracture set in the area shown in the contoured stereographic plot to the left:

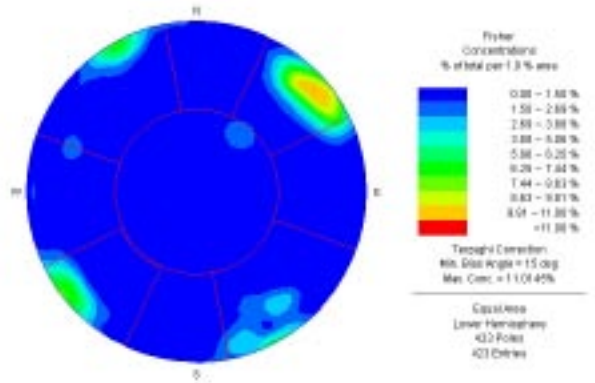
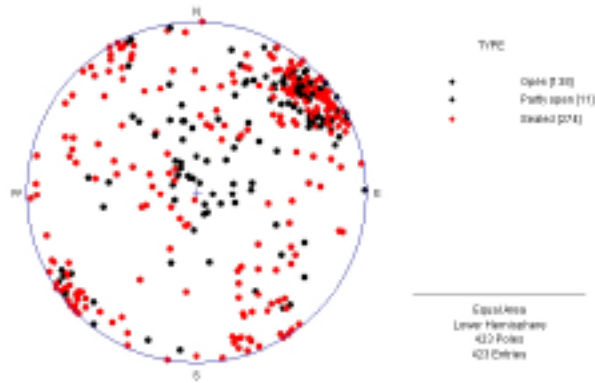
116 poles
K value = 29
Mean pole = 152/09

NW fracture set in the area shown in the contoured stereographic plot to the left:

38 poles
K value = 21
Mean pole = 064/09

Fractures with other orientations have not been divided into sets

ZFMNE1188

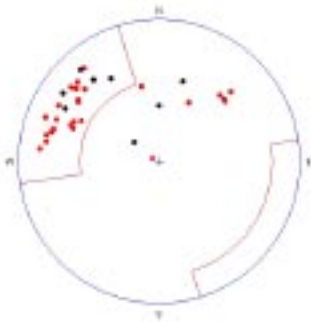
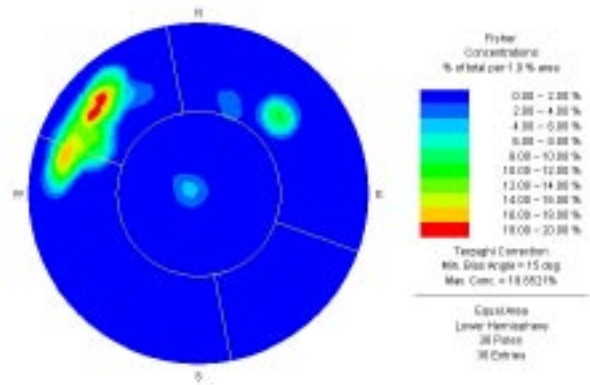
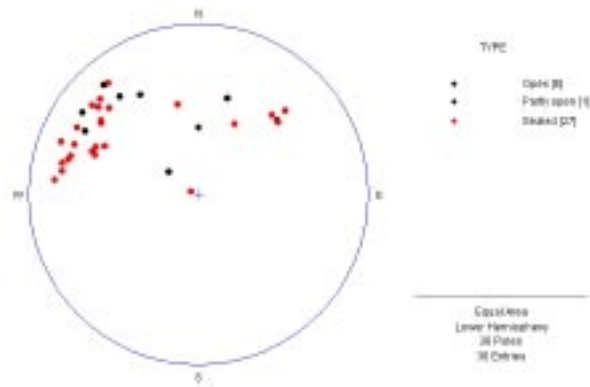


NW fracture set:
215 poles
K value = 27
Mean pole = 049/06

NE fracture set:
77 poles
K value = 12
Mean pole = 147/04

Fractures with other orientations have not been divided into sets

ZFMNE1189

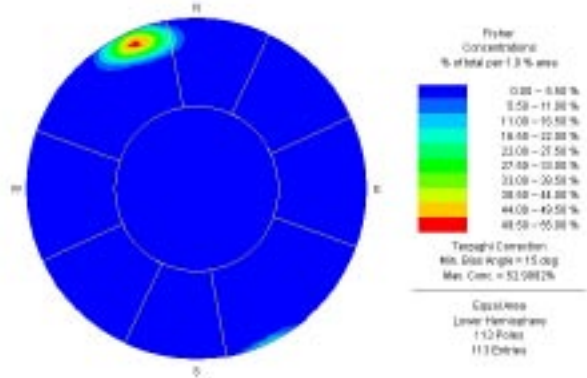
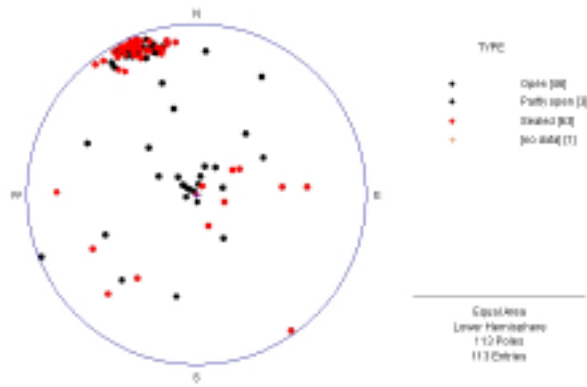


NE fracture set in contoured stereographic plot above:
 20 poles
 K value = 33
 Mean pole = 308/25

NE fracture set in the area shown in the stereographic plot to the left:
 24 poles
 K value = 29
 Mean pole = 301/24

Fractures with other orientations have not been divided into sets

ZFMNE1192

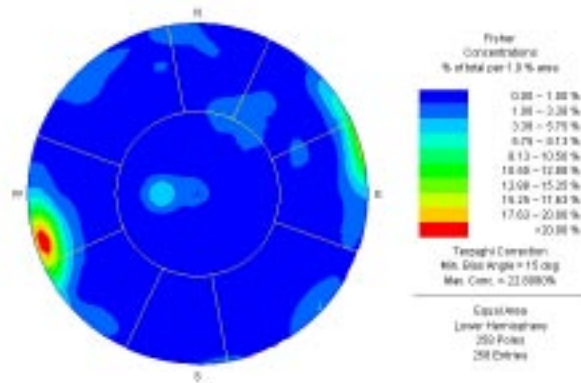
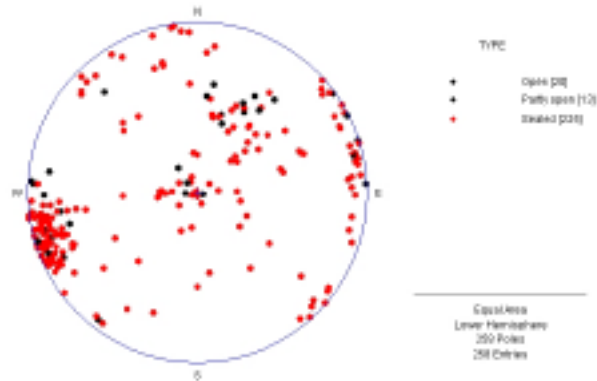


NE fracture set:
 71 poles
 K value = 87
 Mean pole = 337/09

Gently-dipping fracture set:
 29 poles
 K value = 25
 Mean pole = 025/84

Fractures with other orientations have not been divided into sets

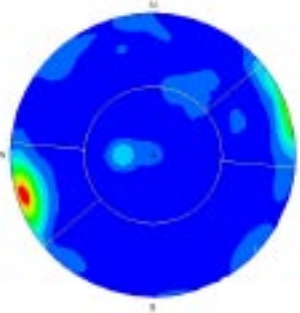
ZFMNS0404



NS fracture set in contoured stereographic plot above:
 110 poles
 K value = 33
 Mean pole = 257/04

Gently-dipping fracture set in contoured stereographic plot above:
 68 poles
 K value = 13
 Mean pole = 344/83

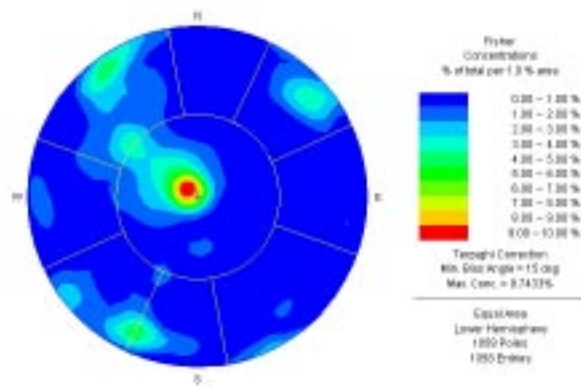
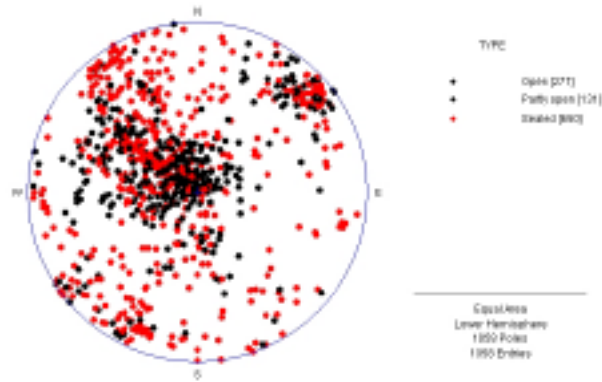
NE fracture set in contoured stereographic plot above:
 25 poles
 K value = 15
 Mean pole = 319/03



NS fracture set in the area shown in the contoured stereographic plot to the left:
 132 poles
 K value = 29
 Mean pole = 252/03

Fractures with other orientations have not been divided into sets

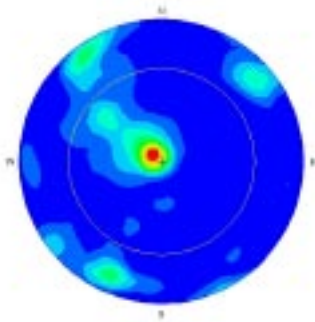
**ZFMNE00A2 at deeper crustal levels in KFM02A (DZ6)
and KFM04A (DZ1, DZ2 and DZ3)**



Gently-dipping fracture set in contoured stereographic plot above :
534 poles
K value = 18
Mean pole = 297/79

NE fracture set in contoured stereographic plot above:
218 poles
K value = 10
Mean pole = 323/15

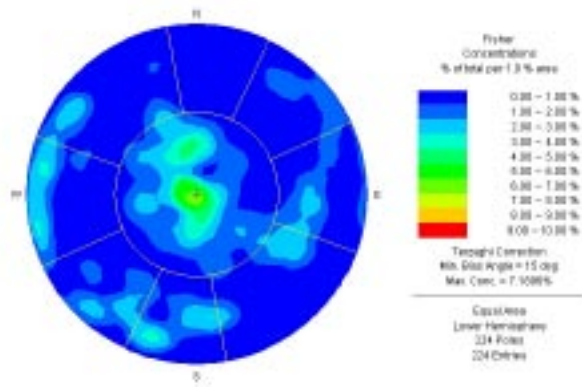
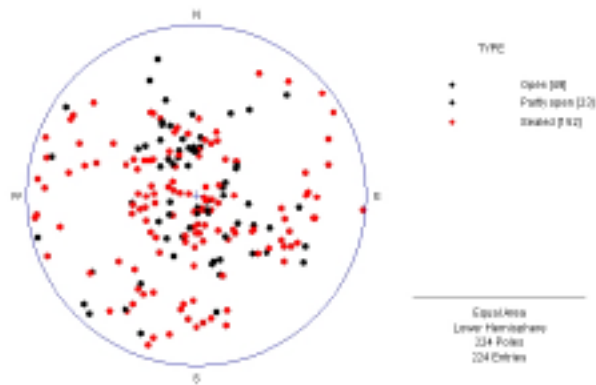
NW fracture set in contoured stereographic plot above:
183 poles
K value = 13
Mean pole = 223/2



Gently-dipping fracture set in the area shown in the contoured stereographic plot to the left:
672 poles
K value = 9
Mean pole = 295/75

Fractures with other orientations have not been divided into sets

ZFMNE00A3

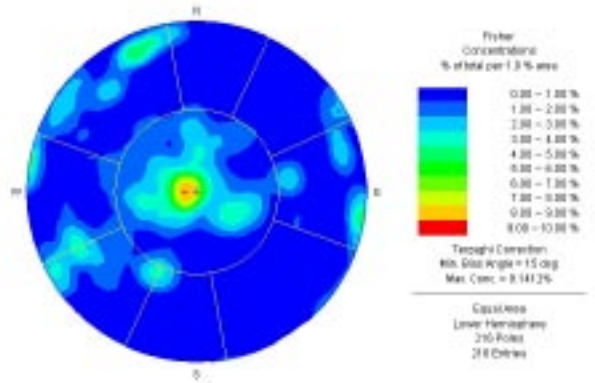
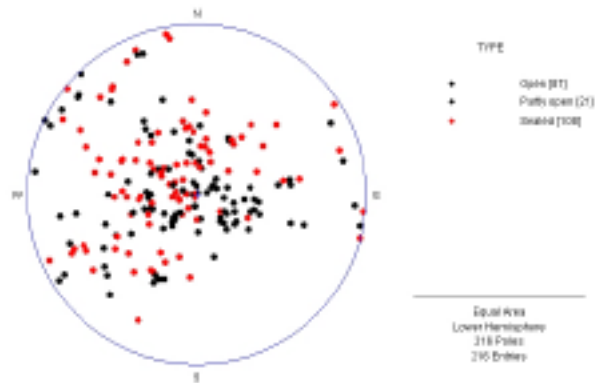


Gently-dipping fracture set:

139 poles
K value = 13
Mean pole = 304/86

Fractures with other orientations have not been divided into sets

ZFMNE00A4



Gently-dipping fracture set:

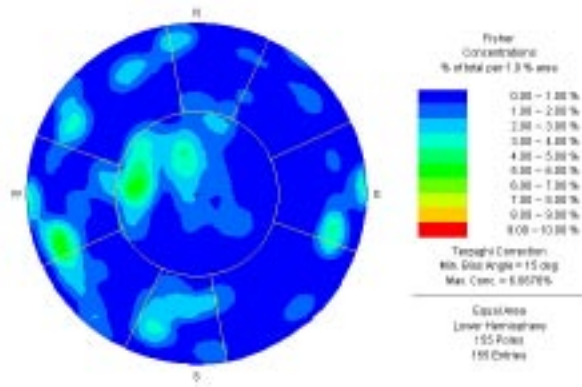
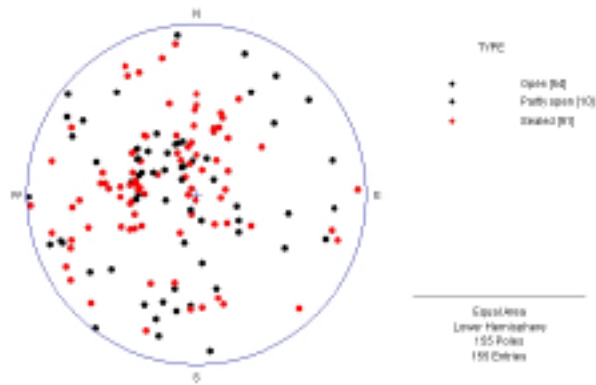
139 poles

K value = 13

Mean pole = 312/86

Fractures with other orientations have not been divided into sets

ZFMNE00A5



Gently-dipping fracture set

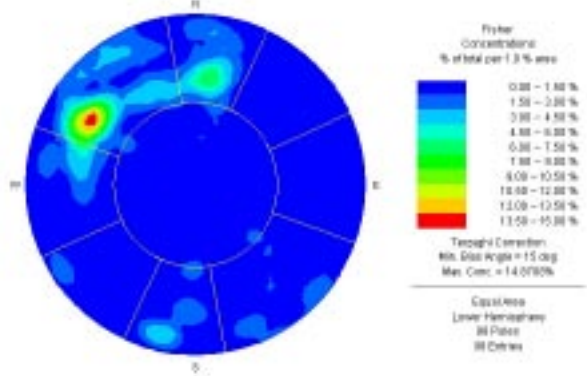
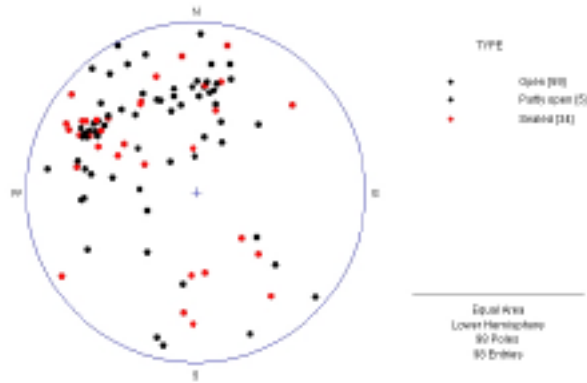
83 poles

K value = 12

Mean pole = 308/76

Fractures with other orientations have not been divided into sets

ZFMNE00A6

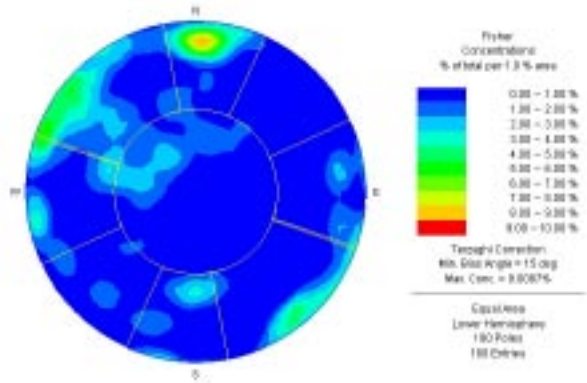
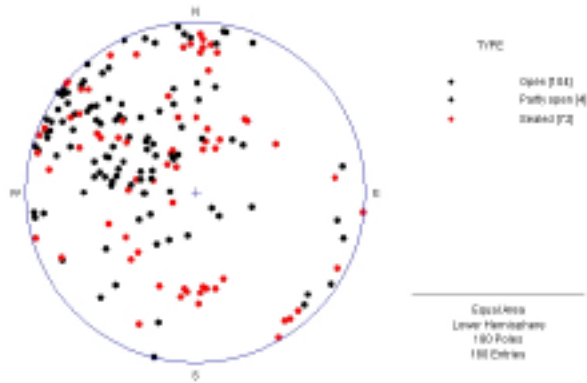


NE fracture set:
46 poles from 46 Entries
K value = 11
Mean pole = 315/20

EW fracture set:
24 poles
K value = 9
Mean pole = 007/15

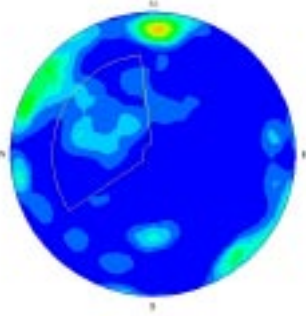
Fractures with other orientations have not been divided into sets

ZFMNE00A7



NE fracture set in contoured stereographic plot above:
 68 poles
 K value = 12
 Mean pole = 313/11

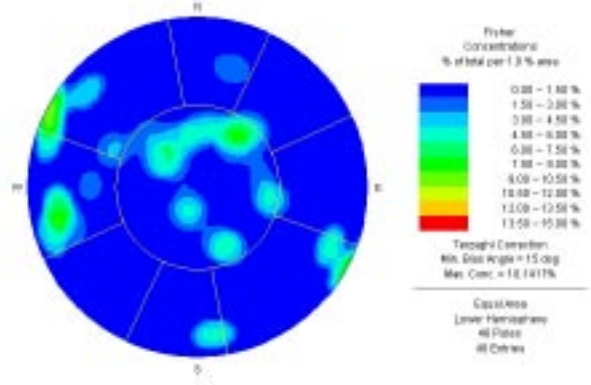
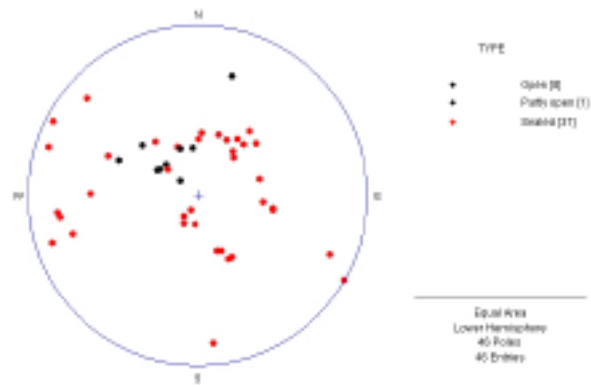
EW fracture set in contoured stereographic plot above:
 31 poles
 K value = 11
 Mean pole = 006/1



Gently-dipping fracture set in the area shown in the contoured stereographic plot to the left:
 61 poles
 K value = 15
 Mean pole = 298/56

Fractures with other orientations have not been divided into sets

ZFMNE00B1



Gently-dipping fracture set

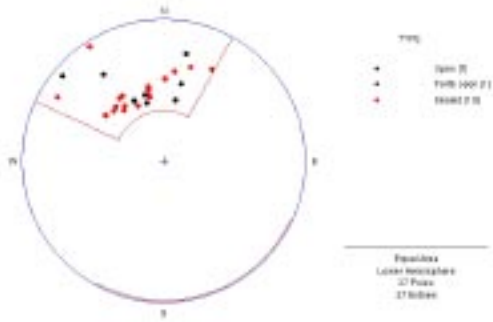
32 poles

K value = 9

Mean pole = 038/78

Fractures with other orientations have not been divided into sets

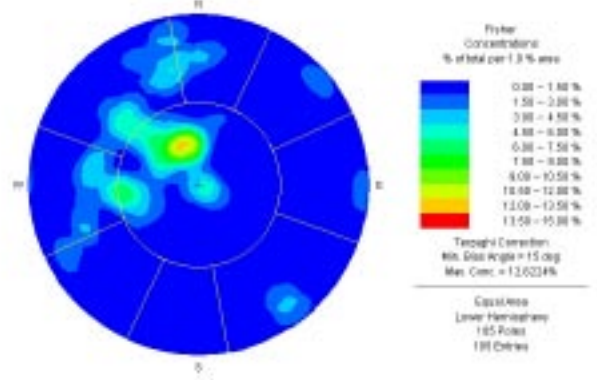
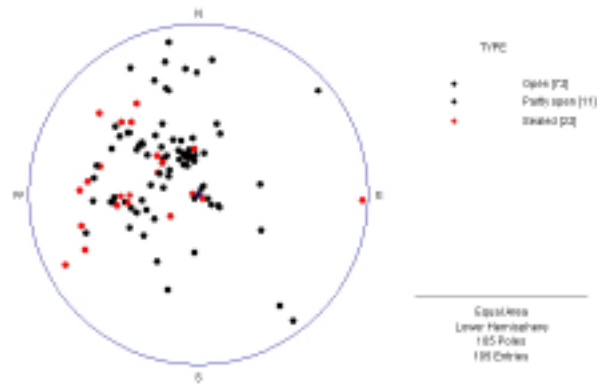
ZFMNE00B4



All fractures:
27 poles
K value = 9
Mean pole = 338/38

Few data. No contoured plot and no division into fracture sets carried out

ZFMNE00B6



Gently-dipping fracture set:

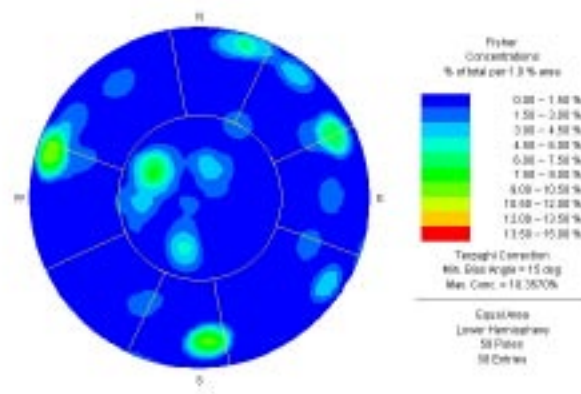
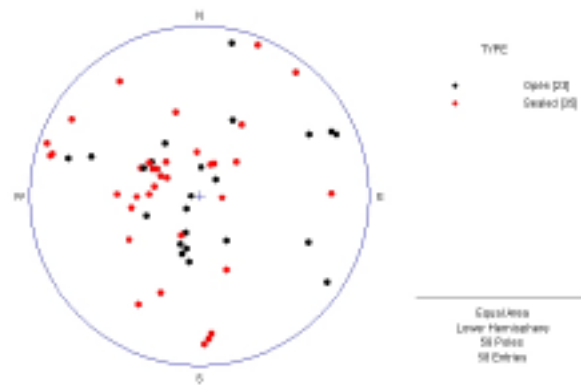
67 poles

K value = 15

Mean pole = 038/15

Fractures with other orientations have not been divided into sets

ZFMNE0866



Gently-dipping fracture set:

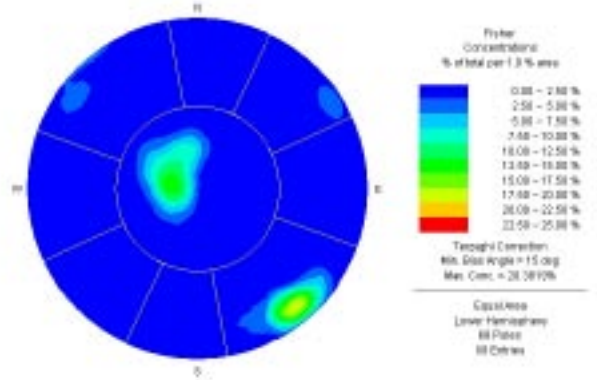
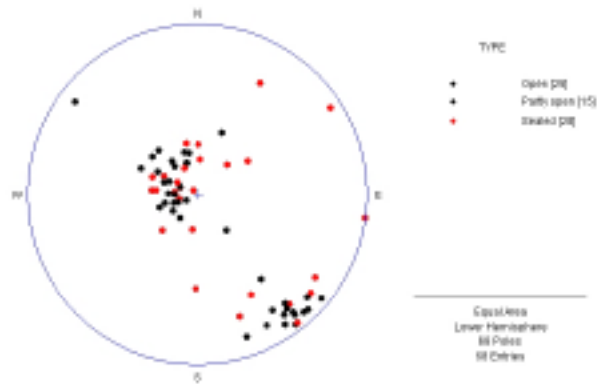
32 poles

K value = 13

Mean pole = 001/11

Fractures with other orientations have not been divided into sets

ZFMNE1187



Gently-dipping fracture set:

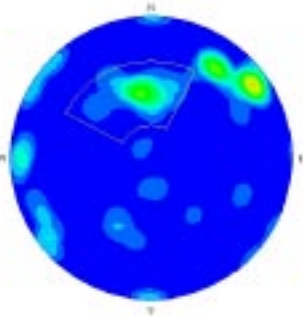
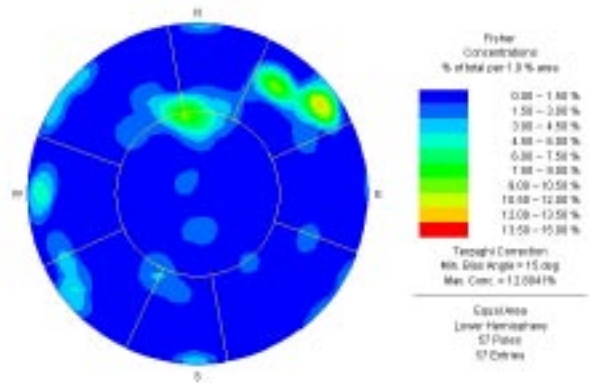
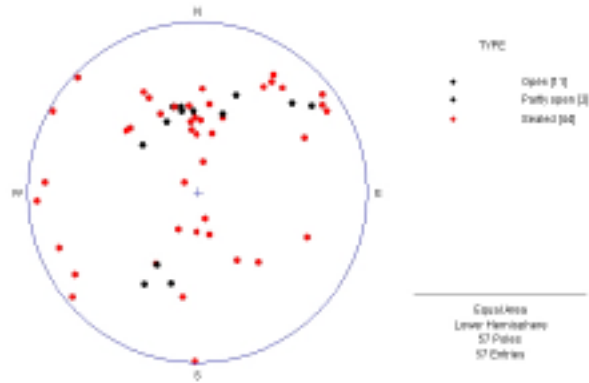
41 poles
 K value = 28
 Mean pole = 307/78

NE fracture set:

23 poles
 K value = 34
 Mean pole = 141/12

Fractures with other orientations have not been divided into sets

ZFMNE1195



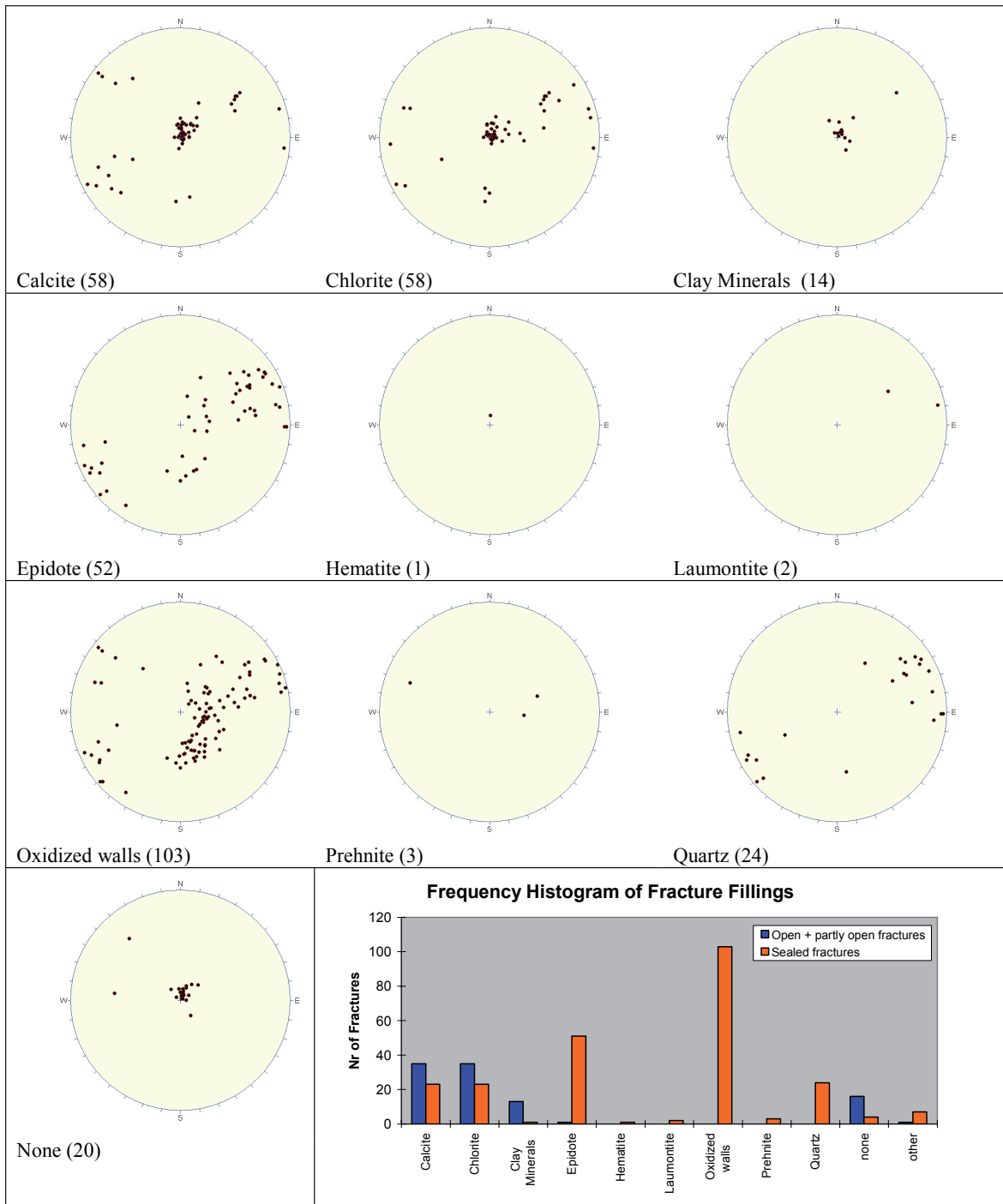
Moderately-dipping fracture set in the area shown in the contoured stereographic plot to the left:
 24 poles
 K value = 28
 Mean pole = 350/50

Fractures with other orientations have not been divided into sets

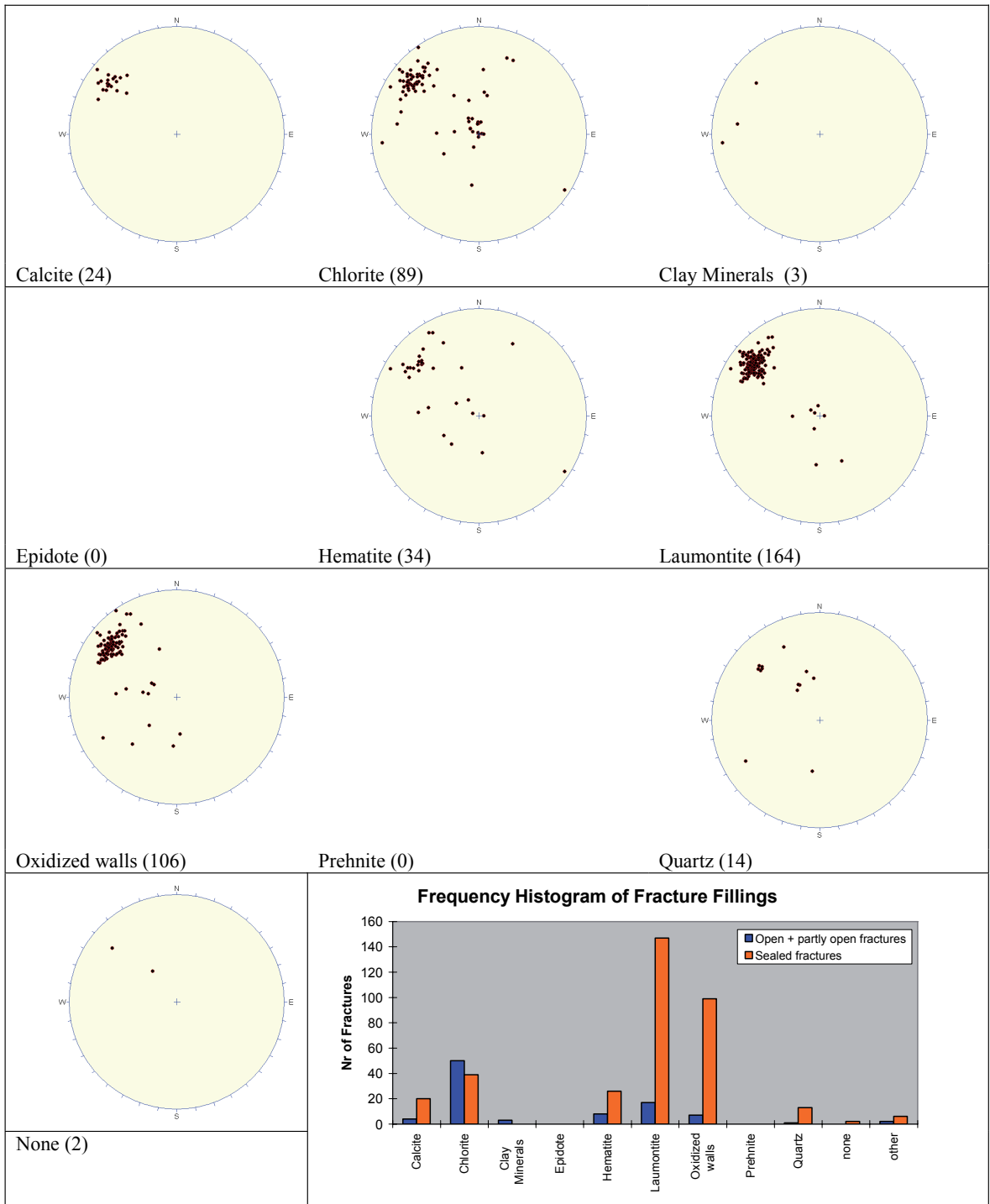
Mineral coating or filling along fractures in deterministic deformation zones

The minerals commonly present as coatings or fillings along fractures in each deterministic deformation zone are shown in the form of a histogram and a series of equal area stereographic projections for each zone. Only data from the fixed point intersections in cored boreholes are analysed here (see Section 3.1). The selection of these minerals is also addressed in the main text in this report (see Section 3.1).

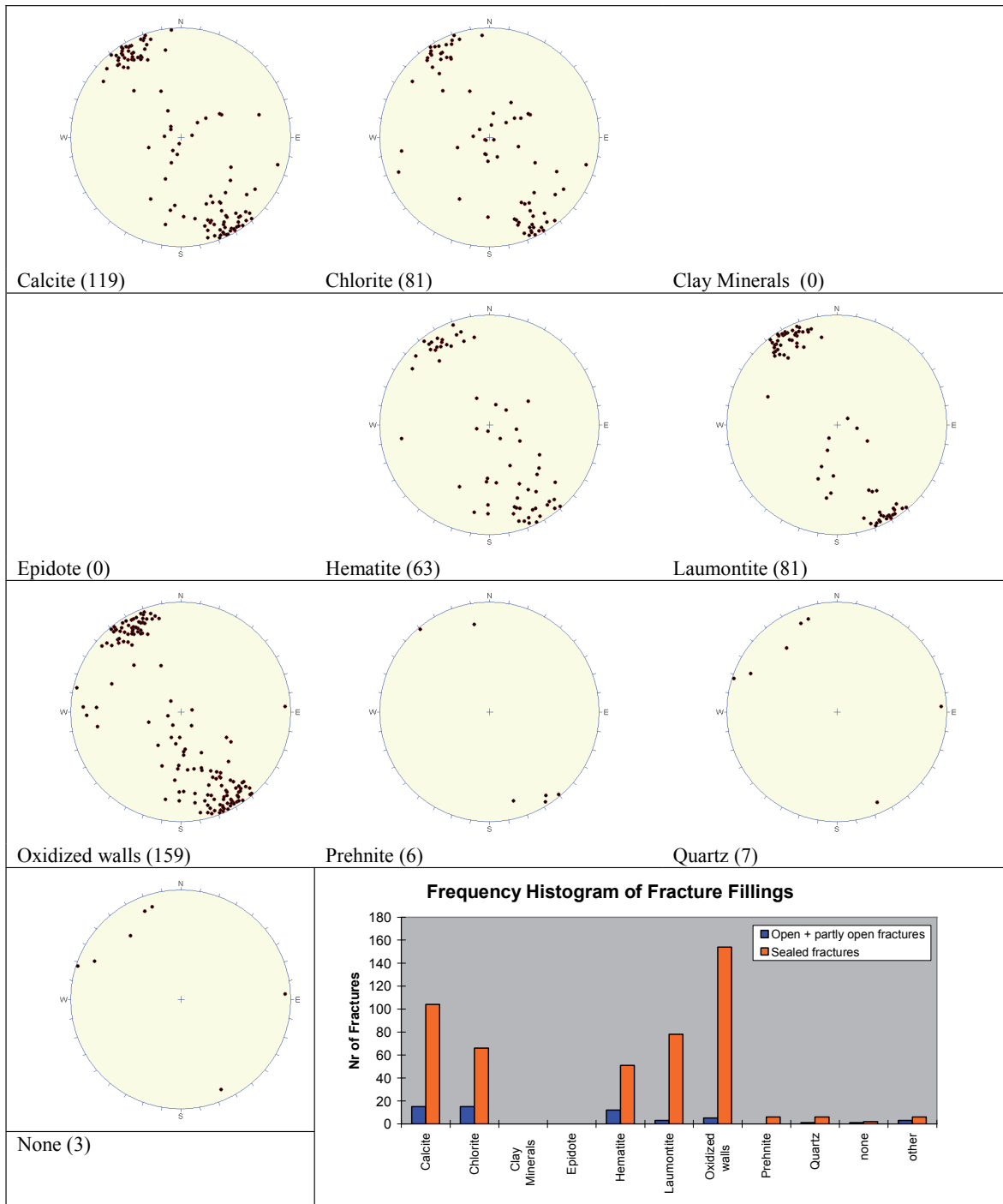
Mineral coatings or fillings along open and partly open fractures are distinguished from those along sealed fractures in the histogram. For each zone, the orientations of fractures that contain a particular mineral filling or coating are presented as poles to planes in the lower hemisphere of a series of equal area stereographic projections. The number of oriented fractures that contain a particular mineral coating or filling is indicated in parentheses.



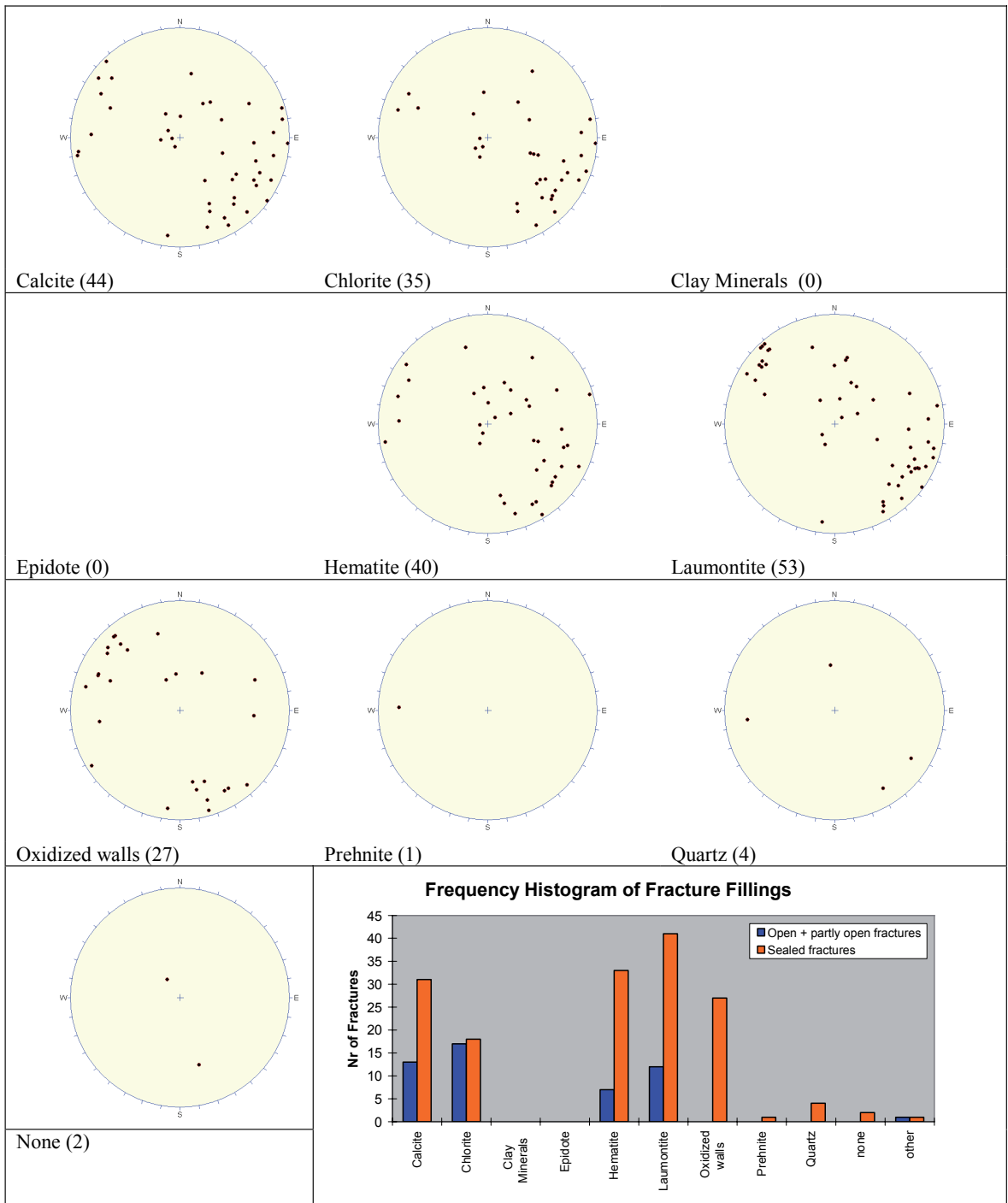
ZFMNW1194



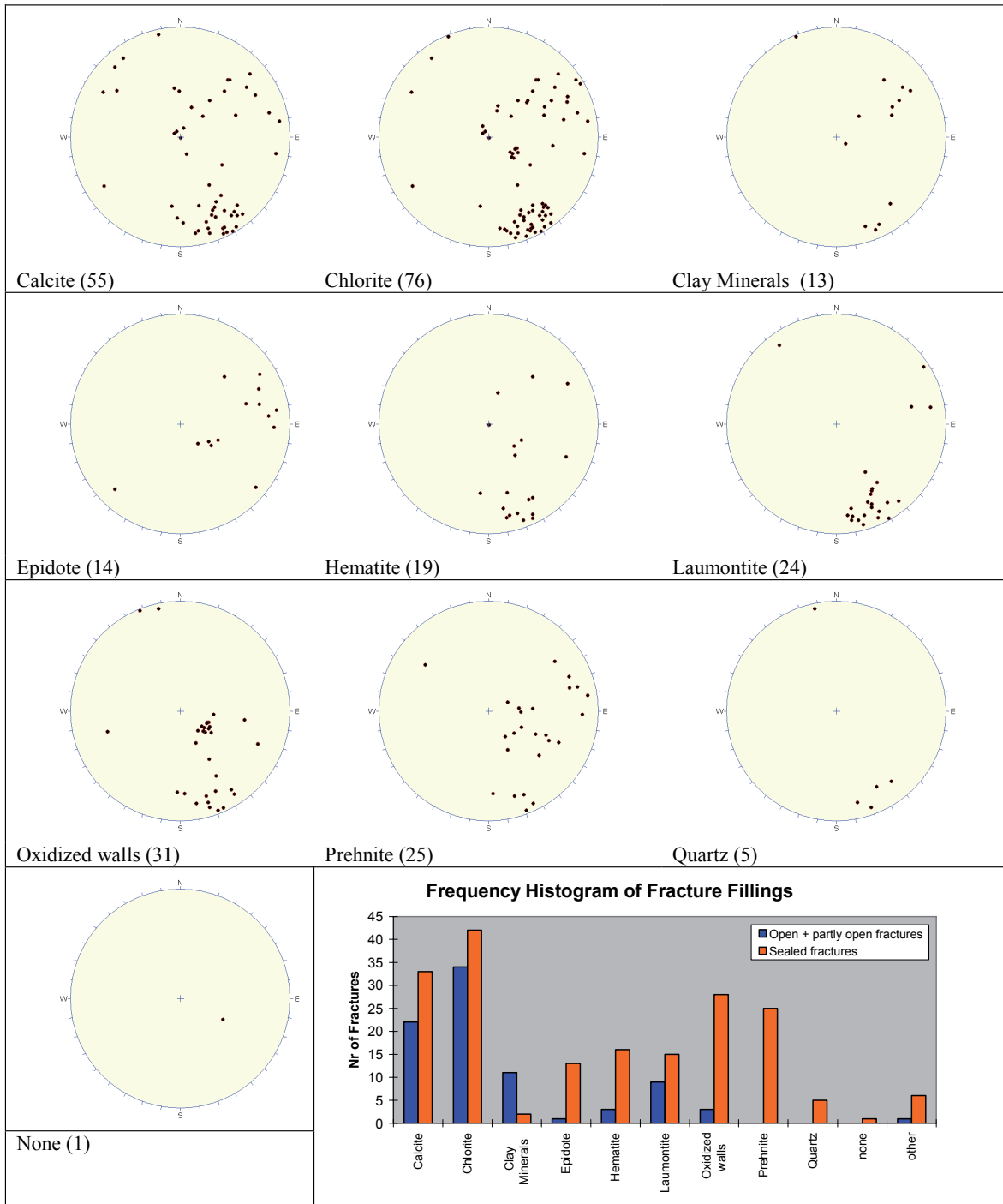
ZFMNE0061



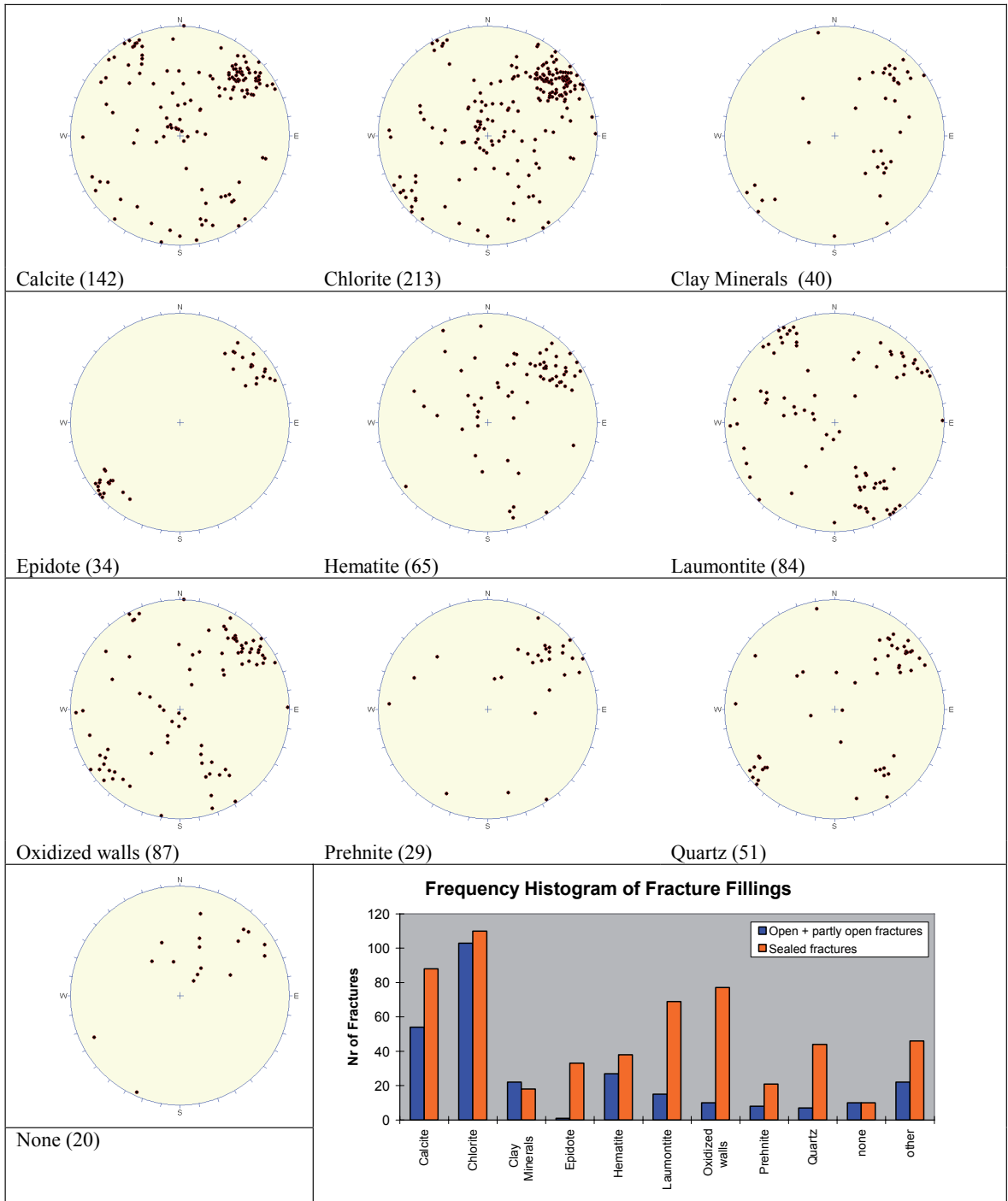
ZFMNE062A, B



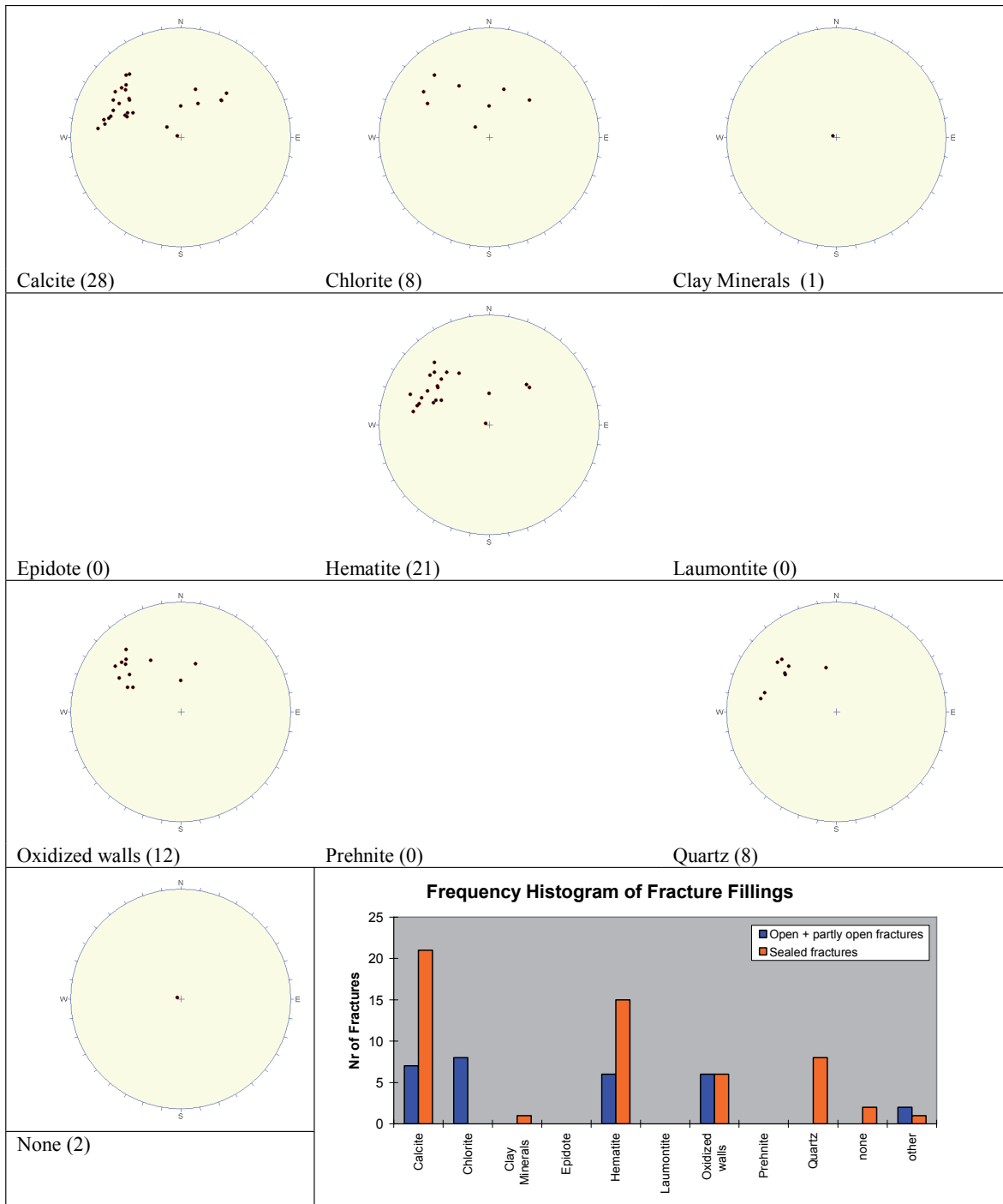
ZFMNE103A, B



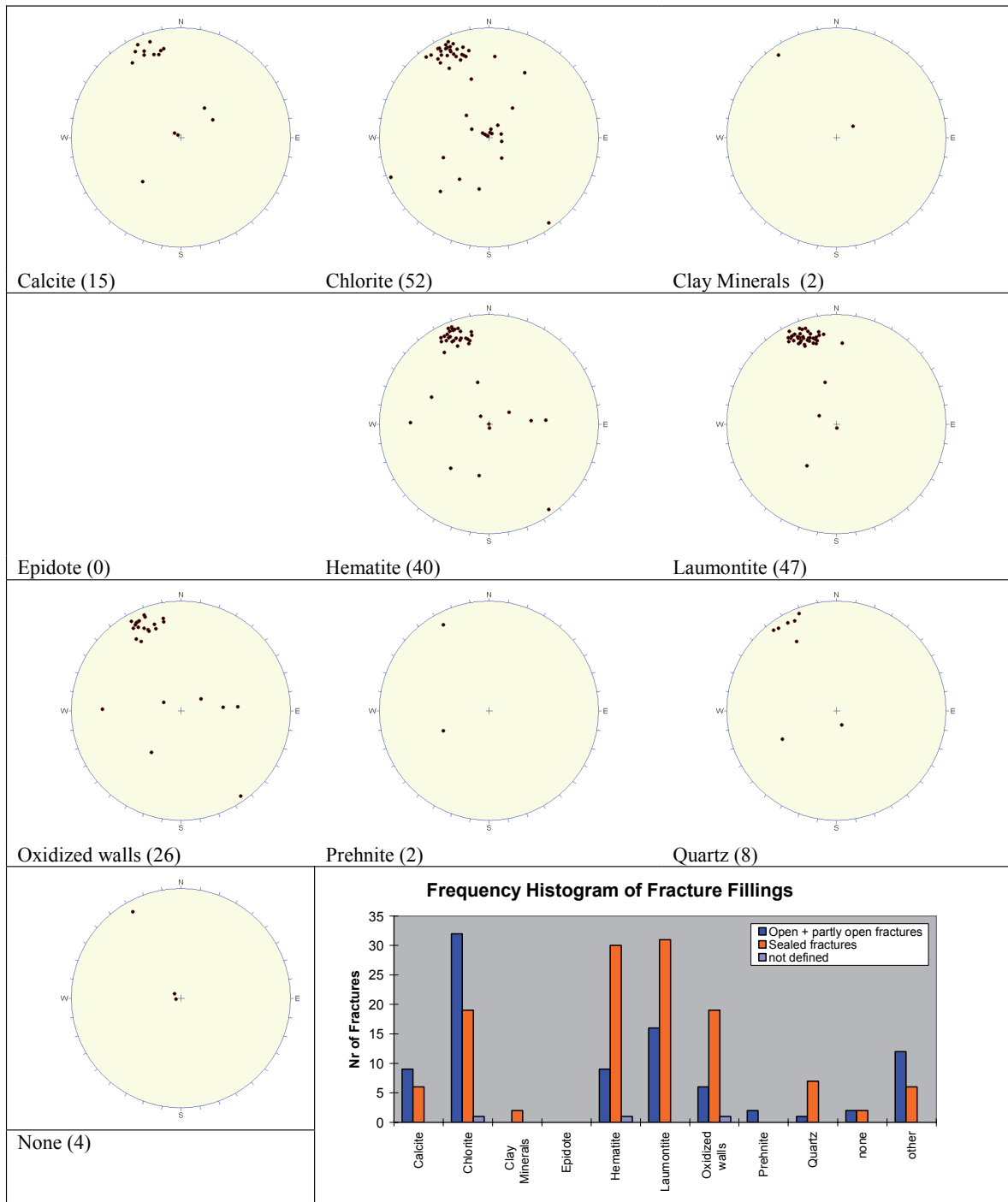
ZFMNE0401



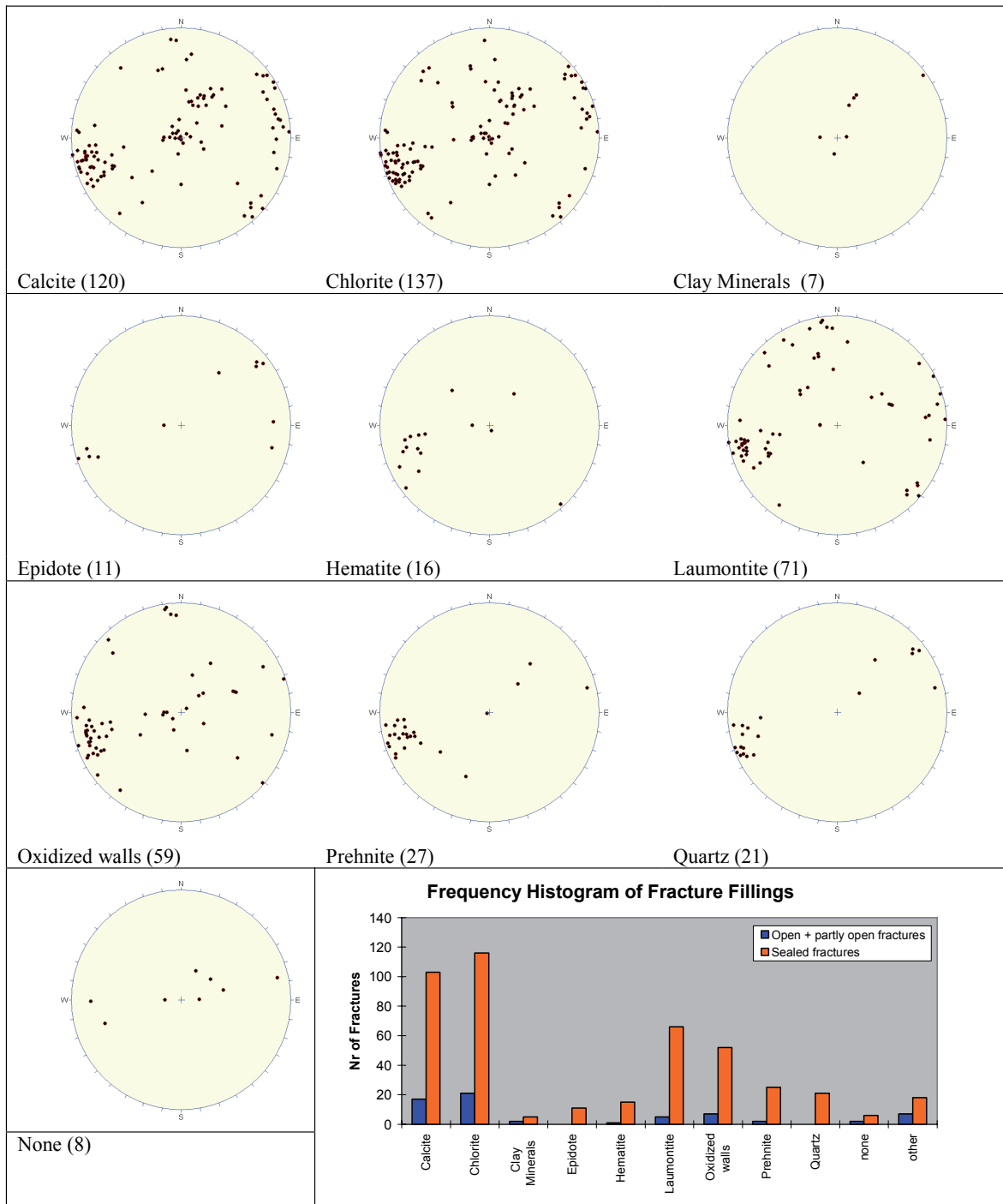
ZFMNE1188



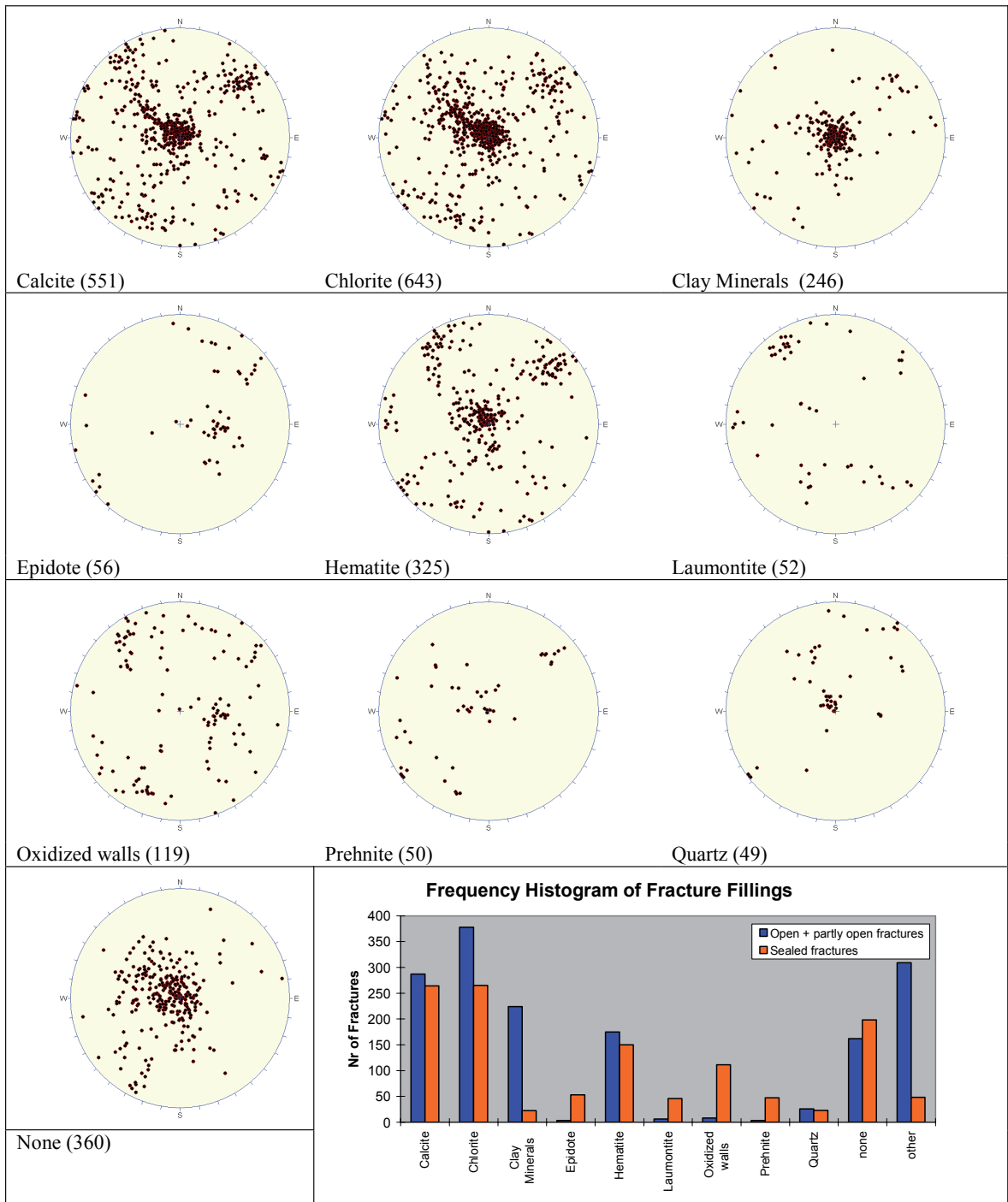
ZFMNE1189



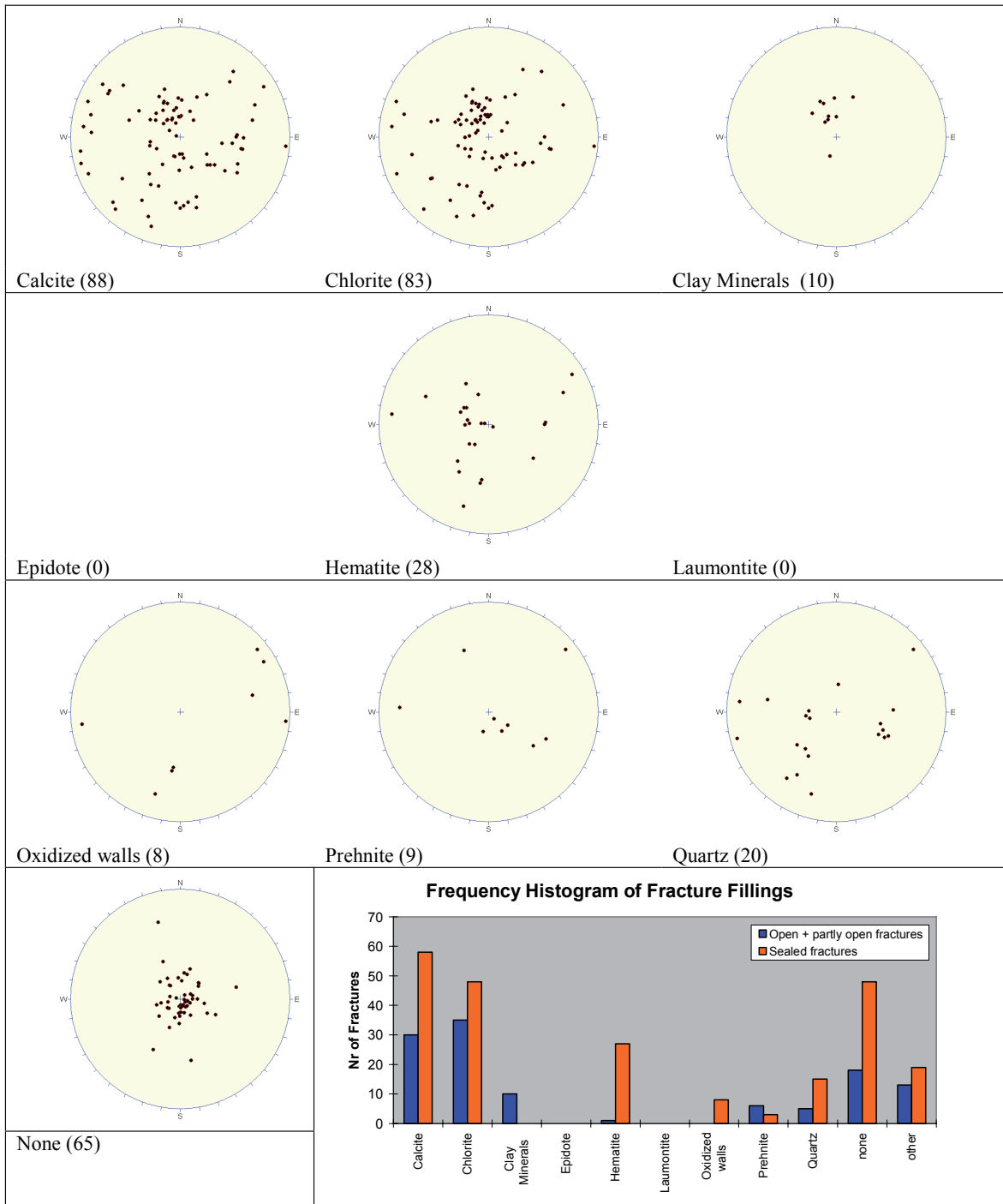
ZFMNE1192



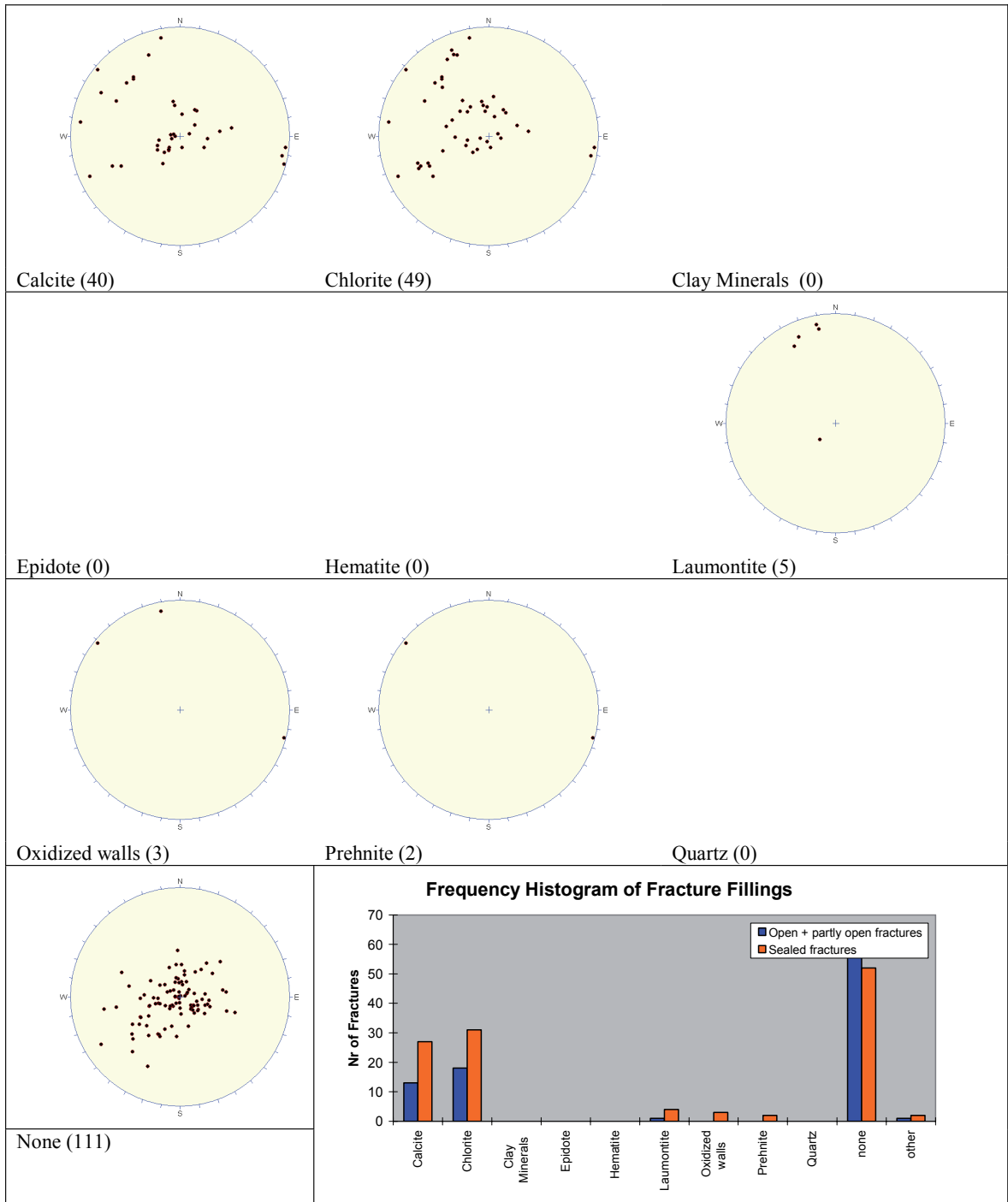
ZFMNS0404



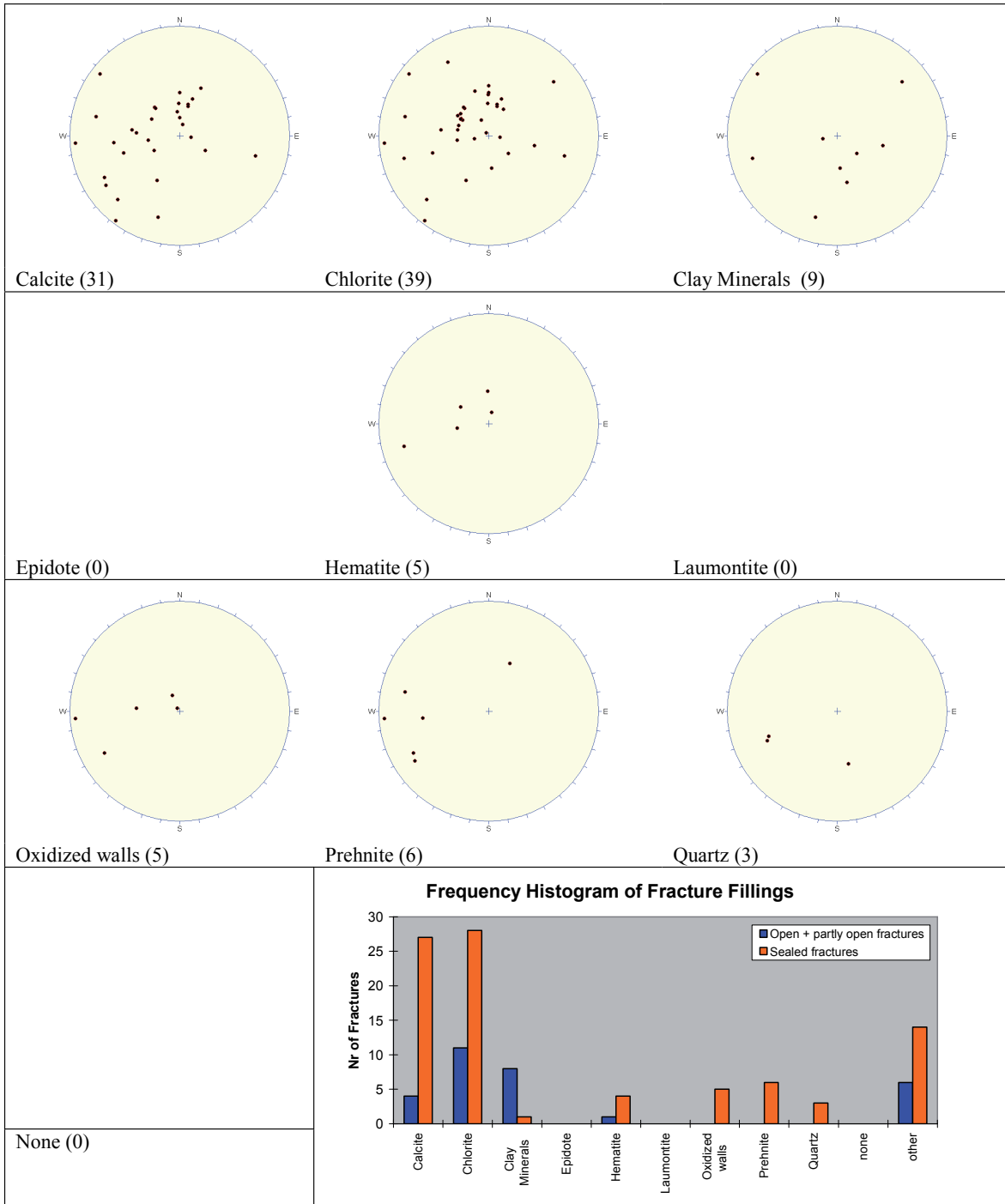
ZFMNE00A2



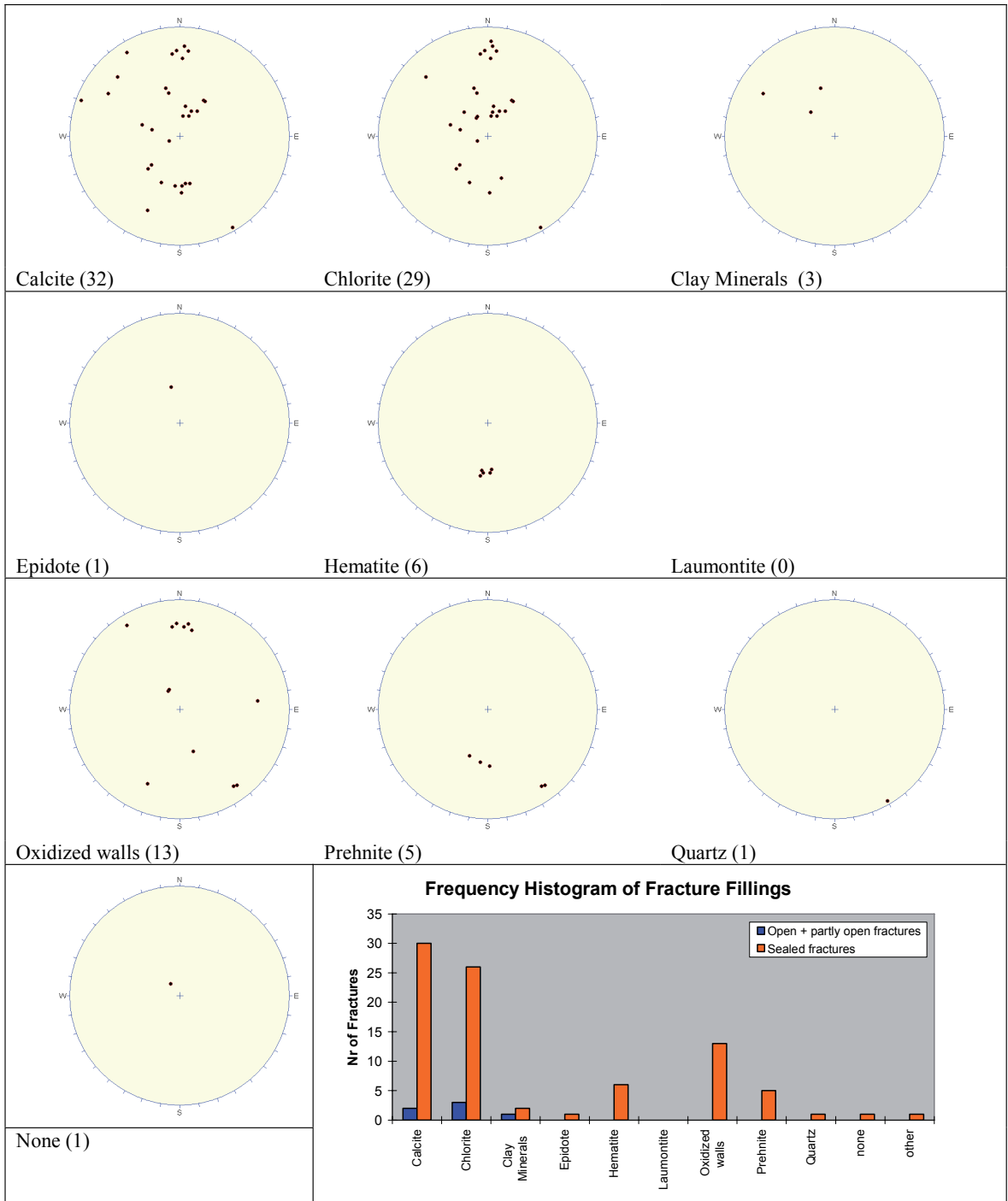
ZFMNE00A3



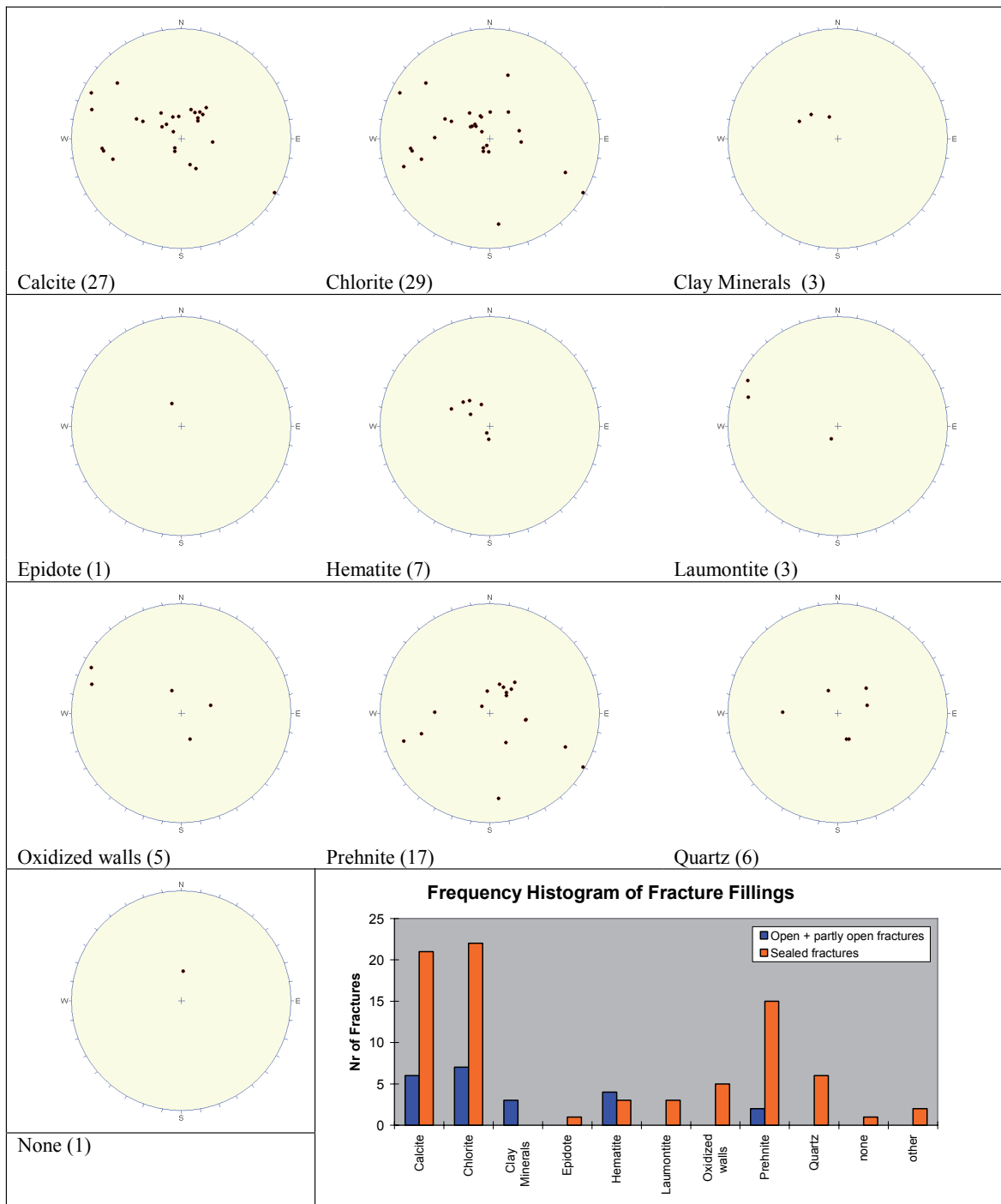
ZFMNE00A4



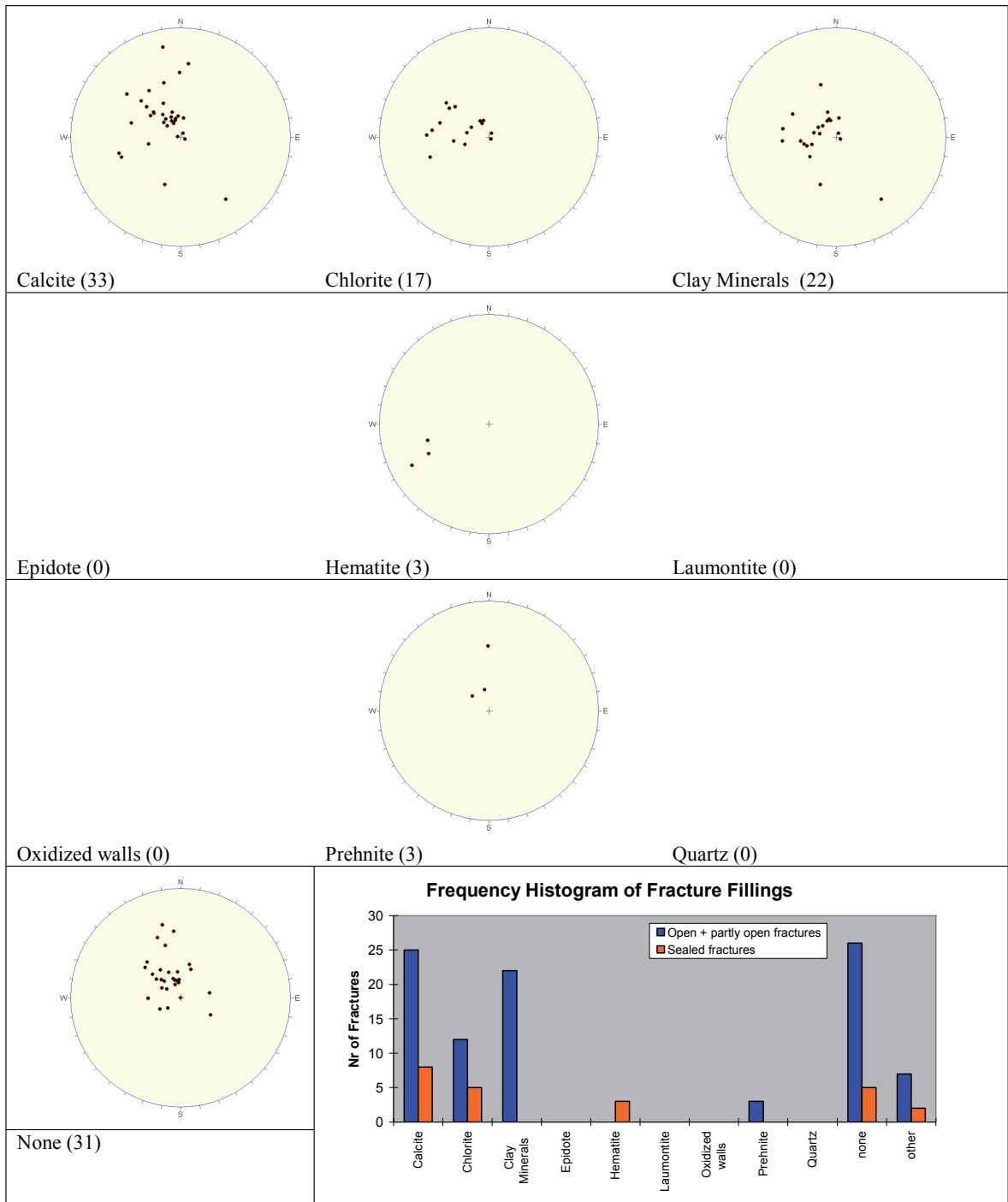
ZFMNE00A5



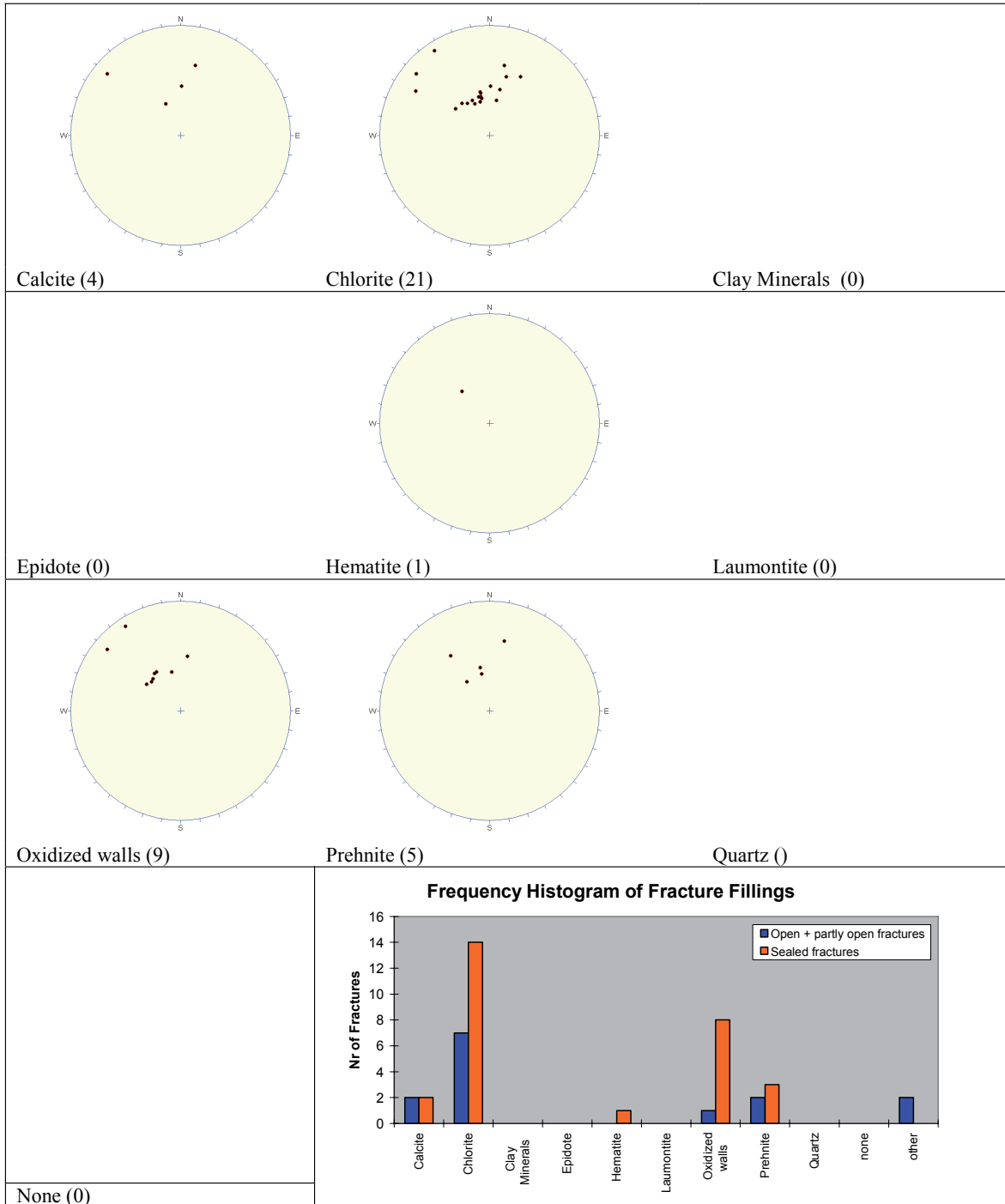
ZFMNE00A7



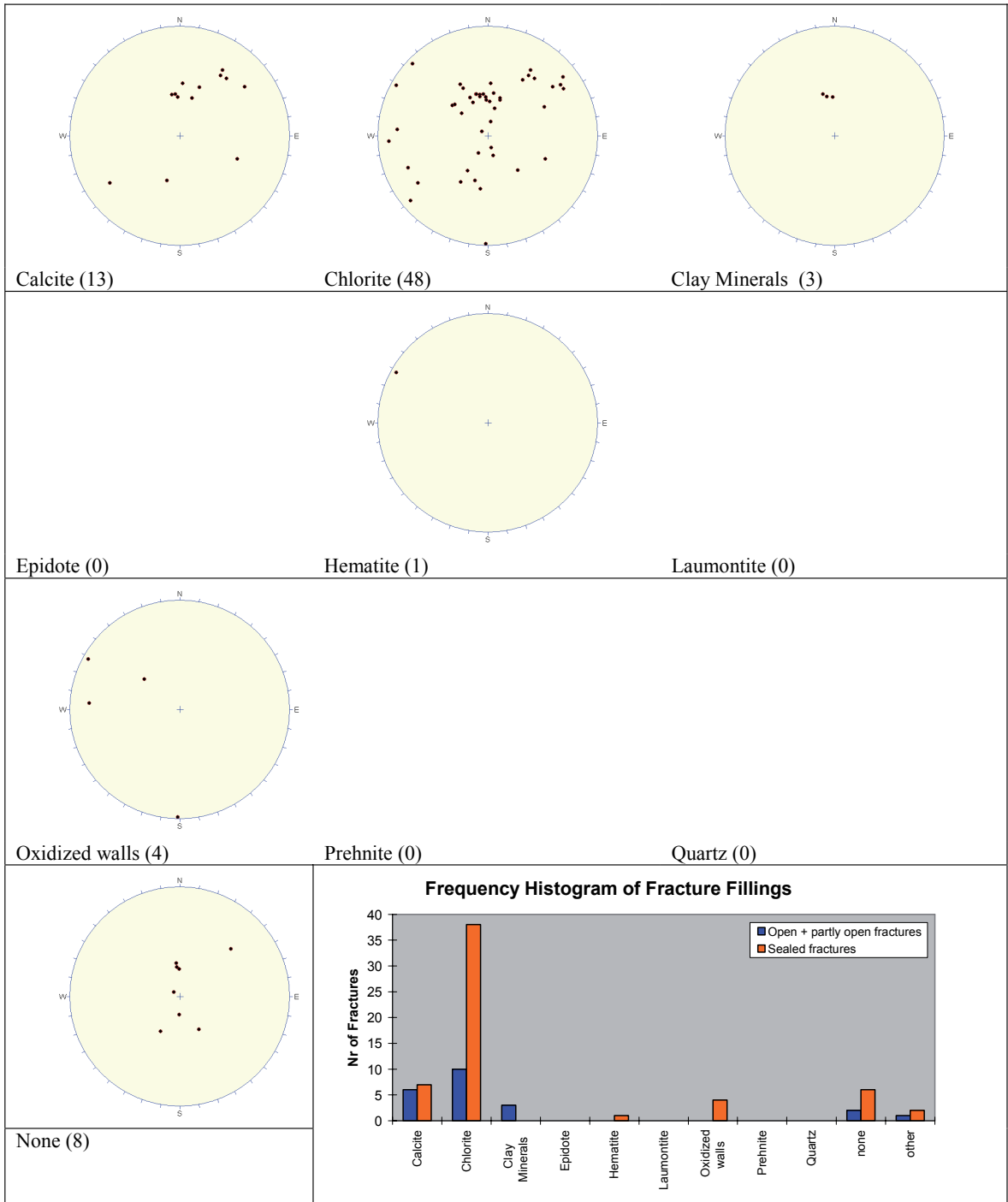
ZFMNE00B1



ZFMNE00B4



ZFMNE00B6



ZFMNE1195